

2012-2015 Monitoring and Research Summary

Wetlands Restoration at Huntley Meadows Park

*W. Lee Daniels, Sara Koropchak, Kathryn Haering, Pat Donovan,
and Daniel Evans*

**Dept. of Crop & Soil Environmental Sciences
Virginia Tech
wdaniels@vt.edu**

Tess Thompson, James Jones, and Laura Lehmann
**Dept. of Biological Systems Engineering
Virginia Tech**

G. Richard Whittecar, Ben Hiza, and Stephen Stone
**Dept. of Ocean, Earth & Atmospheric Sciences
Old Dominion University**

Zach Agioutantis
**Dept. of Mining Engineering
University of Kentucky**

April 11, 2015

Table of Contents

Introduction and Overall Objectives 3

Shallow Groundwater Monitoring 6

 Methods 6

 Results to Date 9

Vegetation Monitoring..... 17

 Introduction 17

 Methods 17

 Sampling methods 17

 Accomplishments to Date 19

 March 2014..... 19

 June-September 2014 19

 October-December 2014..... 20

 Future sampling/plot establishment timing (2015) 20

 Winter/early spring 2015 20

 Summer 2015..... 20

 Fall 2015 20

 Results to Date 20

 Hydrophytic Vegetation Test..... 20

 Species Richness, Diversity, and Evenness..... 21

 Vegetation Transitions..... 21

 Summary of Vegetation Findings to Date..... 27

Groundwater Evaluation and Monitoring 28

 Data Collection and Maintenance 29

 Interpretations..... 30

Surface Water Monitoring 37

 Progress to Date 37

 Results to Date 42

Weather Station and ET Estimators 44

Objectives.....	44
Direct Measurement of Evapotranspiration	45
Estimating Evapotranspiration	50
Progress to Date	54
Results to Date	57
Development and Deployment of Website.....	61
Building a Water Budget for Huntley Meadows and Testing Wetbud.....	62
Background on Regional Water Budget Studies and ET Estimates.....	62
Developing a Site-Specific Water Budget for Huntley Meadows	67
Testing Wetbud	67
Overall Summary and Conclusions	69
Literature Cited	70
Appendix 1. Groundwater Well Logs.....	75

Introduction and Overall Objectives

Huntley Meadows Park is the site of a major wetlands restoration program and an associated collaborative research program. The park was established in 1975 and covers approximately 1,500 acres. The central wetland area is one of the largest non-tidal wetlands of its kind in Northern Virginia. Since the late 1970s, the central wetland has transitioned from a flooded forested wetland, into a hemi-marsh, and then to a lake marsh due to beaver damming activities. However, as a result of recent consecutive droughts, siltation from upstream development north of the park, beaver activities, herbivorous feeding habits of Canada geese, and natural succession, the wetland has deteriorated to a dry marsh/wet meadow with uniform shallow water levels. These conditions promoted the development of large stands of invasive species such as broad-leaved cattail (*Typha latifolia* L) within the park, reducing habitat, and thus wildlife diversity.

In 2012, Wetland Studies and Solutions Inc. (WSSI) developed a Final Wetlands Restoration Plan (Figure 1) for the central wetlands area of the park. The project's overall goal is to increase biodiversity and ecological function (e.g. water quality) by restoring the central wetland area to a hemi-marsh system, with presumed higher levels of biodiversity and ecological function. The hemi-marsh will contain roughly 50 percent open water and 50 percent vegetated wetland in the winter, will dry out in the summer, will have more woody shrubs than currently present, and will have fewer non-desirable herbaceous plants, such as cattails. The restored wetland system will provide annual forage and a diversity of habitat quality for target plant and animal species that were once observed at the wetland and will prevent the dominance of invasive plant species. Furthermore, the total area of seasonally ponded wetlands will increase, enhancing habitat values for wading birds and other species of critical interest to the park.

To create and maintain the hemi-marsh condition, water control structures (ditch plugs, low earthen berm and a water level control outlet; see Figure 1) were installed over the summer and fall of 2013. These structures are used to raise the overall water surface and to vary the ponded water level to mimic seasonal changes typical of hemi-marshes. Additional habitat features (e.g. deeper pools and brush piles) were also developed as a part of the overall plan.

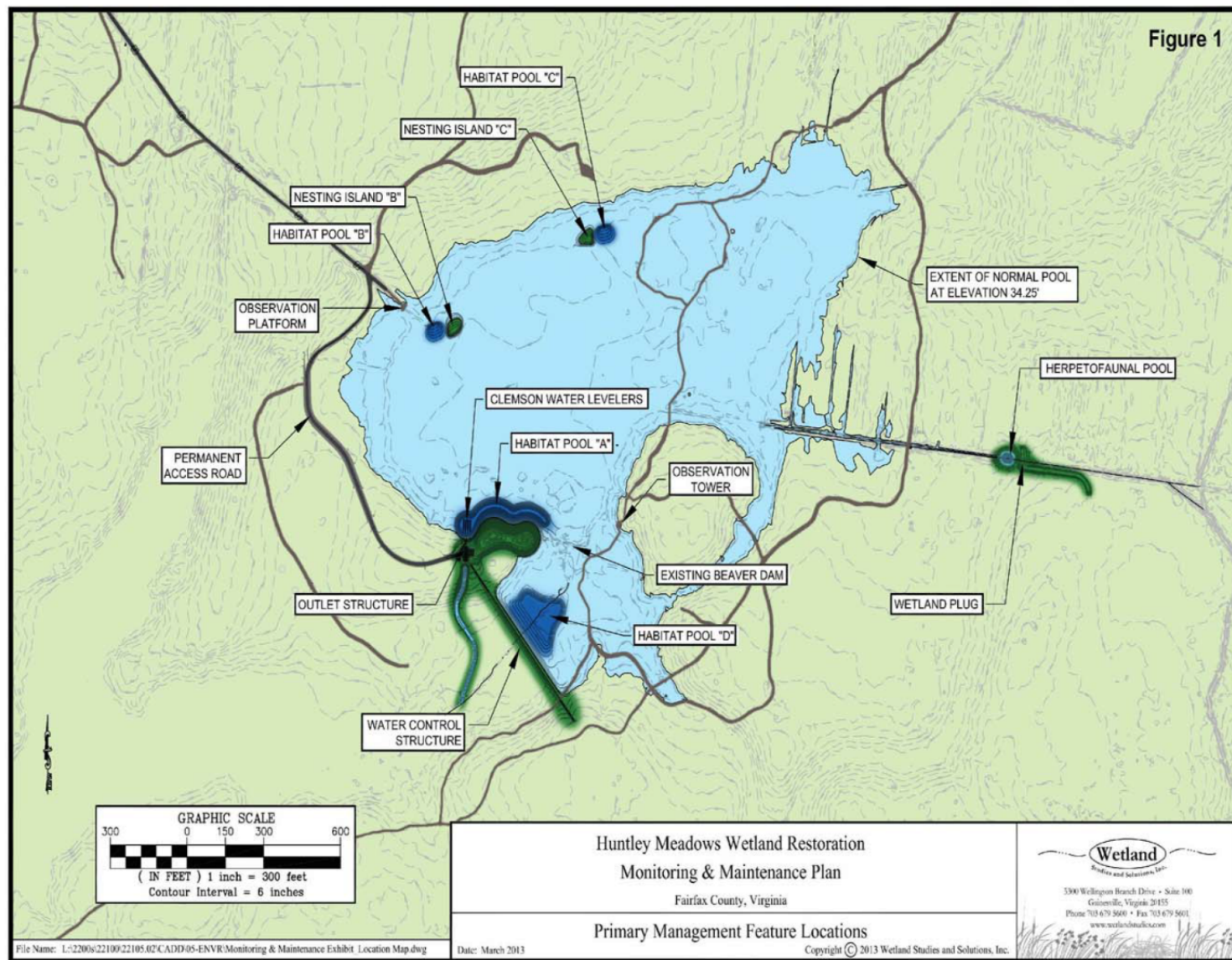


Figure 1. Summary map of Huntley Meadows Park wetland restoration plan (Wetland Studies and Solutions Inc., 2013).

In 2012, Virginia Tech (VT) and Old Dominion University (ODU) agreed to develop and implement a combined monitoring and research program at the park funded by WSSI and the Peterson Family Foundation. This was accomplished via an addendum contract to their pre-existing (est. 2008) cooperative research project entitled *Wetland Water Budget Modeling*, the centerpiece of which has been the development of a wetland water budget prediction and planning tool called *Wetbud*. Current work for this research program is focused on the following objectives:

1. Instrument and monitor all aspects of water level and water budget components for the Huntley Meadows site.
2. Test and calibrate Wetbud (basic and advanced versions) at Huntley Meadows via application of the model using site-specific data sets and comparison with actual variations in water levels (open water and groundwater) over multiple seasons.
3. Determine the net effect of the current installation of the new water control structure on (A) water levels and (B) vegetation community response to raised surface and groundwater levels and more frequent inundation.
4. Investigate several methods to determine actual evapotranspiration (AET) at the Huntley Meadows site and their relative effects on modeled (via Wetbud) vs. actual fluctuations in surface and groundwater.

This report focuses primarily on our specific efforts and results to date to meet objectives 1, 3 and 4. We have also made considerable progress over the past two years in developing and testing the Wetbud model, but those results are being reported separately. However, over the current year (2015) we are moving forward with the site-specific testing of Wetbud for suitable portions of the Huntley Meadows wetlands.

Shallow Groundwater Monitoring

Methods

Four transects of shallow groundwater monitoring wells (Figure 2) were installed in October 2012 to determine local groundwater conditions before and after construction of the new water control structures. The relationship of the shallow wells around the central wetland to the rest of the site's monitoring array is shown in Figure 3. Three groundwater wells (A, B and C) were installed along all four transects as described below and two additional wells were placed into the open water/emergent portion of the marsh for Transects 1 and 3 where it was clear that the area around the well supported extended winter/spring ponded conditions. Along each transect, well A was placed at the edge of the seasonally ponded area dominated by herbaceous vegetation, immediately adjacent to the woody shrub/scrub or forested edge. Well B was placed farther into the surrounding forested area at an elevation presumed to be just above seasonal flooding based on local vegetation and soil indicators. Well C was placed even farther uphill on each transect at an elevation presumed to be above the potential 100 year flood level and clearly into a presumed upland environment.

Shallow groundwater monitoring wells were installed in October 2012 by hand using a 3.5" soil auger. The wells were constructed of 2.0" PVC and well screen, most have a 1' riser, and were installed to variable depths (~ -2 ft to -5 ft) depending on landscape position. The top of the riser was modified with a special PVC fitting to accommodate the well loggers as described below. The lower 12" (30 cm) of each well consists of standard slotted well screen terminating in a solid well point. The rest of the well + riser above the screened increment is solid 2" PVC. The well boring annulus was sand filter packed and the upper 6 in. was filled with a pelletized bentonite plug to minimize surface water charging of the well bore. Bentonite was mounded around the top of the well bore and replaced when necessary. Each well is protected by a locked metal cap and a small concrete pad installed by WSSI personnel. All wells were instrumented with Odysseytm capacitance water level loggers with a reported sensitivity of 1 mm. Water levels are recorded hourly and downloaded monthly with a laptop. The riser for well 2A was extended in November 2013 to keep the logger above flood levels following closure of the outlet control structure. The risers for the two ponded locations were also lengthened to keep the loggers above possible inundation. Water level data are transformed into an Excel format and manipulated with SigmaPlottm V. 12.2.

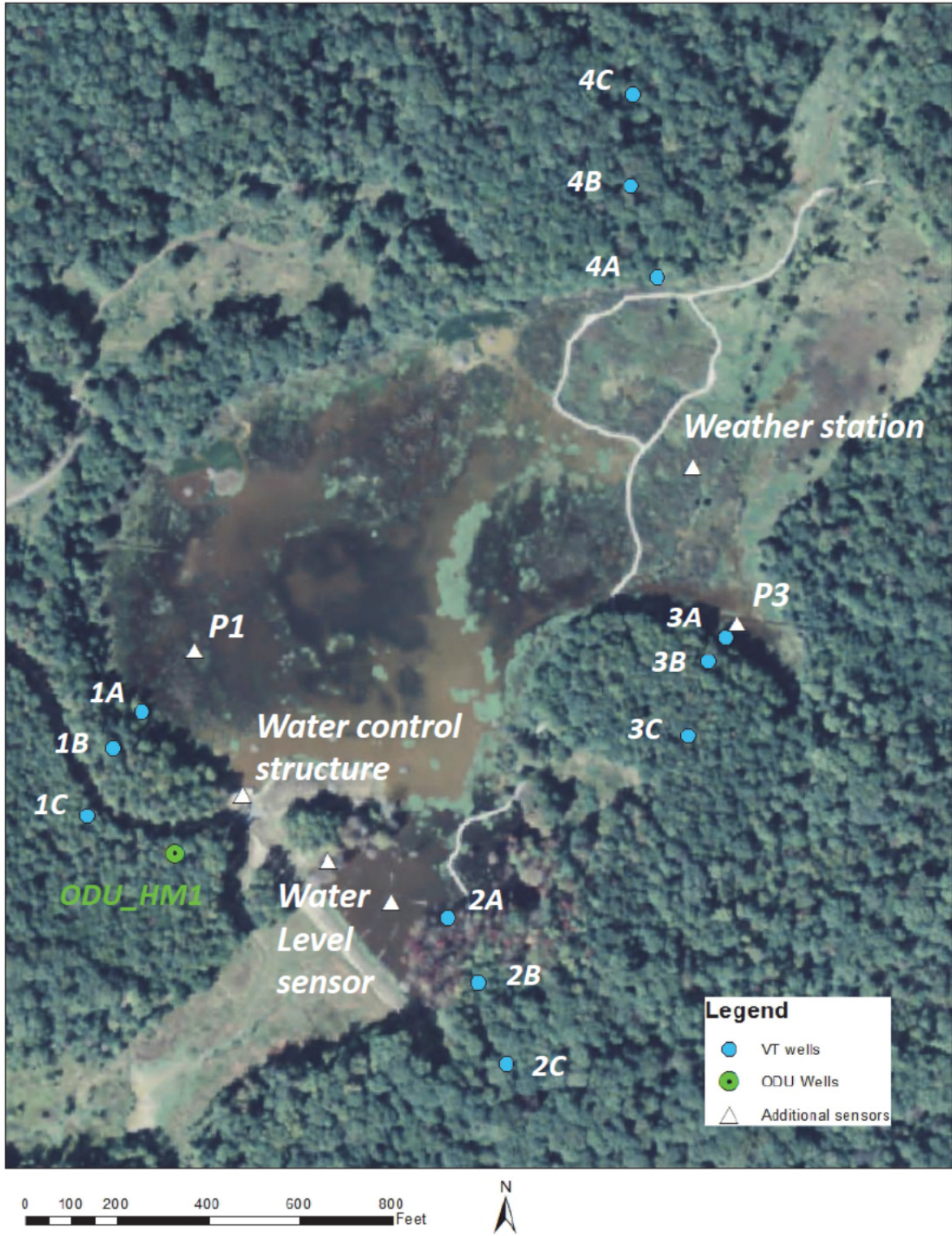


Figure 2. Local detailed map of monitoring locations in and around central wetland at Huntley Meadows Park.

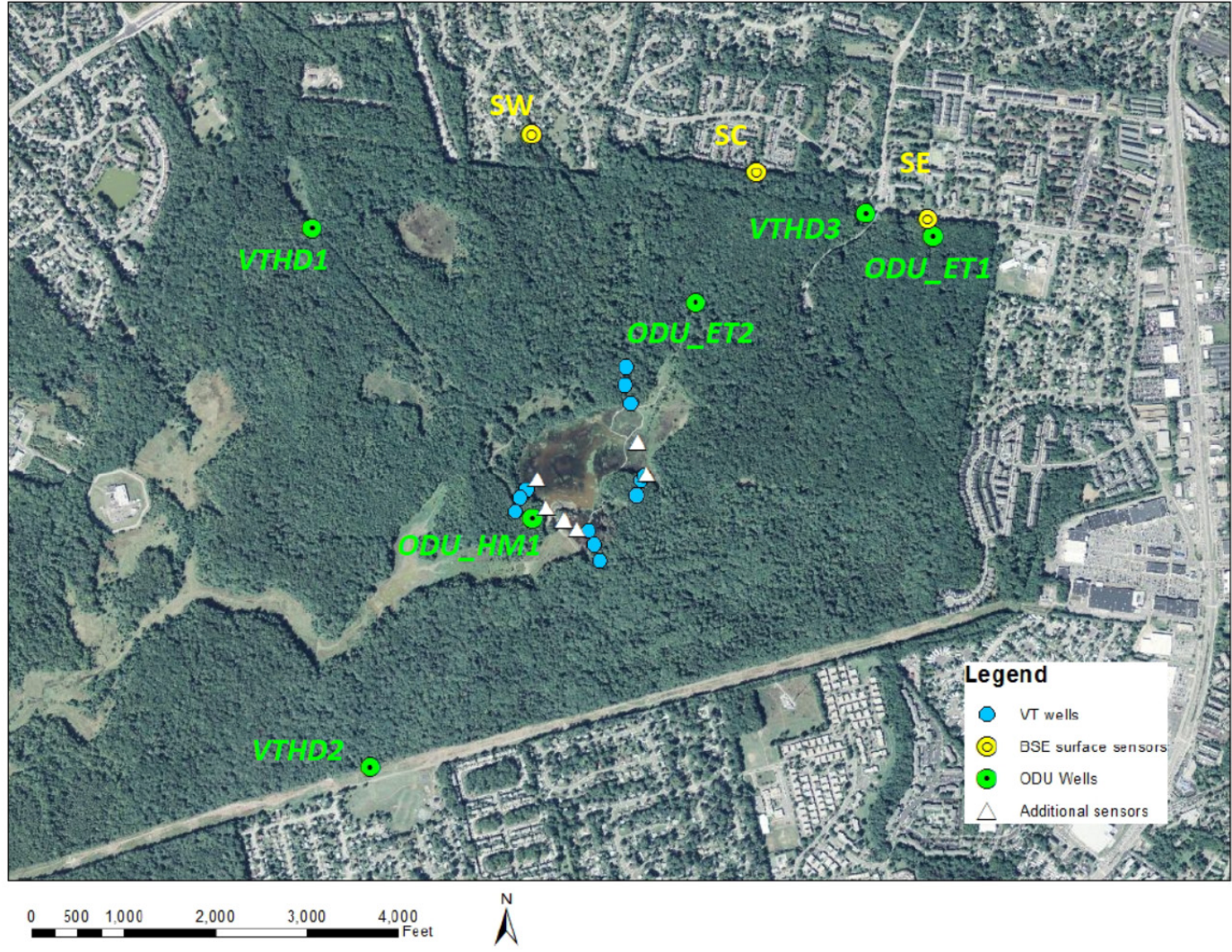


Figure 3. Area map of all monitoring locations at Huntley Meadows Park. See Figure 2 for detailed locations in wetland area at center of the park.

Results to Date

The berm and outlet water control structure associated with the wetland restoration project at Huntley Meadows were constructed over the spring and summer of 2013. The project was completed in September and the slide gates on the water control structure were raised to elevation 34.25 feet on October 4, 2013. The following week, a multi-day rain event (> 6.0 in) produced significant local runoff and the system quickly filled to 34.35 feet, water flowed over the newly constructed berm, and ponded water extended above all of the A and P monitoring locations and approached a number of the B locations.

The shallow groundwater levels at all 12 main transect locations and the two associated ponded locations are shown in Figures 4-9. Overall, the respective groundwater levels for the three primary wells (A, B and C) along all four transects clearly show the combined effects of (1) seasonality, (2) differences in local elevation/topography, and (3) the distinct impact of the new water control structures installed over the summer and fall of 2013. Water levels at all A-B-C locations display the typical “hydroperiod” for forested wetlands in our region due to differences in seasonal evapotranspiration (ET) rates vs. precipitation. The flat response at the bottom of the hydrographs for certain wells reflects the bottom of a “dry well” rather than uniform summer groundwater levels. Groundwater levels rise in the late fall, reach a relatively stable maximum in mid- to late-winter, and then drop rapidly once the trees leaf out again in the spring and ET rises. It is also notable that all wells, particularly those in the middle (B) and highest (C) local landscape positions showed pronounced short-term responses to major rainfall events that were superimposed over their longer-term seasonal hydroperiod. As expected, wells located at position A were less variable in their hydroperiod than those located in the middle and higher landscape positions and the overall depth to the winter high water table increased with local elevation. Finally, all wells at all locations showed a pronounced effect of the installation of the water control structures over the summer of 2013. Differences among well response along the transects are discussed below.

Along Transect 1, the surface was never ponded over the winter/spring of 2012/2013, but remained saturated close to the soil surface or ponded for the majority of time after the construction was completed in the late summer of 2013 (Figure 4). Groundwater levels at both the intermediate (B) and higher (C) local elevations indicate that activation of the water control structures caused a significant increase in the overall elevation of the winter high water table and decreased its short- to medium-term fluctuations. The dramatic effect of the heavy rainfall event in September of 2013 was clearly expressed in wells A and C at this location, but interestingly was not expressed in the middle elevation well. Water levels at the Transect 1 ponded location (P1 in Figure 5) showed a dramatic seasonal hydroperiod fluctuation (>25 in.) with a significant deep subsoil drying event over the first year, but the surface remained ponded and the overall water levels rose significantly once the water control structures were activated.

Transect 2 was originally located along a slightly lower area of the pre-construction landscape where the adjacent pre-existing draining stream channel was incised. This local drainage effect apparently had allowed the forested edge to be maintained at a lower elevation than the other transects. Here, relative water levels along the transect (Figure 6) exhibited a similar overall seasonal hydroperiod and landscape position response to Transect 1, but the effect of the installation of the water control structures was much more pronounced due to its lower elevation and direct proximity to the retaining berm. The overall height and length/duration of near-surface (e.g. < 12 in. from surface) saturation in the middle landscape position (B) appears to have been significantly increased by the new water management regime. The subsoil saturated zone along Transect 3 (Figure 7) was also significantly elevated for much longer duration at locations A and B following construction in 2013, while the primary effect at the upland location (C) appears to be a decrease in short-term winter variability. The ponded well location at Transect 3 (P3 in Figure 8) responded in similar fashion to Transect 1; imposition of the new water management system eliminated the deep summer drying event and deepened overall ponded water levels.

The local landscape for Transect 4 (Figure 3) differs from the other three transects in that the area immediately within the forested zone is extremely flat and low-lying and the marsh/forest edge (A) location is slightly higher in elevation than other transects. The middle (B) and upland (C) well locations were therefore located at a considerably longer distance away from the marsh edge and we assumed would be less sensitive to the effects of the new water management regime. Surprisingly, this assumption was incorrect; all three well locations exhibited higher, more prolonged and less variable (B and C; Figure 9) near-surface winter/spring soil saturation and or ponding (at C). This may be due to the hydrologic/subsoil drainage influence of the north trending arm of the marsh zone that lies parallel to the east of locations 4B and 4C. It is also interesting to note that neither of the two higher elevation wells exhibited a response to the large October 2013 rain event.

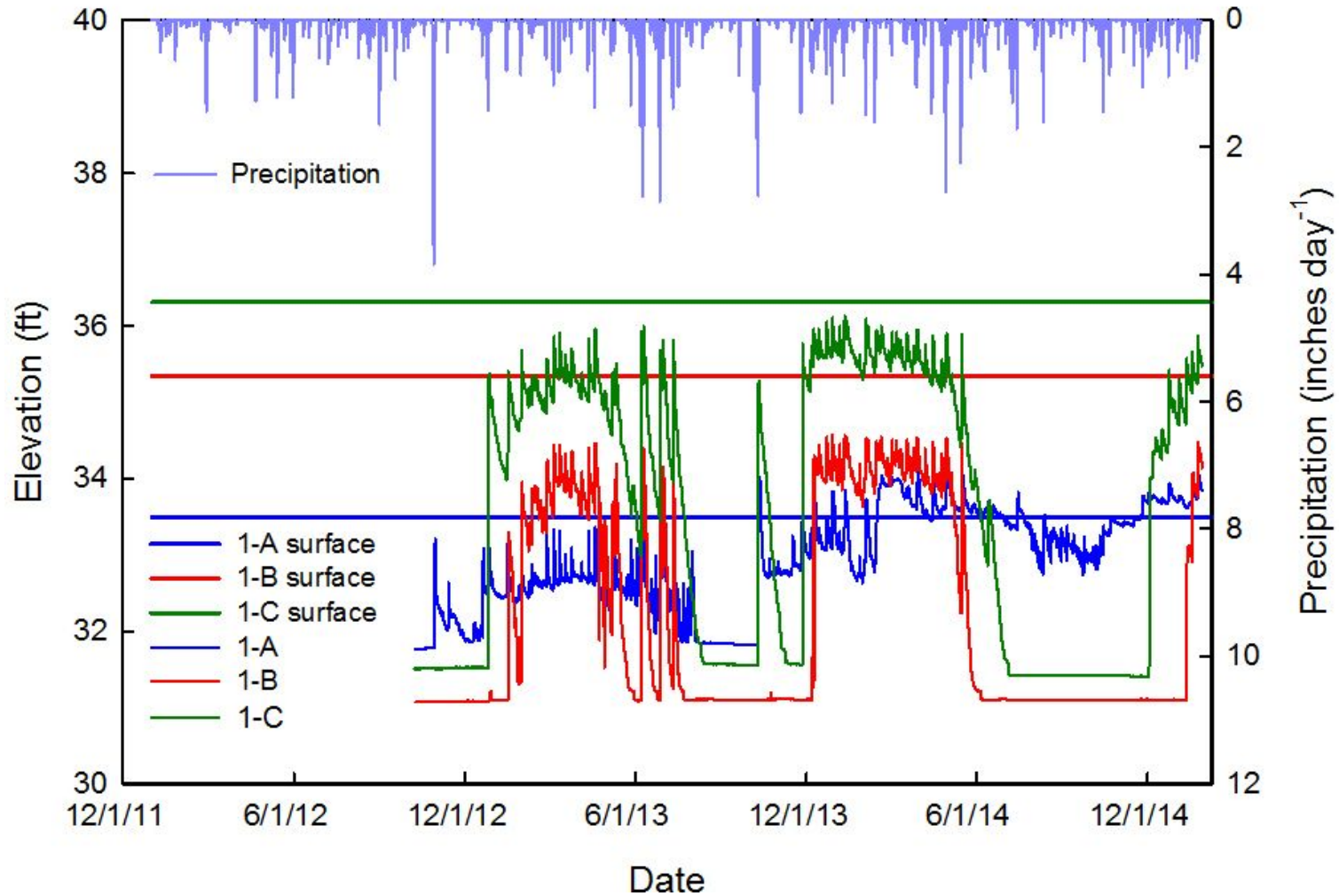


Figure 4. Shallow groundwater levels for wells on Transect 1. The solid lines represent the ground surface elevation at each well. Precipitation (Reagan National Airport) is also shown at the top of the figure. Flat well signals during the summer months denote dry wells.

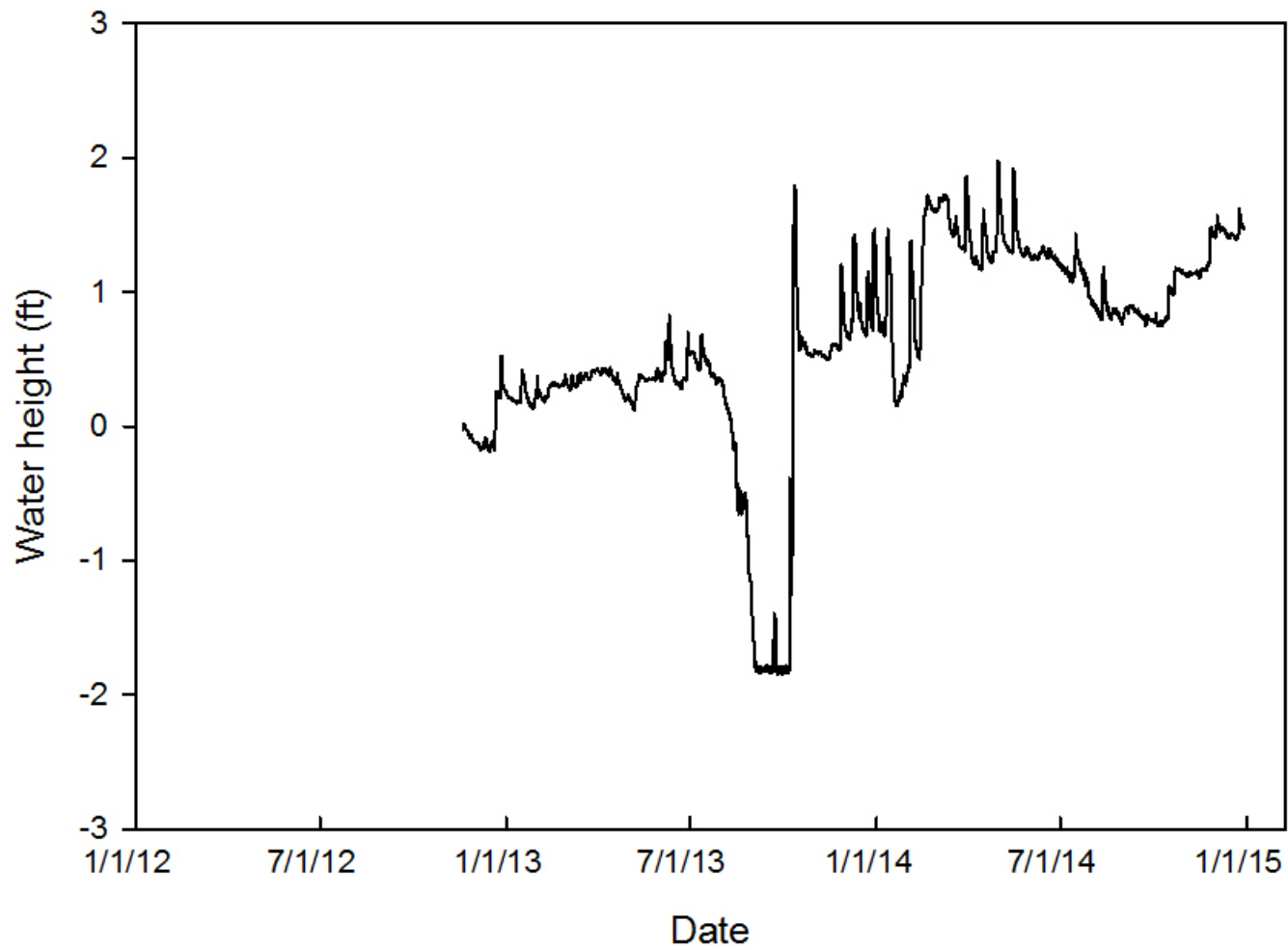


Figure 5. Water levels for the extended Transect 1 well located in the ponded area (P1). The top of the sediment surface = 0. Flat well signals during the summer months denote dry wells.

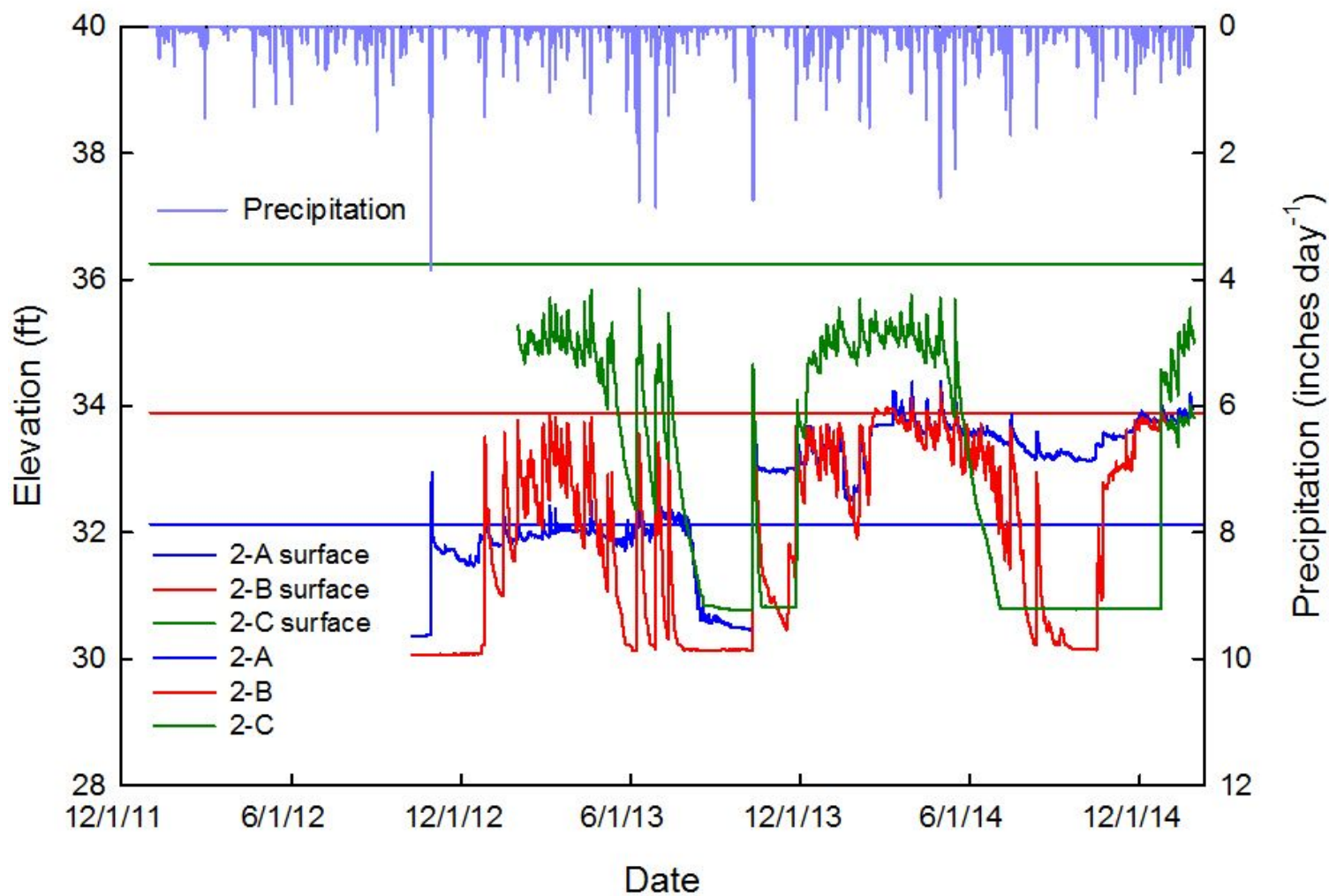


Figure 6. Shallow groundwater levels for wells on Transect 2. The solid lines represent the ground surface elevation at each well. Precipitation (Reagan National Airport) is also shown at the top of the figure. Flat well signals during the summer months denote dry wells.

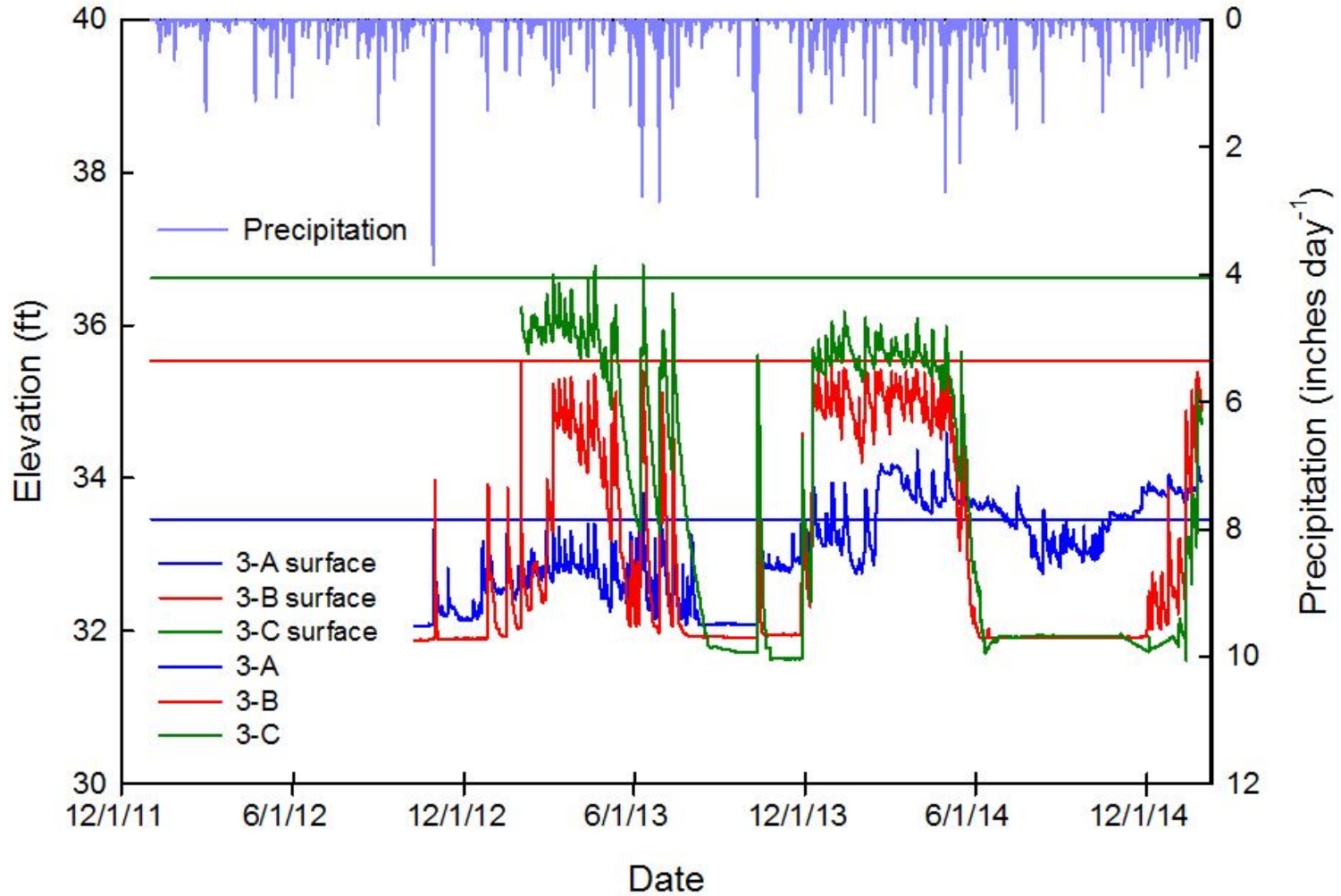


Figure 7. Shallow groundwater levels for wells on Transect 3. The solid lines represent the ground surface elevation at each well. Precipitation (Reagan National Airport) is also shown at the top of the figure. Flat well signals during the summer months denote dry wells.

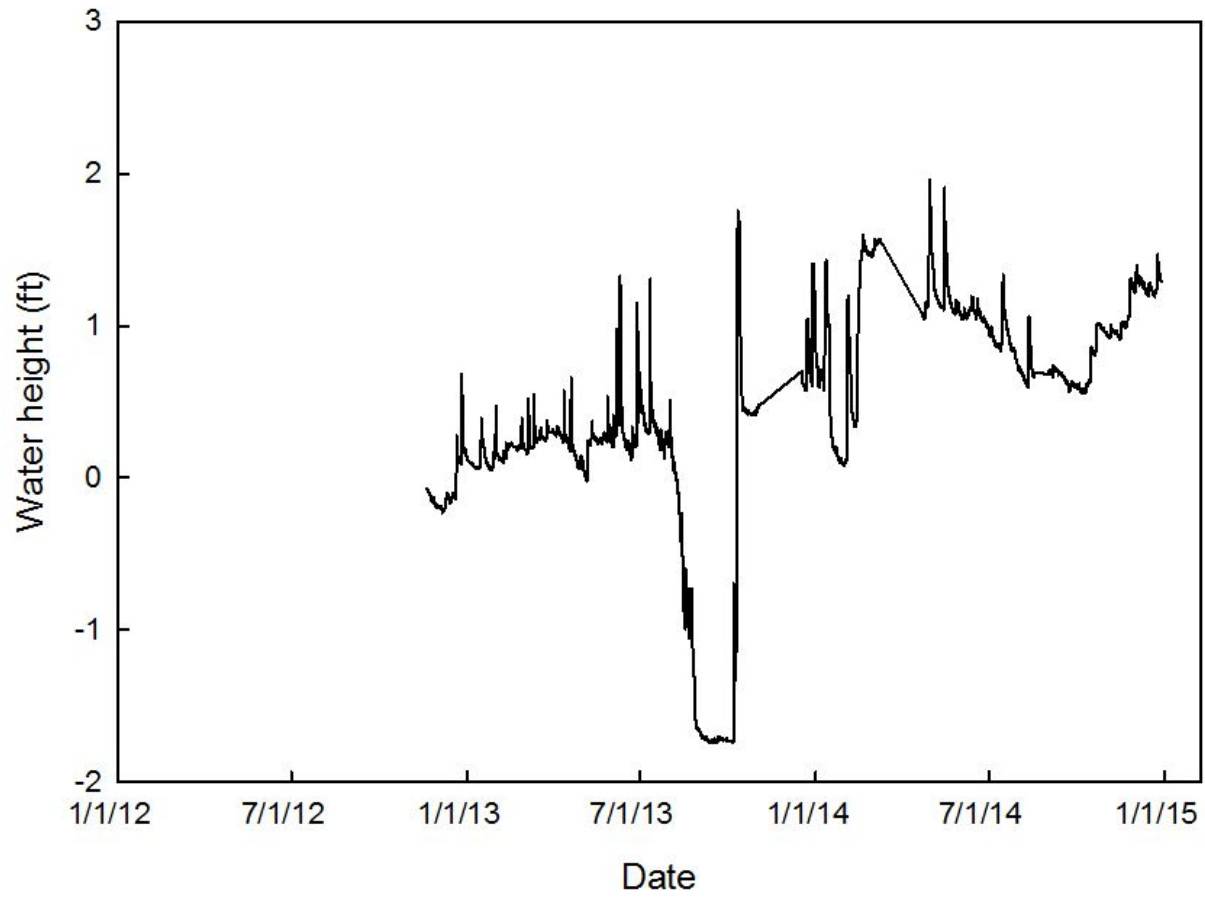


Figure 8. Water levels for the extended Transect 3 well located in the ponded area (P3). Top of the sediment surface = 0.

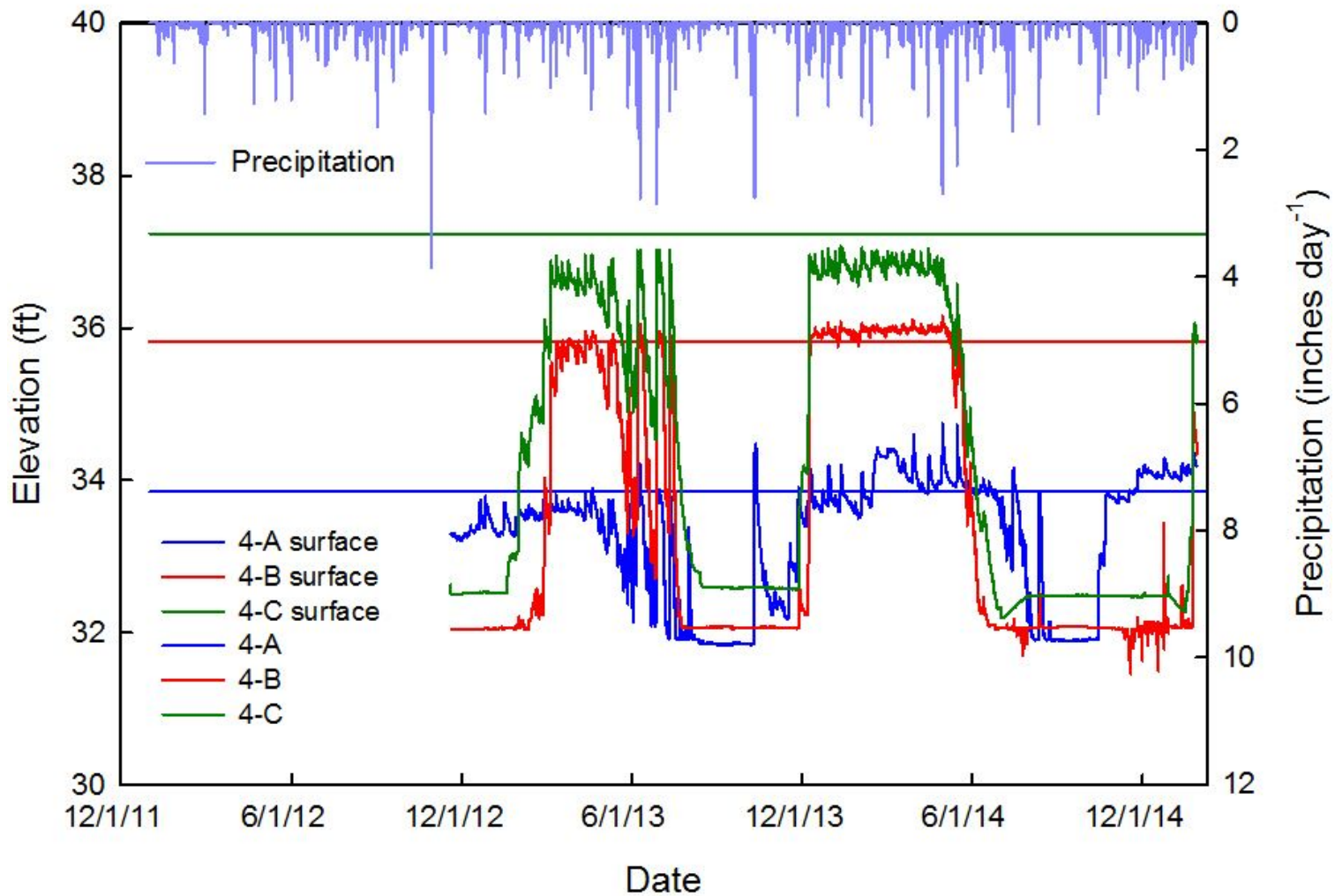


Figure 9. Shallow groundwater levels for wells on Transect 4. The solid lines represent the ground surface elevation at each well. Precipitation (Reagan National Airport) is also shown at the top of the figure. Flat well signals during the summer months denote dry wells.

Vegetation Monitoring

Introduction

We have installed our vegetation monitoring plots adjacent to the shallow groundwater wells (Figure 2) in order to allow direct comparison of vegetation and hydrologic data. The wells are located in areas of interest to us when observing vegetation response to changes in the overall saturation/flooding regime. Wells labeled as “P” are distinctly in ponded areas (approximately 0.5 to 2 ft of standing water year-round), wells labeled as “A” are in a transition zone from ponded to shrub/scrub fringe or forest, wells labeled as “B” are approximately in a transition zone from wet forest to relatively upland forest, and wells labeled as “C” are considered upland. Although no ponded well is present on Transect 4, an additional set of vegetation plots was added to the ponded area beyond location A (4P). These designations were assigned prior to the change in water level management, and well IDs for transect 2 have been adjusted to match our definitions for the purpose of statistical analysis.

Our vegetation monitoring program aims to answer the following questions:

1. How do vegetation communities differ among the four flooding categories (P, A, B, C)?
2. How does vegetation (cover, composition) in the original normal pool respond to increased water levels?
3. How does the vegetation in the new normal pool (previously not flooded) change, particularly in transition zones?
4. How does vegetation outside of the new normal pool change with increased water levels?
5. How do tree survival and growth vary within species in the various flood levels, particularly in transition zones?
6. How do tree communities change with new flooding regimes?

Methods

Sampling methods

Using each well as a plot center, we have established permanent woody species monitoring plots (Figure 10). Woody plots are circular plots with a 32.8 ft. radius (10 m). In each woody plot, we identify all trees (>3.94 in. (10 cm) DBH, >22.96 ft. (7 m) tall), saplings (<3.94 in. DBH, >22.96 ft. tall), shrubs (<22.96 ft. tall), and vines present, determine percent cover, and ensure that all trees with a DBH > 3.94 in. are tagged with inconspicuous numbered tags. Percent cover is determined for each species within each size class, and saplings will be counted for each present species.

Also associated with each well are four 3.3 x 3.3 ft (1 m²) permanent herbaceous monitoring plots (Figure 10). Plots are located along local contours at approximately the same elevation as the well. Within each herbaceous plot, we record the percent cover of all species present and total percent cover. Identifiable unknown species are collected for identification in the Massey Herbarium on the Virginia Tech campus. Unknown species with few distinguishing characteristics and/or rare species are left in the plot for identification during the next sampling trip.

Lastly, we sample vegetation transects between wells to observe the change in vegetation over time across the hydrologic gradient. Beginning at the most ponded well, we assess 1 m² plots every 16.4 ft (5 m) to assess the general wetland status of the present vegetation (aquatic, emergent, upland, etc.) and make notes of the dominant species present. New transects begin at every well, however once transects are clearly into upland vegetation, they are terminated. Observations for transects were first recorded in March 2014 to attempt to describe the initial vegetation status, and again in September 2014 to describe the vegetation transition soon after flooding. Detritus and/or litter present were described in March 2014 and will be used as a proxy for estimating the pre-flooding late summer 2013 vegetation.

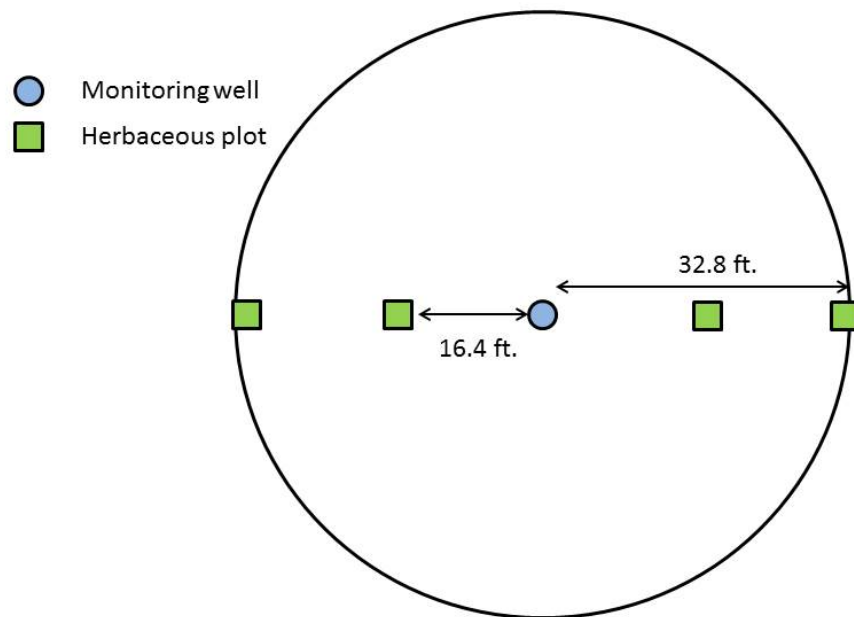


Figure 10. Diagram of vegetation monitoring plot design utilized at Huntley Meadows. Woody species are tallied within the larger 32.8 ft. (10 m) main plot and herbaceous vegetation is assessed in four quadrats located across the local contour.

Analysis methods

Raw vegetation data will be used to calculate richness, evenness, and diversity for all strata. These calculated data will be analyzed using a two-way ANOVA to determine whether there are any differences among transects or well types. As stated above, Transect 2 was reclassified since well 2A actually became ponded after the implementation of the new water management plan, well 2B is transitioning from the ponded area, and well 2C is now in a transition from wet to upland forest. In the future, we will compare these data to water level data for a more accurate assessment, but two of the ponded wells have not yet been surveyed and thus an accurate assessment of those well elevations is not possible at this time. The full vegetation dataset will also be used to calculate “50/20 rule” for dominance to determine whether hydrophytic vegetation is present at each well.

Multivariate statistics will be performed on individual strata, as data are collected in different formats (e.g. basal area and stem count for trees, percent cover for herbaceous). We are in the process of acquiring an appropriate multivariate statistical program (PC-ORD) and plan to complete ANOSIM, NMDS, and PCA analyses of the 2014 vegetation data in the late winter of 2015. Eventually, we will use these methods to compare multiple years of each sampling plot in order to quantify plant community change.

Accomplishments to Date

March 2014

- 1) Permanent plots were located and inconspicuous monuments for corners of herbaceous plots were installed. We did not need to move any plots due to disturbance. Herbaceous plots were placed approximately parallel to the shoreline at 5 and 10 m from either side of the well. We installed a set of vegetation plots (1 woody and 4 herbaceous) in the ponded portion of well transect 4, although there is no well there.
- 2) Ensured that all trees within woody plots were ID'd, measured, and tagged [> 4 in. (10 cm) DBH].
- 3) Attempted to quantify herbaceous vegetation in newly flooded herbaceous plots and on non-upland transects to provide an approximate picture of pre-flooding vegetation. This assessment involved identification of the detritus, operating under the assumption that most of the detritus was from the previous growing season (and representative of pre-wetland expansion vegetation).

June-September 2014

- 1) Conducted two summer full vegetation surveys in late June and early September.
 - a. Assessed both herbaceous and woody vegetation
 - b. Identified collected plants from June and entered data.

- c. Identified some unknowns from September.

October-December 2014

- 1) Completed unknown species ID
- 2) Updated vegetation database
- 3) Calculated and analyzed 2014 Shannon-Wiener diversity, richness, evenness, and 50/20 dominance for all plots.

Future sampling/plot establishment timing (2015)

Winter/early spring 2015

- 1) Perform multivariate statistics on 2014 vegetation data
- 2) Assess woody survival, tag any trees that are now > 4 in. (10 cm) DBH

Summer 2015

- 1) Conduct vegetation surveys in mid-summer and late-summer.
- 2) Begin ID of unknown species.

Fall 2015

- 1) Complete ID of unknowns
- 2) Data analysis of 2015 woody data
 - a. Survival
- 3) Data analysis for summer 2015 herbaceous data
 - a. 50/20 dominance
 - b. Richness
 - c. Shannon-Wiener diversity
 - d. Evenness
 - e. Multivariate analysis of communities (PCA, ANOSIM, etc.)

Results to Date

Hydrophytic Vegetation Test

Dominant species were determined for each plot in all five strata and combined to determine the overall number of dominant species, as well as the proportion of dominant species that were facultative (FAC), facultative-wet (FACW), or obligate (OBL) hydrophytic species. If 50% or more of the dominant species were FAC, FACW, or OBL, then the plot was deemed to have hydrophytic vegetation (Table 1). However, if the percent of dominants that were also wetland species was only marginally greater than 50%, particularly if upland (UPL) species were present or a large proportion of species were FAC, the plot was given a “Maybe” designation. The presence of a “Maybe” designation simply indicates that the plot might have hydrophytic

vegetation, but will need confirmation of hydric soils and wetland hydrology to designate it as a wetland.

Based on the dominance test, 9 of the 15 plots have definitively hydrophytic vegetation and 5 may have hydrophytic vegetation. Three of the B plots and two C plots may have hydrophytic vegetation, and one C plot definitely has hydrophytic vegetation. Plots where the vegetation was not definitively hydrophytic or upland rarely contained any OBL or FACW dominant species, and when these species were present, they occurred with UPL species. It is probable that the vegetation communities in these “Maybe” plots will become more hydrophytic in response to the new flooding regime, as they are intermediate between hydrophytic and upland species.

Species Richness, Diversity, and Evenness

Species richness, Shannon-Wiener diversity, and Evenness were calculated for all five strata and analyzed by a series of ANOVAs to determine whether there were any differences among transects or well type (P, A, B, C). There were no differences in species richness among transects, however there were significant differences in sapling species richness ($p=0.022$) and herbaceous species richness ($p<0.001$) among well types (Table 2). In both strata, ponded wells had the lowest species richness, and the upland forested plots (C) had the highest species richness.

Shannon-Wiener diversity of herbaceous species differed both among well type ($p<0.001$) and transect ($p=0.007$) (Table 3). Ponded wells had the lowest diversity, compared to the other three well types. Diversity was highest in transect 1 and lowest in transect 4, though transects 2 and 3 did not differ from transects 1 or 4. There were no differences in diversity in any of the other vegetation strata. There were no differences in evenness in any of the vegetation strata (Table 4).

Vegetation Transitions

Well-to-well transects were sampled in March and September 2014 to provide a cursory picture of the change in vegetation across the wetland to non-wetland gradient (Table 5). It is early to draw any major conclusions, but it appears as though areas that were already wet and became wetter are transitioning more rapidly than upland areas that are experiencing higher water levels. For example, areas with solely emergent vegetation in March, such as the transect from 1P to 1A, now have a mixture of emergent and floating vegetation. The first two sampling points in the transect from 3P to 3A have transitioned from a community of entirely emergent vegetation in March to a community of entirely floating vegetation in September. It is unclear at this point if or when the originally more upland communities (e.g. B and C locations) will begin to support more wetland plant species. However, it is clear that these transects will provide a very interesting picture of the changing vegetation community over time.

Table 1. Dominance test for 2014 vegetation plots.

Well transect (1-4)	Well ID (P, A, B, C) *	Corrected well ID (P, A, B, C) †	# Dominant species ≠	# Dominant wetland species (FAC + FACW + OBL)	# Dominant FAC species	% Dominants = wetland species	% Wetland species = FAC	Hydrophytic vegetation?
1	P	P	4	4	0	100.0	0.0	Yes
1	A	A	7	6	3	85.7	50.0	Yes
1	B	B	8	5	3	62.5	60.0	Maybe
1	C	C	11	8	4	72.7	50.0	Yes
2	A	P	7	7	5	100.0	71.4	Yes
2	B	A	9	4	3	44.4	75.0	No
2	C	B	8	5	2	62.5	40.0	Yes
3	P	P	4	4	0	100.0	0.0	Yes
3	A	A	9	7	4	77.8	57.1	Yes
3	B	B	10	6	5	60.0	83.3	Maybe
3	C	C	12	7	7	58.3	100.0	Maybe
4	P	P	6	6	1	100.0	16.7	Yes
4	A	A	9	9	5	100.0	55.6	Yes
4	B	B	8	5	4	62.5	80.0	Maybe
4	C	C	8	5	5	62.5	100.0	Maybe

*Wells labeled as “P” are distinctly in ponded areas, wells labeled as “A” are in a transition zone from pond to forest, wells labeled as “B” are approximately in a transition zone from wet forest to relatively upland forest, and wells labeled as “C” were considered upland.

†Designations were assigned prior to flooding, and well IDs for transect 2 have been adjusted to match our definitions for the purpose of statistical analysis.

≠ Based on 50/20 dominance test (USACE 2010).

Table 2. Species richness in the five strata of 2014 vegetation.

Well transect (1-4)	Corrected well ID (P, A, B, C) *†	Trees		Saplings		Shrubs		Vines		Herbaceous	
		Mean plot richness (n=4)	Standard deviation	Mean plot richness (n=4)	Standard deviation	Mean plot richness (n=4)	Standard deviation	Mean plot richness (n=4)	Standard deviation	Mean plot richness (n=16)	Standard deviation
	P	2.0	2.8	0.8 B	1.5	4.5	1.7	0.0	0.0	2.6 B	1.8
	A	4.3	2.6	3.0 AB	1.4	7.5	2.1	0.5	1.0	8.3 A	3.4
	B	5.8	1.5	4.3 A	1.7	5.0	1.4	1.0	1.2	6.2 A	2.8
	C	5.3	4.0	4.7 A	1.5	6.0	3.0	1.0	1.7	6.8 A	2.9
1		3.3	2.9	3.0	2.6	6.3	2.2	0.0	0.0	7.1	3.2
2		7.0	1.0	4.7	1.5	6.0	1.0	0.0	0.0	4.6	3.6
3		4.0	4.3	3.3	2.4	5.3	2.5	1.0	1.2	5.9	3.8
4		3.5	1.3	1.8	1.3	5.5	3.1	1.3	1.5	5.8	3.1

*Wells labeled as “P” are distinctly in ponded areas, wells labeled as “A” are in a transition zone from pond to forest, wells labeled as “B” are approximately in a transition zone from wet forest to relatively upland forest, and wells labeled as “C” were considered upland.

†Designations were assigned prior to flooding, and well IDs for transect 2 have been adjusted to match our definitions for the purpose of statistical analysis.

Table 3. Shannon-Wiener diversity in the five strata of 2014 vegetation.

Well transect (1-4)	Corrected well ID (P, A, B, C) *†	Trees		Saplings		Shrubs		Vines		Herbaceous	
		Mean Shannon- Wiener Diversity (H') (n=4)	Standard deviation	Mean Shannon- Wiener Diversity (H') (n=4)	Standard deviation	Mean Shannon- Wiener Diversity (H') (n=4)	Standard deviation	Mean Shannon- Wiener Diversity (H') (n=4)	Standard deviation	Mean Shannon- Wiener Diversity (H') (n=16)	Standard deviation
	P	0.29	0.59	0.17	0.35	0.95	0.64	0.00	0.00	0.62 B	0.49
	A	0.62	0.64	0.41	0.49	1.22	0.46	0.00	0.00	1.58 A	0.41
	B	1.07	0.17	0.91	0.66	1.06	0.30	0.00	0.00	1.23 A	0.54
	C	1.07	0.72	1.20	0.44	1.09	0.58	0.22	0.39	1.44 A	0.41
1		0.55	0.58	0.59	0.74	1.13	0.35	0.00	0.00	1.49 A	0.46
2		1.15	0.26	1.05	0.39	1.25	0.34	0.00	0.00	1.01 AB	0.69
3		0.73	0.92	0.83	0.65	0.89	0.62	0.00	0.00	1.28 AB	0.66
4		0.64	0.46	0.17	0.35	1.09	0.56	0.17	0.34	0.97 B	0.46

*Wells labeled as “P” are distinctly in ponded areas, wells labeled as “A” are in a transition zone from pond to forest, wells labeled as “B” are approximately in a transition zone from wet forest to relatively upland forest, and wells labeled as “C” were considered upland.

†Designations were assigned prior to flooding, and well IDs for transect 2 have been adjusted to match our definitions for the purpose of statistical analysis.

Table 4. Species evenness in the five strata of 2014 vegetation.

Well transect (1-4)	Corrected well ID (P, A, B, C) *†	Trees		Saplings		Shrubs		Vines		Herbaceous	
		Mean Plot Evenness (E) (n=4)	Standard deviation	Mean Plot Evenness (E) (n=4)	Standard deviation	Mean Plot Evenness (E) (n=4)	Standard deviation	Mean Plot Evenness (E) (n=4)	Standard deviation	Mean Plot Evenness (E) (n=16)	Standard deviation
	P	0.16	0.33	0.16	0.32	0.57	0.38	0.00	0.00	0.56	0.39
	A	0.37	0.34	0.30	0.34	0.60	0.15	0.00	0.00	0.77	0.10
	B	0.63	0.12	0.56	0.39	0.66	0.08	0.00	0.00	0.71	0.23
	C	0.67	0.14	0.78	0.13	0.61	0.17	0.20	0.35	0.82	0.19
1		0.37	0.33	0.37	0.43	0.63	0.15	0.00	0.00	0.81	0.13
2		0.59	0.12	0.69	0.12	0.69	0.14	0.00	0.00	0.64	0.35
3		0.39	0.45	0.56	0.40	0.49	0.33	0.00	0.00	0.78	0.32
4		0.46	0.31	0.16	0.32	0.65	0.16	0.15	0.31	0.60	0.21

*Wells labeled as “P” are distinctly in ponded areas, wells labeled as “A” are in a transition zone from pond to forest, wells labeled as “B” are approximately in a transition zone from wet forest to relatively upland forest, and wells labeled as “C” were considered upland.

†Designations were assigned prior to flooding, and well IDs for transect 2 have been adjusted to match our definitions for the purpose of statistical analysis

Table 5. Summary of well to well transects sampled in March and September 2014.

			March 2014		September 2014	
Starting well	Ending well	Distance from starting well (m)	Dominant veg (Algae, submersed, floating, emergent, wet area plants, upland) or no vegetation present	Water depth (m)	Dominant veg (Algae, submersed, floating, emergent, wet area plants, upland) or no vegetation present	Water depth (m)
1P	1A	5	Emergent	1	Emergent/floating	0.75
1P	1A	10	Emergent	1	Emergent/floating	0.75
1P	1A	15	Emergent	0.5	Emergent/floating	0.25
1A	1B	5	Wet area	0.5	Wet area	0.1
1A	1B	10	No vegetation present/visible	0.5	Wet area	<0.01
1A	1B	15	No vegetation present/visible	0.25	Wet area	<0.01
1A	1B	20	Upland	0.25	Wet area	0
1A	1B	25	Upland	0.1	Wet area	0
1A	1B	30	Upland	0.1	Wet area	0
2A	2B	5	No vegetation present/visible	1	No vegetation present/visible	0.75
2A	2B	10	No vegetation present/visible	1	No vegetation present/visible	0.75
2A	2B	15	No vegetation present/visible	0.75	No vegetation present/visible	0.5
2A	2B	20	No vegetation present/visible	0.75	No vegetation present/visible	0.5
2A	2B	25	No vegetation present/visible	0.5	Emergent	0.25
2A	2B	30	Emergent	0.5	Emergent/floating	0.25
2A	2B	35	Wet area	0.25	Wet area	0.1
2A	2B	40	Upland	0.1	Upland	<0.01
2A	2B	45	Upland	0.1	Upland	<0.01
2B	2C	5	No vegetation present/visible	0.1	No vegetation present/visible	<0.01
2B	2C	10	Upland	<0.01	Upland	0
2B	2C	15	Upland	<0.01	Upland	0
2B	2C	20	Upland	<0.01	Upland	0
2B	2C	25	Upland	<0.01	Upland	0
2B	2C	30	Upland	<0.01	Upland	0
2B	2C	35	Upland	<0.01	Upland	0
2B	2C	40	Upland	<0.01	Upland	0
2B	2C	45	Upland	<0.01	Upland	0
2B	2C	50	Upland	0	Upland	0
2B	2C	55	Upland	<0.01	Upland	0
3P	3A	5	Emergent	0.5	Floating	0.4
3P	3A	10	Emergent	1	Floating	0.75
3P	3A	15	Emergent	0.5	Emergent/floating	0.4
3P	3A	20	Emergent	0.3	Emergent/floating	0.25
3A	3B	5	Upland	0.15	Upland	0.01
3A	3B	10	Upland	<0.01	Wet area	0
3A	3B	15	Upland	0	Wet area	0
3A	3B	20	Upland	0	Wet area	0
4P	4A	5	Emergent	0	Emergent	0.5
4P	4A	10	Emergent	0.5	Emergent	0.25
4P	4A	15	Boardwalk		Boardwalk	
4P	4A	20	Emergent	0.5	Emergent	0.1
4P	4A	25	Wet area	0.25	Emergent	0.01
4A	4B	5	Wet area/upland	0.1	Wet area/upland	<0.01
4A	4B	10	Upland	<0.01	Upland	0
4A	4B	15	Upland	<0.01	Upland	0
4A	4B	20	Upland	<0.01	Upland	0
4A	4B	25	No vegetation present/visible	0.01	Upland	0
4A	4B	30	Upland	0	Upland	0
4A	4B	35	Upland	0.01	Upland	0
4A	4B	40	Upland	0.01	Upland	0
4A	4B	45	Upland	0	Upland	0
4A	4B	50	Upland	0	Upland	0
4A	4B	55	Upland	0	Upland	0
4A	4B	60	Upland	<0.01	Upland	0

Summary of Vegetation Findings to Date

Lower species richness and diversity at the ponded wells seem to be driven by a more limited plant community that can establish and maintain in higher water levels, as well as locally novel environmental conditions that the plant community has not yet responded to. For example, the ponded well in transect 2 (well A, renamed well P for statistical analyses) has an abundance of dead non-aquatic species and only now (after 2014 vegetation surveys) are some aquatic species such as floating pennywort (*Hydrocotyle ranunculoides*) establishing. The low herbaceous diversity observed in transect 4 was driven by an abundance of the non-native invasive, *Microstegium vimineum*, that represented over 90% of herbaceous cover in several plots. It is unlikely that the plant community will change much in this transect where *M. vimineum* has taken over. We will continue to quantify these plant communities and will soon begin our multivariate analyses to quantify whole community responses to changing water levels.

The well-to-well transects have begun to paint a picture of the changing plant community. Sampling points that were already established with hydrophytic vegetation are transitioning to vegetation tolerant to wetter conditions. It is expected that this change will become more pronounced over time, but it is unclear how the original (pre-2013) transitional upland communities will change in response to a higher water levels. We will continue to record our observations of these well to well transects at least annually to monitor changes in the plant community.

Groundwater Evaluation and Monitoring

Introduction

Huntley Meadows Park sits in Hybla Valley. This valley contains many interbedded mud (silt+clay) and sand sheets because of its long and complex history of deposition and erosion. The results of this history govern the present-day movement of groundwater into and under the Huntley Meadows central wetlands. The pattern of aquifers and confining beds and the spatial distribution of recharge/infiltration zones will control seasonal variations in water available to the wetland. Much of the field work, well construction, and hydrologic analyses done to date was necessary to understand these patterns in, around, and under the wetland. The outcome of this hydrogeologic analysis will guide the construction of the Wetbud Advanced Model.

The geologic history of the Potomac River basin controls the hydrostratigraphy in Hybla Valley; prior studies in the valley provided important clues about the characteristics, extent and thicknesses of the aquifers there. As much as 1.6 miles (2.5 km) wide, this broad curved valley marks one of the paths of the ancestral Potomac River. During one of the low-stands of the ocean caused by growth of Pleistocene ice sheets, the river cut a deep valley into the Cretaceous sediments that are hundreds of feet thick in this part of the Coastal Plain. Coarse Cretaceous sediments and mud beds underlie the highlands north and west of the valley as well as the somewhat higher ground lying to the southeast (Mixon et al., 1989). After the valley was carved, each time the ice sheets melted and made the sea levels rise, the valley was filled by an estuary and collected sediments washed in by streams or carried in by the tides (Litwin et al, 2010). Following each of those high-stands of the sea during warmer times, ocean levels dropped more than once due to the re-growth of continental glaciers in Canada and Antarctica. During those low-stands, the Potomac River carved a different route, leaving the stream sediments just deposited in Hybla Valley to be gullied by smaller streams tributary to the Potomac. After the formation of steep-sided deep gullies, as sea levels rose again, fine-grained estuarine sediments carpeted the valley floor and filled most of the gullies (Milan Pavich, USGS, unpublished data; Pavich et al., 2010). Since that high-stand, the ocean levels dropped again and then subsequently rose to their present elevation.

Analyses of soil maps and of drill hole data from several sources - test borings made prior to the wetland reconstruction; USGS studies of the valley stratigraphy (e.g. Litwin et al, 2010); construction of wells by VT and ODU personnel; examination of soil profiles made with hand augers - confirm the general pattern of aquifers and confining beds reported by prior studies. This interpretation of the hydrostratigraphy guided the selection of the deep well locations (VTHD1, VTHD2, VTHD3, ODU HM1). According to that interpretation, around most of the margins of the valley, at the base of the steep hillsides, lie somewhat sandy soils and surficial deposits that are relatively permeable. These would be stream deposits washed into the valley and deposited as fans that may extend far into valley, perhaps completely under the wetland at the center of the valley. During a Pleistocene low-stand of the sea, these deposits were deeply

gullied; those gullies subsequently were refilled with mud beds that have a low permeability. These thick “clays” underlie much of the valley floor, including the lowlands containing the large central wetland in the park. Sands that underlie the thick clay beds are thought to connect hydrologically to recharge (infiltration) zones formed on the sandy surficial deposits and soils around the margins of the valley. The four deep groundwater monitoring wells were placed at locations and depths in an attempt to measure water level fluctuations both in recharge zones (VTHD1, VTHD3) and in the confined aquifers below the “clay beds” under the Huntley Meadows wetlands (VTHD2, ODU HM1).

Well Construction

ODU and VT constructed and outfitted six wells, five of which presently produce water level data. Two wells were drilled by truck-mounted auger to approximately 17 ft (5.4 m; VTHD1), 42 ft (13.4 m; VTHD2), and to 39.5 ft (12.0 m; ODU HM1). Three of these were drilled by hand auger to depths of 12 ft (3.8 m) (VTHD3) and 10 ft (3.1 m) (ODU_ET1 and ODU_ET2). Construction details are shown in the well completion reports in Appendix 1. The four deeper wells were constructed to better understand the more regional groundwater flow setting; the two shallow wells were constructed to better evaluate the differences in evapotranspiration (ET) rates via the White (1932) method vs. other estimation methods and discussed in more detail later.

Data Collection and Maintenance

Well	Data Collection			
VTHD3	12/16/13	5/30/14	8/19/14	10/24/14
VTHD2	12/17/13	5/30/14	8/20/14	11/7/14
VTHD1	12/16/13	5/30/14	8/20/14	11/7/14
ODU_ET2				10/24/14
ODU_ET1				10/24/14

All of the wells are being maintained in the same manner. Approximately four times per year water level and temperature data are collected from the Solinsttm Leveloggers in the wells. When data are downloaded a manual measurement of depth to water is also taken to ensure the transducers have maintained accuracy, the wells and equipment are inspected, and any damaged components are repaired or replaced. Once the data are collected it is compensated for barometric pressure via Solinst Levelogger software using pressure readings from a transducer suspended in the casing of the VTHD2 well. A final step will be for WSS to survey the elevation of the top of the well casings in the late winter or early spring of 2015.

Interpretations

The following are interpretations and graphs of water levels from the data collected up through 11/7/2014. Precipitation data on the graphs is from the Washington Reagan National weather station GHCND:USW00013743).

VTHD1 and VTHD3 (screened intervals 6.8-17.3 ft (2.07-5.24 m) and 6.6-12.2 ft (2.01-3.72 m), respectively).

The two hydrographs (Figures 11 and 12) show responses to precipitation at the same times, although the magnitude of the response is greater in VTHD3 (Figure 12). The more muted response in the deeper well could be due to a combination of the greater depth of the screens at VTHD1 and a higher specific yield of the soils around VTHD1. Slug tests have been performed at both well locations and the results from the slug tests will be used to test this hypothesis. The water table is highest in both wells from mid-December to late-May. This period of higher water levels is likely due to the effect of the vegetation going dormant during this time. VTHD1 and VTHD3 are likely in the same unconfined aquifer.

VTHD2 (screened interval 32.0-42.0 ft (9.75-12.80 m))

The water level in VTHD2 (Figure 13) rises slowly in response to seasonal recharge from mid-December to mid-May with muted responses to individual rain events, especially when compared to both VTHD1 and VTHD3. The muted signal indicates that the dense clay seen at the base of VTHD1 and VTHD3 forms a broad aquitard across much Hybla Valley. The recharge replenishing the aquifer below may have to travel hundreds of meters from infiltration areas around the edges of the valley bottom.

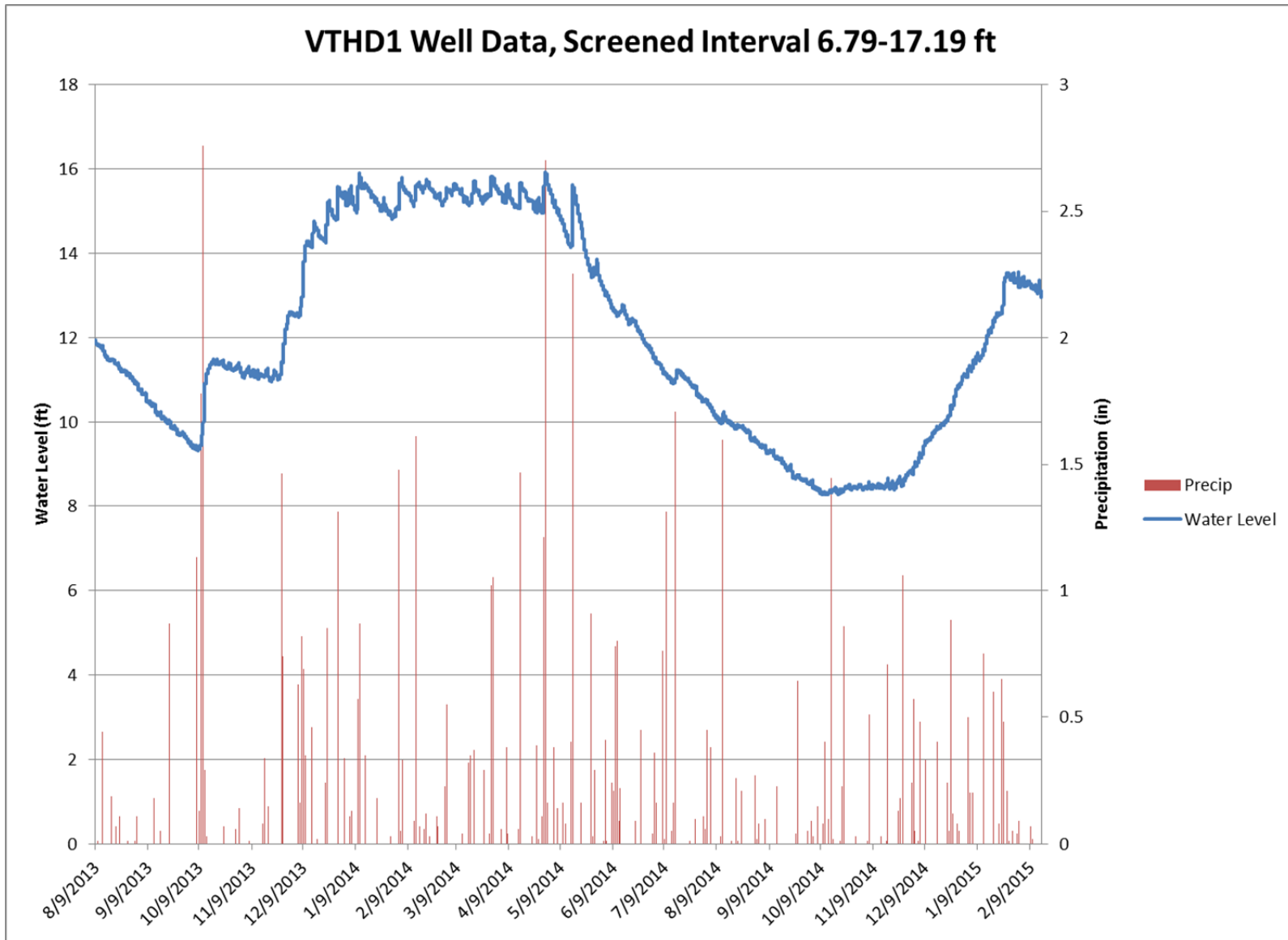


Figure 11. Water levels and associated precipitation for Well VTHD1.

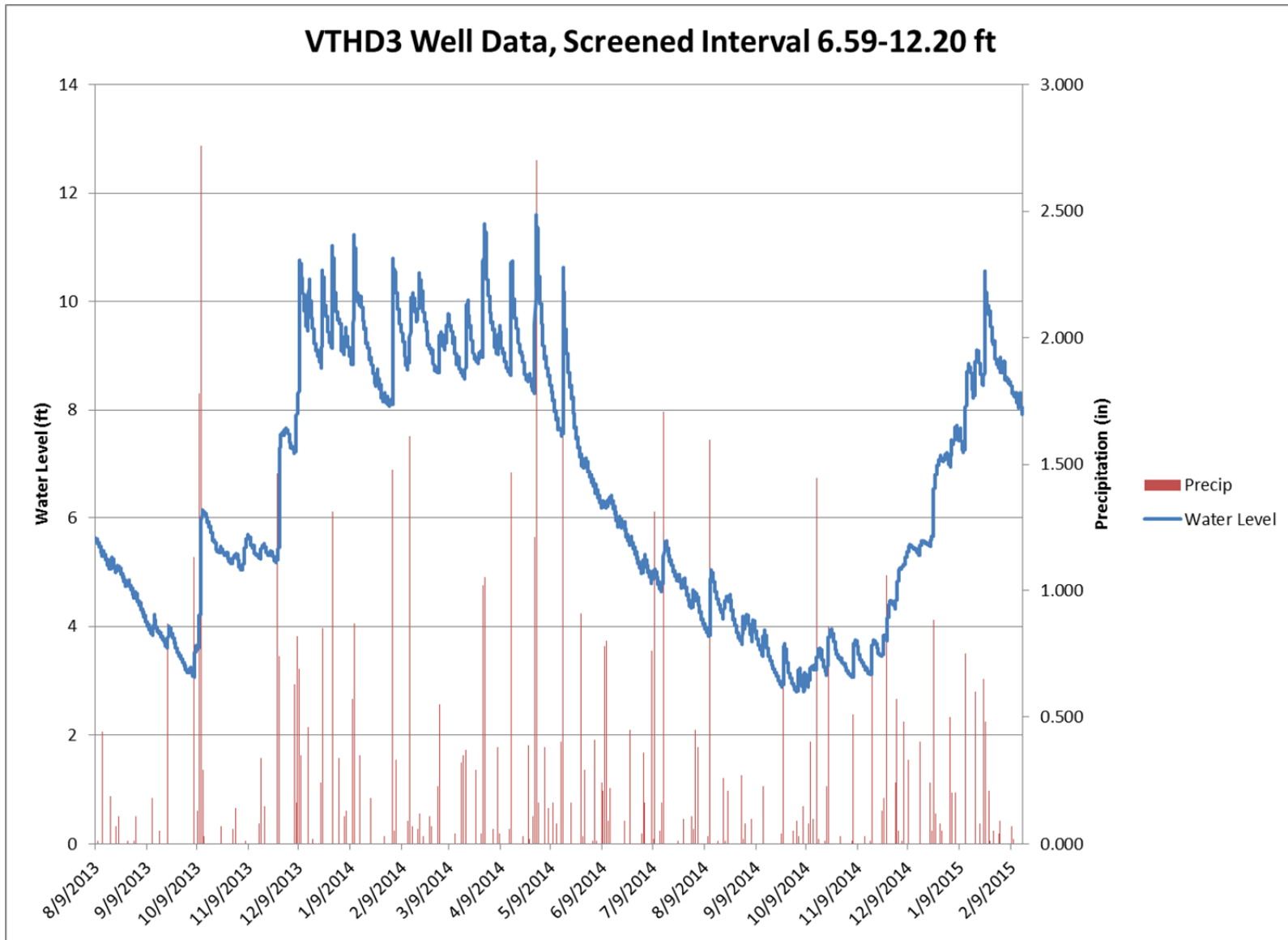


Figure 12. Water level data and associated precipitation for well VTHD3.

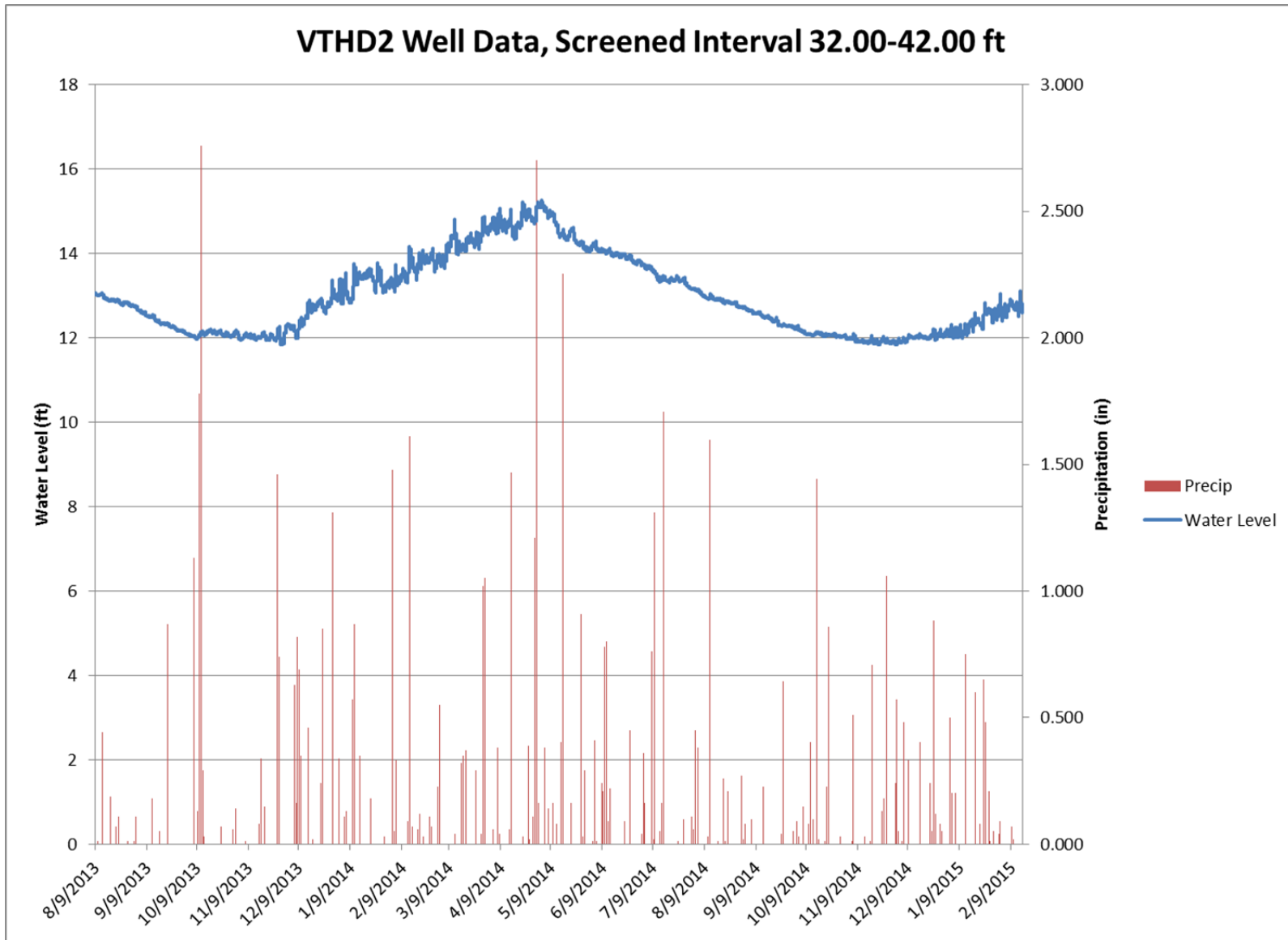


Figure 13. Water levels and associated precipitation for well VTHD2.

ODU_ET1 and ODU_ET2 (screened intervals 2.0-10.0 ft (0.61-3.04 m) and 1.0-10.0 ft (0.30-3.04 m), respectively).

These two shallow wells were emplaced into the surface aquifer connected to the wetland at Huntley Meadows Park. Unlike the other wells ODU maintains, these wells have long screens in order to monitor the diurnal flux due to evapotranspiration (ET). White (1932) noted that water levels fluctuated daily in monitoring wells near a river in Escalante Valley, Utah and developed a method of determining the rate of loss due to ET using that fluctuation. He deduced that transpiration by vegetation and evaporation from soil caused by the heat of the day withdraws water from the riparian zone; this loss stops at night (e.g. midnight to 04:00) when there is no solar energy or residual heat to drive the process. If there is a steady seepage of groundwater to the site, the water table recovers during the evening. Comparison of the long-term decline of the water table over several days and the short-term recovery during each evening permits calculation of an ET estimate. This method provides a low-impact, cost-effective means for direct measurement of actual ET rates within the watershed. The intent is to compare estimates using the White (1932) method with those calculated by the Penman-Monteith equation, the Thornthwaite equation, and also the Bowen's Ratio instrument array, all discussed below.

The well ODU_ET2 is in an area mapped by the National Wetlands Inventory (NWI) as forested/shrub wetlands. The well ODU_ET1 is in a non-wetland forested "upland" setting similar to that surrounding Huntley Meadows Park. These two settings provide representative samples for two local vegetative communities and will be used to parameterize the variation in the effects of ET across the watershed spatially and temporally. These data may be used later in an Advanced Model scenario within Wetbud.

Data collection at ODU_ET1 and ODU_ET2 (Figures 14 and 15) began August 22nd of 2014 so significant comparisons to the other wells at Huntley Meadows are not yet possible. The hydrographs from both wells show the water levels slowly decreasing from late August to late October which agrees with the other wells in the park. The spring and summer of 2015 should provide the most interesting data from these wells as this will be the time evapotranspiration will affect these locations the greatest. The pressure transducer in ODU_ET2 (5 mm resolution) has been replaced with a more accurate unit (2.5 mm resolution) in order to better constrain the effect of evapotranspiration in the freshwater forested and shrub wetlands within Huntley

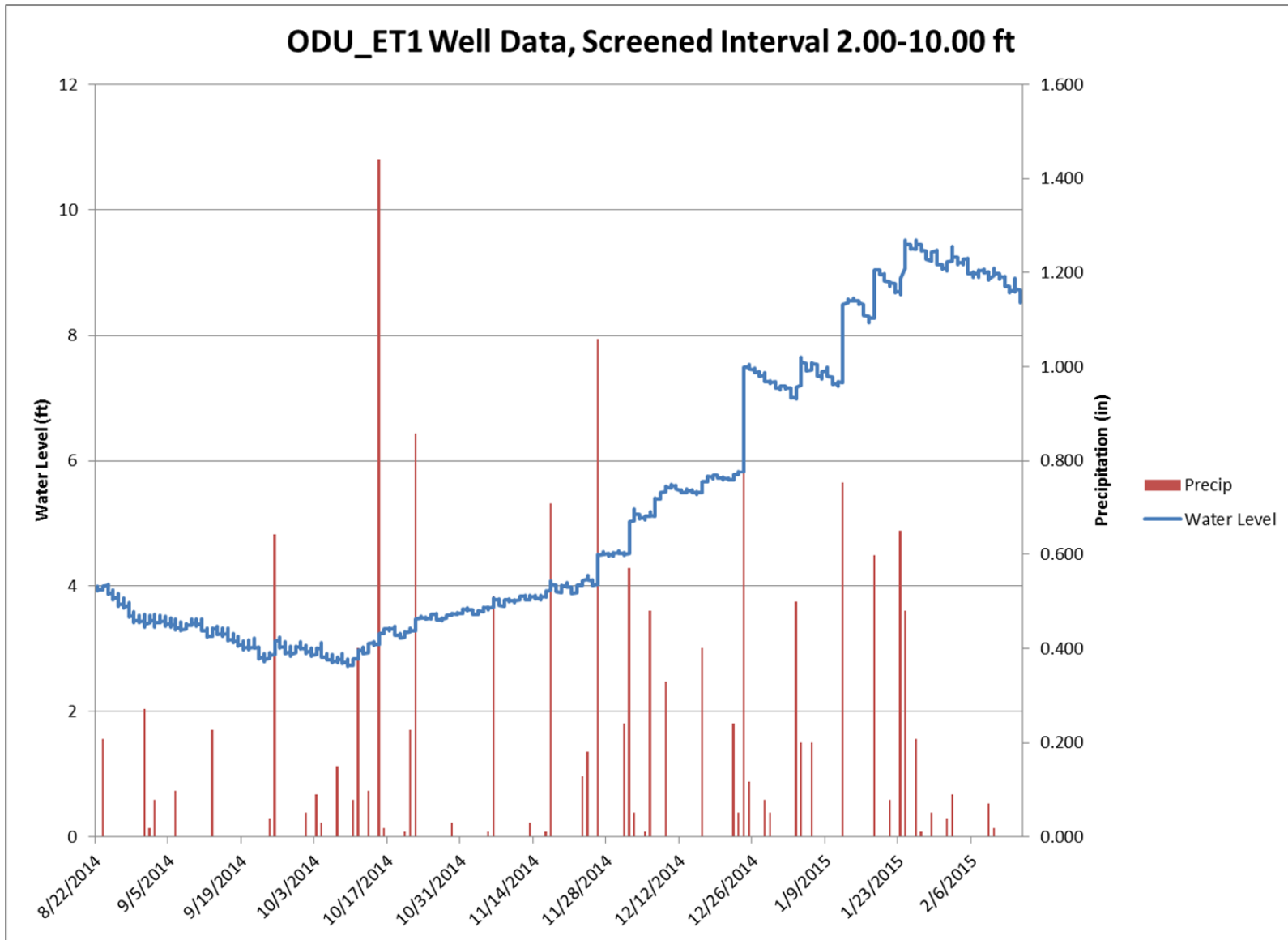


Figure 14. Water level and associated precipitation data for well ODU ET1.

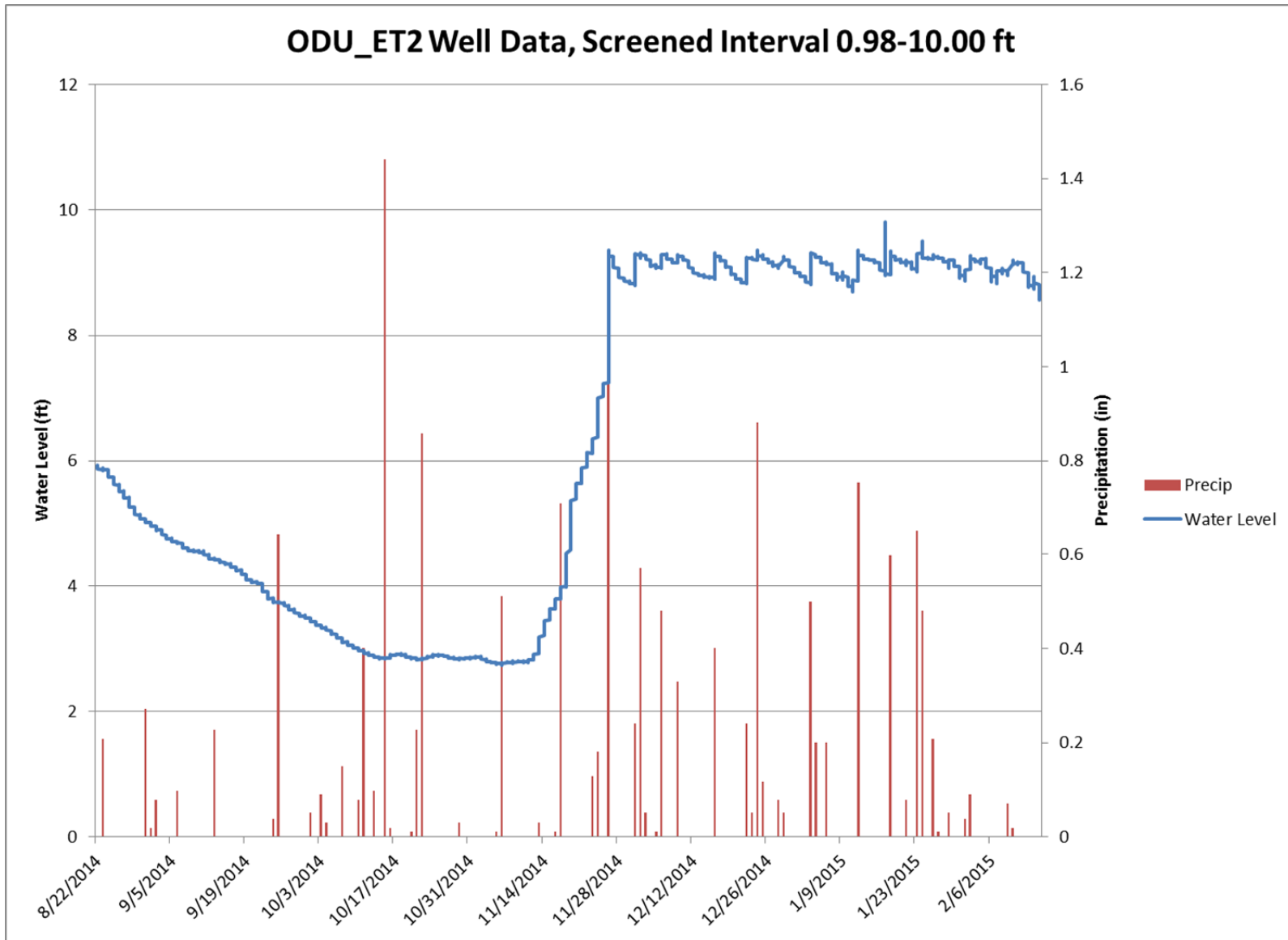


Figure 15. Water level and associated precipitation data for well ODU ET2.

Surface Water Monitoring

As part of the overall water budget and to provide data for testing the Wetbud model, monitoring of surface water inflows to and outflows from the Huntley Meadows wetland was necessary.

Progress to Date

The overall wetland watershed was delineated and the main tributary inflows were identified: the primary area contributing surface flows to the wetland is the suburban neighborhood north of the park (Figure 3). Given the dense forest cover in the rest of the watershed and the lack of significant perennial channels, it was assumed that surface runoff from the remainder of the watershed was minor compared to the urban inputs. Surface runoff from the neighborhood is directed into a stormwater collection system consisting of dry detention ponds and concrete-lined trapezoidal channels (Figure 16). These channels discharge into unlined channels at the northern edge of the park. While the ideal monitoring point for surface water inflows is just upstream of the wetland, a site visit showed there were no monitoring locations within the park that would provide reliable stage-discharge relationships. The forested area in the northern part of the park contains multiple channels with extensive woody debris. Field evidence indicated these streams routinely flow out-of-bank at high flows, making discharge measurements difficult and any stage-discharge relationship inaccurate at high flows (Figure 17).

Hobo U20-001-04 pressure transducers (0-13 ft. range; ± 0.02 ft.) were installed March 10-11, 2014 in three of the tributary channels where the channel was relatively uniform and where a reliable stage-discharge relationship could be developed. The sensors were placed inside a slotted PVC pipe to minimize vandalism and damage from debris (Fig. 18). Data from the unvented pressure transducers are corrected using barometric pressure data from a fourth pressure transducer near the water control structure that is not submerged. It should be noted that the SE tributary was diverted in the past and no longer discharges to the Huntley Meadows wetland. Nonetheless, this watershed is being monitored because it has similar landuse, geology, and slope as the contributing watersheds and provided an accessible monitoring location. Data from this watershed will be combined with information from the other two watersheds to determine runoff rates per acre, which will be used to estimate runoff from the ungaged catchments.



Figure 16. Central inflow channel (SC) to Huntley Meadows Park.



Figure 17. Inflow channel conditions within forested area north of the central wetland. Given the channel irregularities and frequent out-of-bank flows, this area was not suitable for discharge monitoring.



Figure 18. Installation of pressure transducers at monitoring location SC.

Because the urban tributaries are relatively uniform, flows will be estimated using Manning's equation:

$$q = \frac{1.49}{n} R^{2/3} S^{1/2} \quad (1)$$

where q is the stream discharge in cfs, n is the Manning's roughness coefficient, R is the hydraulic radius, A/P , where A is the cross sectional flow area (ft.^2) and P is the wetted perimeter (ft.), and S is the channel slope (ft./ft.). Channel geometries were determined by surveying the channels with a laser level. Manning's n values were estimated as 0.018, 0.018 (summer) and 0.015 (winter), and 0.05 (below bankfull), for the SW, SC, and SE monitoring points, respectively. These roughness values will be verified by measuring stream discharge at each point at multiple discharges.

Outflows from the Huntley Meadows wetland are controlled by a sheet pile water control structure and an outlet structure. The outlet structure consists of four Clemson beaver pond levelers and two sets of two slide gates (Figure 19). After passing over the second set of slide gates, water discharges to the downstream channel via a concrete box culvert. If the depth of water upstream and downstream of the slide gates, as well as the slide gate location, are known, then flows over the gates can be calculated. To monitor water levels within the water control structure, two Campbell Scientific (CSI) CS451-L30 vented pressure transducers (0.1% accuracy) were installed. One pressure transducer was installed upstream of the second set of slide gates on January 17, 2014 and the second pressure transducer was installed downstream of the slide gates on November 12, 2014. To continuously monitor the location of the second set of slide gates, two Honeywell S&C AQLT shaftless waterproof linear position transducers were installed in July and August 2014. Due to sensor malfunction, only one of the position transducers is currently installed. It is anticipated that a replacement position transducer will be delivered and installed in March 2015. Water levels, gate elevations, and water temperature data are stored by a CSI CR1000 data logger and then transmitted to the main control panel at the project weather station using a 900 MHz spread spectrum radio and a 900 MHz 9 dBd Yagi antenna. A 12 V sealed battery and 10W solar panel are used to power the data logger and sensors.

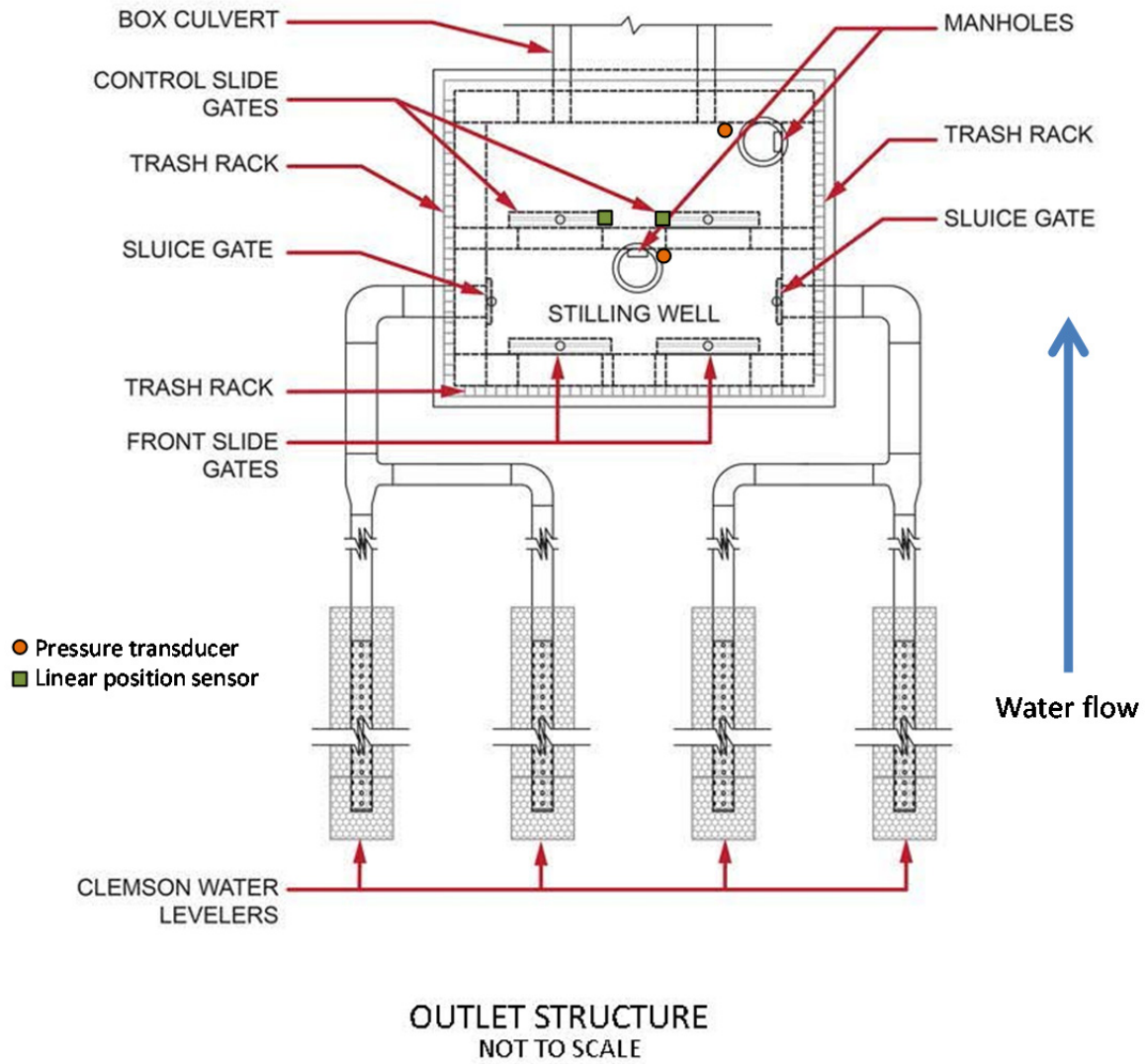


Figure 19. Plan view of Huntley Meadows pond outlet control structure (schematic courtesy of WSSI).

In addition to monitoring water levels, water temperature, and gate positions at the outlet structure, water levels are also being monitored in Habitat Pool “D” at the water control structure using a CSI SR50A-L175 Sonic Ranging Sensor. Because the sonic sensor measures the distance to an object, it can continue to monitor the pond even when dry. Air temperature corrections for the sonic sensor are measured using a CSI 109-L175 temperature probe. Data from the sonic water level sensor are stored in a CSI CR206X data logger adjacent to the habitat pond and then transmitted to the project weather station using a 900 MHz spread spectrum radio and a Yagi antenna. The data logger is powered by a 12-V sealed battery and a solar panel.

Results to Date

Stage data from the three monitored streams are downloaded monthly, pressure corrected, and stored in the project SQL database. Figure 20 shows hourly precipitation totals and estimated stream discharge during a high intensity storm event in August 2014. Baseflow in each of the three tributaries is consistently low (< 1 cfs). However, during storm events, there is a rapid increase in stream stage, as would be expected in urbanized watersheds. The storm event on August 12, 2014 totaled 2.34 in., with a maximum 30-min. intensity of 2.1 in./hr. A total of 4.2, 5.4, and 6.6 acre-ft. of runoff from the SW, SC, and SE watersheds, respectively, were recorded for the 60-hr period shown in Figure 20. This runoff volume corresponds to an average of 0.59 in./acre for the urban area north of the park, or a 0.57-ft. increase in water depth in the wetland, which is reflected in the increase in the pool water level shown (later) in Figure 23.

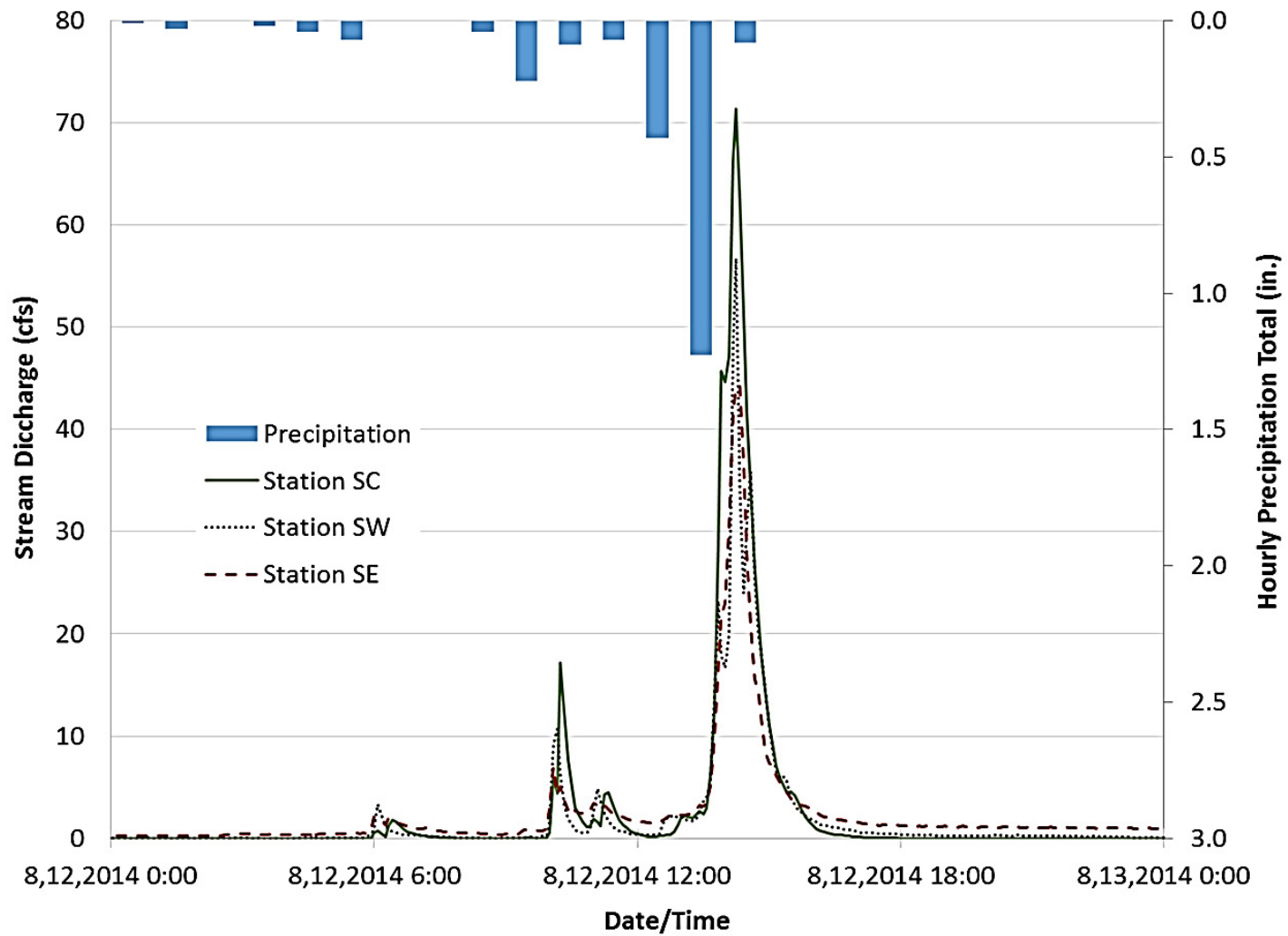


Figure 20. Hourly precipitation totals and stream discharge estimates for the three monitored tributaries north of Huntley Meadows Park.

Weather Station and ET Estimators

Objectives

Multiple studies have shown that evapotranspiration can account for up to 40% of the water loss in certain wetlands (Arnold et al., 2001; Bradley, 2002) and may account for a much higher proportion in isolated wetlands with limited surface water and groundwater interactions. The overall goal of installing the Bowen Ratio Energy Balance System (BREBS; a.k.a. the weather station) is to provide accurate measurements of evapotranspiration (ET) rates, as well as weather data needed to estimate reference crop ET using the Penman-Monteith equation. Comparisons will also be made to the standard Thornthwaite method. By measuring the actual ET (AET) and calculating the reference crop ET, crop coefficients for the wetland vegetation communities at Huntley Meadows can be determined. These data will enable park managers to better understand the overall water balance in the Huntley Meadows wetland, will be used to test the Wetbud model, and will improve wetland ET predictions in the mid-Atlantic region.

ET is a complex process dependent on several weather factors, such as temperature, solar radiation, humidity, and wind speed in addition to crop type and growth stage. To avoid the development of separate ET equations for an array of different crops, the concept of reference crop evapotranspiration (ET_0) was introduced (Trajkovic and Kolakovic, 2009). Historically, grass and alfalfa were used as reference crops, but since these crops do not grow throughout the world, the United Nations Food and Agriculture Organization (UN-FAO) redefined a reference crop as a dense, low growing green crop. Following Allen et al. (1998), ET_0 is defined as the ET of a hypothetical 0.39 ft. high crop that provides full ground coverage, and has no shortage of water, a canopy resistance of 21 s/ft., and an albedo of 0.23. The older literature (e.g. Thornthwaite; Penman) often refers to similar estimates of the hypothetical maximum rate of ET as *potential ET* (PET), but this is not necessarily tied to a specific crop canopy condition in the same manner as ET_0 (although the Thornthwaite method was developed for a well-watered grass).

While a reference crop ET estimation provides an initial ET value for use in the wetland water budget, wetland vegetation may not transpire at the same rate as the reference crop. The relationship between the reference crop ET (ET_0) and the actual evapotranspiration can be determined by crop coefficients, K_c . The K_c represents an integration of effects of crop height, crop-soil resistance, and surface albedo that affect the difference between the actual crop and the ET_0 reference crop. If the crop coefficient for a given location is known, the crop ET can be calculated as follows:

$$ET = K_c * ET_0 \quad (2)$$

Crop coefficients are readily available for most agricultural crops to convert reference crop evapotranspiration to actual evapotranspiration. However, few crop coefficients exist for wetland systems. The following sections describe methods for measuring and estimating wetland vegetation ET.

Direct Measurement of Evapotranspiration

Directly quantifying ET requires measurement of the loss of liquid water from the surface, or the gain of water vapor by the atmosphere, through either a mass and/or an energy balance.

Generally, energy balance approaches assume the atmosphere is an open system and describe evapotranspiration as the water vapor flow, or latent heat, through the land-atmosphere interface into an open system. Conversely, a closed system can be assumed and measurements of inputs and outputs of the liquid phase can be measured, with evapotranspiration calculated as the net loss of water from the system (Maidment, 1992). The techniques summarized below provide insight into how mass and energy balance techniques have been implemented, as well as background theory of how they were formulated.

Developing a basin water balance is the process in which water fluxes (AET, precipitation, groundwater recharge, surface and subsurface runoff) and storage changes (soil-water storage changes, groundwater changes, and reservoir changes) are balanced within a given watershed. Basin water balances can be lumped by considering the whole basin or distributed by calculating the water balance in finite sub-units of the basin (Allen et al. 2011; Senay et al., 2011). Under normal conditions, evapotranspiration can be solved for by the following equation:

$$P - ET - Q - \Delta S = E_{rr} \quad (3)$$

where P is precipitation, ET is actual ET, Q is basin discharge, ΔS is change in water storage, and E_{rr} is the discrepancy in the water balance. Theoretically, this discrepancy should be negligible when all of the components of the water balance are measured accurately.

Furthermore, the ΔS term can be expressed as a series of components such that

$$\Delta S = \Delta S_m + \Delta G_w + \Delta S_n + \Delta R_s \quad (4)$$

where ΔS_m = changes in soil water, ΔG_w = groundwater loss/recharge, ΔS_n = changes in snow pack or ice, and ΔR_s is changes in rivers, lakes, and reservoirs. The ΔS term can be considered negligible in some instances when annual water balances are calculated for multiple years. (Viessman, Jr and Lewis, 1996; Senay et al. 2011). Under this assumption, ET on the watershed scale can be taken as follows:

$$P - Q - ET = 0 \quad (5)$$

By knowing P and Q, ET can be estimated.

A similar approach to the water balance method for calculating ET is the use of weighing lysimeters. These devices have been used extensively to provide information on evapotranspiration from agricultural crops (Allen et al., 1991). Weighing lysimeters allow precise determination of the soil water balance, including the ET and flux of water below the root zone to the groundwater table (Feltrin et al., 2011; Schrader et al., 2013). The main body of the device comprises an inner chamber enclosing the unsaturated and saturated soil in a manner that isolates the soil mass hydrologically (Figure 21). Understanding this, the inputs and outputs can be described in a fashion similar to Equation 3.

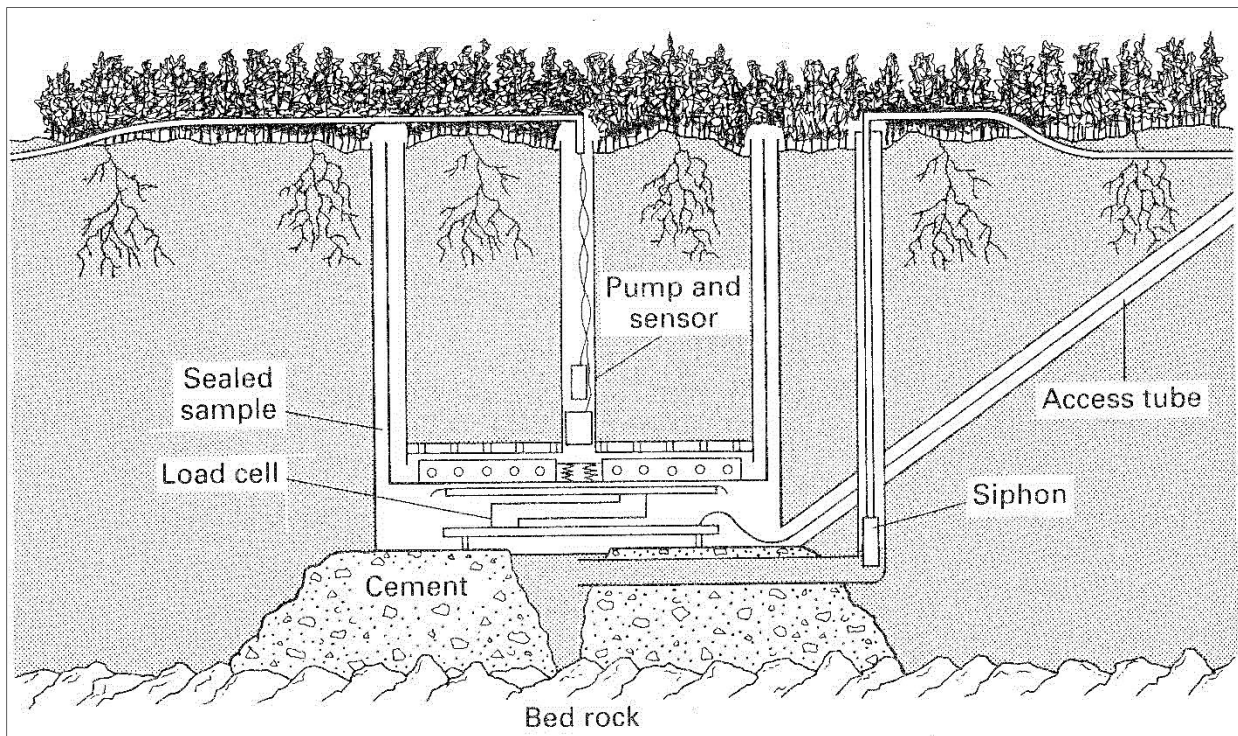


Figure 21. Example of a weighing lysimeter (Maidment, 1992).

While precise measurement of water fluxes is possible using weighing lysimeters, they are not practical for ET measurement from entire vegetation communities or from large plants, such as mature trees. The fluctuation of the groundwater table has been used to estimate ET from forests for decades (White, 1932; Feddes and Lenselink, 1994; Loheide et al., 2005; Bryla et al., 2010). This concept, originally developed by White (1932), quantifies daily groundwater losses to ET through the analysis of well hydrographs and is commonly referred to as the White method (WM). White (1932) noted that water levels fluctuated daily in monitoring wells near a river in Escalante Valley, Utah and developed a method of determining the rate of loss due to ET using that fluctuation. He deduced that transpiration by vegetation and evaporation from soil caused by the heat of the day withdraws water from the riparian zone; this loss stops at night (e.g. midnight to 04:00) when there is no solar energy or residual heat to drive the process. If there is a steady seepage of groundwater to the site, the water table recovers during the evening. The water table response to evapotranspiration is determined by taking the difference between the actual water table elevation at the end of the day and the expected water table elevation, assuming the only water flux in or out of the site is due to ground flow (Cheng et al., 2013). Comparison of the long-term decline of the water table over several days and the short-term recovery during each evening permits calculation of an ET estimate:

$$ET = r(t) - S_y \frac{dWT_g}{dt} \quad (6)$$

where r is the rate of groundwater to and from the well, S_y is the specific yield, dWT_e is the net change in water table elevation, and dt is the change in time. The assumptions that should be met when using the WM are as follows (Loheide et al., 2005):

1. Evapotranspiration by vegetation causes the observed diurnal water table fluctuations;
2. Evapotranspiration values are negligible compared to the groundwater influx between 0:00 and 4:00;
3. The amount of groundwater influx throughout the day is constant, unless there is recharge from precipitation ; and,
4. S_y accurately describes the volume of water extracted from the saturated zone per unit decline in the water table per unit area of the site.

Furthermore, the WM generally requires a high resolution sensor capable of measuring water levels with millimeter accuracy (Feltrin et al., 2011). This method provides a low-impact, cost-effective means for direct measurement of actual ET rates within the watershed (Bryla et al., 2010).

The water balance and WM methods assume the AET is essentially the quantity of water that is unaccounted for in a given water balance. Alternatively, energy-based approaches, such as the

eddy covariance (EC) method, determine vapor flux by measuring sensible (H) and latent heat (λE) (Figure 22). The EC approach calculates the vapor flux by measuring instantaneous fluctuations of atmospheric gases and sensible heat within a given air volume, assuming constant air pressure (Irmak et al., 2014).

The latent heat flux can be converted to an ET rate as follows:

$$ET = \frac{3600\lambda E}{\varepsilon\rho_w} \quad (7)$$

where λE is the latent heat flux, ε is the latent heat of vaporization for water, and ρ_w is the density of water. The calculation of eddy flux requires several simplifying assumptions: the surrounding terrain is homogenous and flat; the water vapor transport processes are constant in time; there is adequate air turbulence to transport the water vapor away from the site; and, the water vapor is transported away from the site in the vertical direction (Baldocchi et al., 1988, Massman and Lee, 2002). A convenient rule of thumb suggests a fetch: instrument height ratio of approximately 100:1 (Smith and Cresser, 2003). While the field measurements for EC are straightforward (3-dimensional windspeed, air temperature, and gas concentration), the data post-processing is extensive, requiring a thorough knowledge of time series and spectral analysis.

The Bowen Ratio Energy Balance (BREB) is another energy-based approach that has been used extensively for the quantification of evaporation over several surfaces, from open water, to grassland, crop land, and forest (Savage et al., 2009). Using BREB, the available solar energy can be partitioned into the sensible and latent heat, from which evapotranspiration is quantified. The Bowen ratio can be expressed as follows:

$$\beta = \frac{H}{\lambda E} \quad (8)$$

The Bowen ratio can be used with the surface energy balance, which for uniform surfaces can be simplified to:

$$R_n = H + G + \lambda E \quad (9)$$

where R_n is net radiation, G is the surface soil heat flux (energy absorbed by the ground), H is the sensible heat flux (energy used to change the air temperature), λE is the latent heat flux (energy used to convert liquid water into water vapor). These quantities are related in the following:

$$\lambda E = \frac{R_n - G}{1 + \beta} \quad (10)$$

$$H = \frac{\beta}{1 + \beta} (R_n - G) \quad (11)$$

By measuring the change in air temperature and water vapor pressure with height above the vegetation, the sensible and latent heat can be determined as follows:

$$H = -\rho_a c_{p_a} K_h \frac{\partial T}{\partial z} \quad (12)$$

$$\lambda E = \frac{\rho_a c_{p_a}}{\gamma} K_v \frac{\partial e}{\partial z} \quad (13)$$

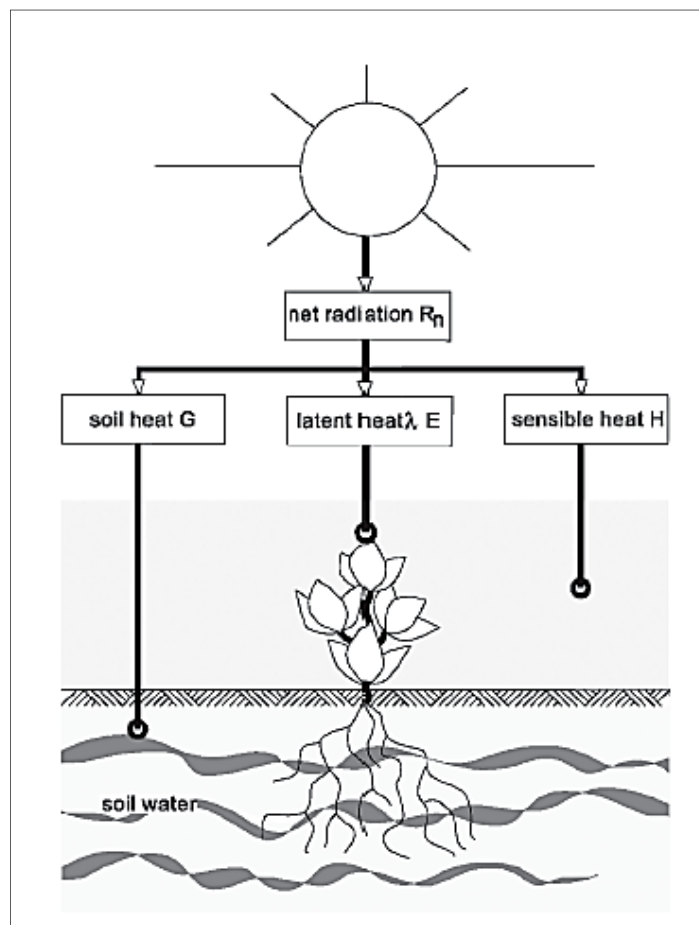


Figure 22. Incoming solar radiation, sensible, latent, and soil heat flux (Feddes and Lenselink, 1994).

Assuming the diffusivity of sensible and latent heat are equal, $K_h=K_v$, respectively (Malek and Bingham, 1993; Perez et al., 1999), the Bowen Ratio can be calculated as follows:

$$\beta = \gamma \frac{\Delta T}{\Delta e} \quad (14)$$

where ρ_a is the density of air, c_{pa} is the specific heat of air, z is height, T is temperature, $\gamma=c_p P/e_r L$, P is the atmospheric pressure, c_p is the specific heat of air at constant pressure, e_r is the ratio between the molecular weights of water vapor and air (0.622), and L is the latent heat of vaporization. The latent heat is the energy source for evapotranspiration, allowing liquid water to change phase into vapor.

The BREB has been widely used since it was initially proposed by Bowen (1926) because it has the advantage of a clear physical concept, few parameter requirements, and a simple calculation method. Unlike the EC technique, the Bowen ratio method does not explicitly require information on wind speed and aerodynamic properties of the surface. As with the EC method, a fetch:height ratio of 100:1 is recommended and high-resolution measurements are required (Rosenberg, 1983, Heilman et al., 1989). However, because the BREB method does not directly measure water vapor transport, accurate wind speed measurements are not required, reducing the importance of the fetch ratio.

Estimating Evapotranspiration

Given the number of factors that affect evapotranspiration, predictions of reference crop ET can be complex; however, there have been several methods developed which use simplified techniques. For example, Thornthwaite (1948) developed a relationship between mean monthly temperatures and PET from a well-watered grass crop, as determined through analyses of water budgets for the eastern United States in areas with adequate moisture for active transpiration. This analysis determined that ET_0 (mm/month) could be estimated using the following equations:

$$PET_0 ET_0 = 16d \left[\frac{10T}{I} \right]^a \quad (15)$$

$$I = \sum_{n=1}^{12} \left[\frac{T}{5} \right]^{1.514} \quad (16)$$

where T is the mean temperature for the month ($^{\circ}\text{C}$), I is the annual thermal index, and d is a correction factor based upon the latitude and the month, and a is given by $0.49+0.0179I-0.0000771I^2+0.000000675I^3$.

While the Thornthwaite method is valuable in its simplicity, the Food and Agricultural Organization (FAO), as well the American Society of Civil Engineers (ASCE), recommend calculating reference crop evapotranspiration using the Penman-Monteith equation (Monteith, 1965; Jensen et al., 1990; Allen et al., 1998; Walter et al., 2000). The Penman-Monteith model is based upon a combination approach which incorporates energy and aerodynamic considerations (Sumner and Jacobs, 2005). Assuming an alfalfa reference crop as described in Jensen et al. (1990), the Penman-Monteith equation for determining ET_0 can be quantified by ASCE-EWRI (2005):

$$ET_0 = \frac{0.408\Delta(R_n - G) + \gamma \frac{C_n}{T + 273} u_2 (e_s - e_a)}{\Delta + \gamma(1 + C_d u_2)} \quad (17)$$

where:

- ET_0 = standardized reference evapotranspiration for 12 cm tall cool season grass in mm day^{-1} ;
- R_n = calculated net radiation at the crop surface in $\text{MJ m}^{-2} \text{day}^{-1}$ at the daily time step or alternatively $\text{MJ m}^{-2} \text{h}^{-1}$ for hourly intervals;
- G = soil heat flux density at the soil surface in $\text{MJ m}^{-2} \text{day}^{-1}$ at the daily time step or alternatively $\text{MJ m}^{-2} \text{h}^{-1}$ for hourly intervals;
- T = mean daily or hourly air temperature at height of 1.5-2.5 m ($^{\circ}\text{C}$);
- u_2 = mean daily or hourly wind speed at height of 2 m (ms^{-1});
- e_s = saturation vapor pressure at height of 1.5-2.5 m (kPa), calculated at time daily as the average of saturation vapor pressure at maximum and minimum air temperatures⁷
- e_a = mean actual vapor pressure at height of 1.5-2.5 m (kPa);
- Δ = slope of the saturation vapor pressure versus temperature curve ($\text{kPa } ^{\circ}\text{C}^{-1}$);
- C_n = numerator constant that changes with respect reference type and respective time step ($\text{K mm s}^3 \text{Mg}^{-1} \text{d}^{-1}$); and,
- C_d = denominator constant that changes with respect reference type and respective time step (s m^{-1}).

The units for the 0.408 coefficient are $\text{m}^2 \text{MJ}^{-1}$, which symbolizes the latent heat of vaporization, λ , and water density, ρ_w , where $\lambda = 2.45 \text{ MJ kg}^{-1}$ and $\rho_w = 1.0 \text{ Mg m}^{-3}$. Furthermore, it should be noted that using hourly time steps and then summing over a 24 hour period should provide better estimates of ET_0 than using data averaged over a 24 hour period (ASCE-EWRI, 2005).

The saturation vapor pressure of the air can be computed as:

$$e_s = \frac{e^{\circ}(T_{\max}) + e^{\circ}(T_{\min})}{2} \quad (18)$$

where T_{\max} and T_{\min} are daily maximum and minimum air temperature, respectively, °C, at the measurement height (1.5-2.0 m), and e° is the saturation vapor pressure function. At the hourly scale, e_s can be calculated as a function of hourly air temperature:

$$e^{\circ}(T)=0.6108 \exp\left(\frac{17.27T}{T+237.3}\right) \quad (19)$$

where $e_s(T)$ is in kPa and T is in °C. Actual vapor pressure, e_a , can be computed in a fashion similar to equation 5 but rather than using mean air temperature, morning dew point temperature is substituted. For hourly calculations, e_a , should be calculated using the relationship with relative humidity:

$$e_a = \frac{RH}{100} e^{\circ}(T) \quad (20)$$

where RH is the mean relative humidity, in percent, and T is the mean air temperature in °C. The psychrometric constant in the Penman-Monteith equation can be calculated by the following (Bos et al., 2009):

$$\gamma=0.000665P \quad (21)$$

where P is atmospheric pressure, kPa, and γ has units of kPa °C⁻¹. If there are no data available for atmospheric pressure, it can be calculated from the elevation of the site (ASCE-EWRI, 2005):

$$P=(2.406-0.0000534z)^{5.26} \quad (22)$$

where z is elevation above mean sea level in meters.

The slope of the saturation vapor pressure-temperature, Δ , can be calculated by:

$$\Delta = \frac{2503 \exp\left(\frac{17.27T}{T+237.3}\right)}{(T+237.3)^2} \quad (23)$$

where Δ has units of kPa °C⁻¹ and T is daily or hourly mean air temperature in °C.

Wind speed is a function of the height above the ground surface. The standard measurement height for wind speed is 2 m, but wind speeds measured at other heights can be adjusted using equation 24:

$$u_2 = u_z \frac{4.87}{\ln(67.8z_w - 5.423)} \quad (24)$$

where u_z and z_w are the wind speed and ground surface height, respectively. It should also be noted the above equation is based upon a logarithmic wind speed profile over a short clipped grass.

Net short wave radiation can be calculated given the relationship between albedo and solar radiation, which is given as:

$$R_n = (1 - \alpha)R_s \quad (25)$$

where R_s is solar radiation and α is albedo, which is generally assumed equal to 0.23 for the reference crop. For net emissivity, the ASCE-EWRI procedure follows the work of Brunt (2011) for the estimation of net emissivity at the hourly and daily time scale, respectively:

$$R_{nl} = \sigma f_c (0.34 - 0.14\sqrt{e_a}) \frac{T_{kmax}^4 + T_{kmin}^4}{2} \quad (26)$$

$$R_{nl} = \sigma f_c (0.34 - 0.14\sqrt{e_a}) T_{Khr}^4 \quad (27)$$

where R_{nl} has units of $\text{MJ m}^{-2} \text{ day}^{-1}$, σ is the Stefan Boltzmann constant ($4.901 \times 10^{-9} \text{ MJ K}^{-4} \text{ m}^{-2} \text{ day}^{-1}$), f_{cd} is a cloudiness function, e_a is actual vapor pressure, T_{kmax} is the maximum absolute temperature in the 24 hour period, T_{kmin} is the minimum absolute temperature within the 24 hour period, T_{Khr} is the average hourly absolute temperature. The cloudiness function can be calculated using equation 28:

$$f_{cd} = 1.35 \frac{R_s}{R_{so}} - 0.35 \quad (28)$$

where R_s/R_{so} is relative solar radiation, R_s is measured or calculated solar radiation, and R_{so} is clear-sky radiation. Clear-sky radiation can be calculated by:

$$R_{so} = (0.75 + 2 \times 10^{-5} z) R_a \quad (29)$$

where z is elevation and R_a is extraterrestrial radiation. Extraterrestrial radiation can be computed using the relationship between the solar constant, solar declination, and the day of the year, as given by:

$$R_a = \frac{24}{\pi} G_{sc} d_r [\omega_s \sin(\varphi) \sin(\delta) + \cos(\varphi) \cos(\delta) \sin(\omega_s)] \quad (30)$$

where G_{sc} is the solar constant ($4.92 \text{ MJ m}^{-2} \text{ day}^{-1}$), d_r is the inverse relative distance factor for the earth-sun, ω_s is the sunset hour angle (in radians), $\varphi=L (\pi/180)$ for L =latitude in degrees, and δ is the solar declination. The parameters d_r and δ can be quantified by the following equations:

$$d_r=1+0.033 \cos\left(\frac{2\pi}{365} J\right) \quad (31)$$

$$\delta=0.409\sin\left(\frac{2\pi}{365} J-1.39\right) \quad (32)$$

where J is the number of the day in the Julian year. Additionally, the sunset hour angle can be calculated by:

$$\omega_s = \arccos(-\tan(\varphi) \tan(\delta)) \quad (33)$$

In many cases, the soil heat flux, G , is assumed negligible in the Penman-Monteith equation; however, the FAO and EWRI provide some guidance in the estimation of this term. For hourly or shorter time steps, G can be estimated as:

$$G_{\text{day}}=0.1R_n \quad (34)$$

$$G_{\text{night}}=0.5R_n \quad (35)$$

where G and R_n are measured at the same time interval and have units of energy. Furthermore, nighttime can be defined when the measured or calculated net radiation is negative. In addition, the coefficient 0.1 in equation 34 represents a small amount of dead thatch underneath the leaf canopy of the short grass reference used in these standardized equations (Bos et al., 2009).

Progress to Date

Monitoring equipment was installed to measure evapotranspiration from the scrub-shrub and forested vegetation within Huntley Meadows Park. Additionally, the meteorological measurements needed to calculate reference crop ET are also being made so that crop coefficients can be determined. A Bowen Ratio Energy Balance System (BREBS) weather station was installed in the Huntley Meadows wetland May 27-30, 2014 in the mixed emergent and scrub-shrub vegetation growing in the northeast section of the wetland. This location was chosen such that the vegetation community of interest would be upwind from the station, but far enough away from the surrounding forest to minimize interference with wind and solar radiation measurements. A Bowen Ratio system was chosen to measure ET, rather than a weighing lysimeter or an eddy covariance system, due to costs, the desire to minimize impacts to the wetland, and the limited fetch in the wetland.

The BREBS station consists of equipment required to conduct an energy balance. Net solar radiation (incoming – outgoing) is measured using a REBS Q* 7.1 radiometer, which can measure wavelengths ranging from 0.25 to 60 μm . To determine the amount of energy absorbed by the ground (and/or overlying water), the amount of water over the ground surface and in the soil, the change in water and/or soil temperature, and the heat flux deeper into the soil are measured. The total amount of energy used to change the temperature of the water and soil are calculated using the water and soil specific heat capacities, respectively. The temperature of the surface water is measured using two CSI 107-L temperature probes. Soil moisture content, soil temperature, and soil heat flux are each measured at three points below the net radiation sensor using the REBS SMP, REBS STP, and REBS HFT sensors (Table 6).

The amount of solar energy used to change the air temperature (sensible heat, H) and the amount of energy used to convert liquid water into water vapor (latent heat, λE) are calculated by measuring the change in air temperature and the change in the vapor pressure, respectively, between two different elevations above the vegetation. The BREBS station uses two sets of air temperature and vapor pressure sensors, separated by a distance of 3.3 ft., to measure the air temperature and vapor pressure differences (e.g. gradients). The lowest sensor is located just above the estimated vegetation height at full growth. These sensors are installed on an automated exchange system that switches each sensor set between the high and low location every 30 minutes. The sensors are exchanged to minimize the effects of sensor bias on the ET estimates. Because the changes in temperature and vapor pressure that must be measured are very small, the sensors used in the BREBS station are more sensitive than similar sensors used in standard weather stations. For example, the air temperature sensors are accurate to 0.01°F, while the CSI 107 temperature probes are only accurate to 1.8°F.

In addition to the sensors used to quantify the overall energy budget, standard weather sensors were installed, including a TR-525M tipping bucket rain gage and a Model 276 Setra barometric pressure sensor. The weather station is powered using a 12-V deep cycle marine battery and a solar panel. The main control panel at the weather station consists of a AM16/32B multiplexer and a CSI CR1000 datalogger, as well as a 900 MHz spread spectrum radio and a Yagi antenna to communicate with the data loggers at the habitat pool and the outlet structure. Data are recorded to the dataloggers every 15 minutes and then are uploaded hourly from all of the CSI data loggers using a Sierra Wireless RavenXTV CDMA cellular modem and the CSI LoggerNet software. The data downloaded from the site are checked for errors and then stored in a SQL database, which is stored on the project server and backed up off site. Additionally, the most recent sensor measurements are graphed and displayed on the Huntley Meadows project web site. There have been issues with respect to power, and these problems have been resolved by installing a maintenance free battery as well as by rewiring the system to shut down when battery voltage drops below 11.5 V.

Table 6. Sensors in Bowen Ratio Energy Balance system.

Instrument	Make	Model	Range/ Accuracy
Net Radiometer	REBS	Q*7.1	0.25 to 60 μm
Soil Moisture Probe	REBS	SMP10064/10065/10066	1.5% SM*
Soil Temperature	REBS	STP14001/STP14002/STP14003	0.02°F/0.012°C
Soil Heat Flux	REBS	HFT-3.1	
Temperature	REBS	THP13007/13008	0.01°F/0.008°C
Tipping Bucket Rain Gauge	Texas Electronics	Series 525	0.004 in./0.1 mm
Barometer	Setra	Model 276	± 0.05 psia
Wireless Modem	Sierra Wireless	RavenXTV CDMA	N/A
Multiplexer	CSI	AM16/32B	N/A
Anemometer	Met One Instruments	Model 034B	± 1.8 mph, $\pm 4^\circ$

*SM =Soil moisture in %.

Results to Date

Figure 23 shows the response of the wetland pool to the storm event on August 12-13, 2015. Prior to the storm event, the water level in the Habitat D pool is just below the elevation of the slide gate and the water in the outlet structure is 0.4 ft. lower than the slide gate (the difference is likely closer to 0.2 ft. lower due to a consistent observed offset between the outlet and pool water surface elevations, which will be investigated further). During the storm event, there is a distinct 0.5-ft. increase in water level in the pool, which corresponds well to the estimated surface inflow of 0.57 ft. from the urban watersheds. The influx of storm runoff is also reflected in the water temperature measurements. The water standing in the outlet control structure is at a constant low temperature before the storm event. The water temperature rises rapidly as the warmer water from the wetland enters the control structure, disrupting the diurnal pattern in wetland water temperatures. The response from the pressure transducer in the outlet structure does not mimic that of the sonic water level sensor in the habitat pool. This unusual response is likely due to turbulence in the outlet structure. Following the storm event, water levels in the outlet structure settle down and mimic water level changes observed in the habitat pool, albeit with the offset mentioned previously.

Another interesting pattern in outlet structure water levels was observed in the two weeks prior to the August 12, 2014 storm event. Figure 24 illustrates precipitation rates and the corresponding water levels in Habitat D pool and the outlet structure. Following each storm event, there is a sharp rise in water levels in the wetland and the outlet structure, followed by a slow drawdown. The sharp drops in outlet water levels are when the outlet structure is pumped dry for maintenance and sensor installation (late July and August). However, there was little precipitation in the first two weeks of August. An interesting diurnal water level fluctuation is observed in the outlet structure that appears to correspond to ET. A similar response is not observed in the habitat pool near the sheet pile dam. Following the storm event on August 12, 2014, the pattern does not continue, possibly because the ET demand is being met by retained infiltrated rainfall as soil water, rather than groundwater.

Measurements made at the weather station are illustrated in Figure 25. For the sake of clarity, measurements from multiple sensors are averaged (two air temperatures and three soil temperatures). This graph shows the net increase in solar radiation during the day and a net loss to the atmosphere at night. During the storm event, radiation levels are decreased, as would be expected under cloudy conditions. The response of both the air temperature and the water temperature to the absorbed solar radiation is also evident, although there is a time lag, particularly for the water temperature.

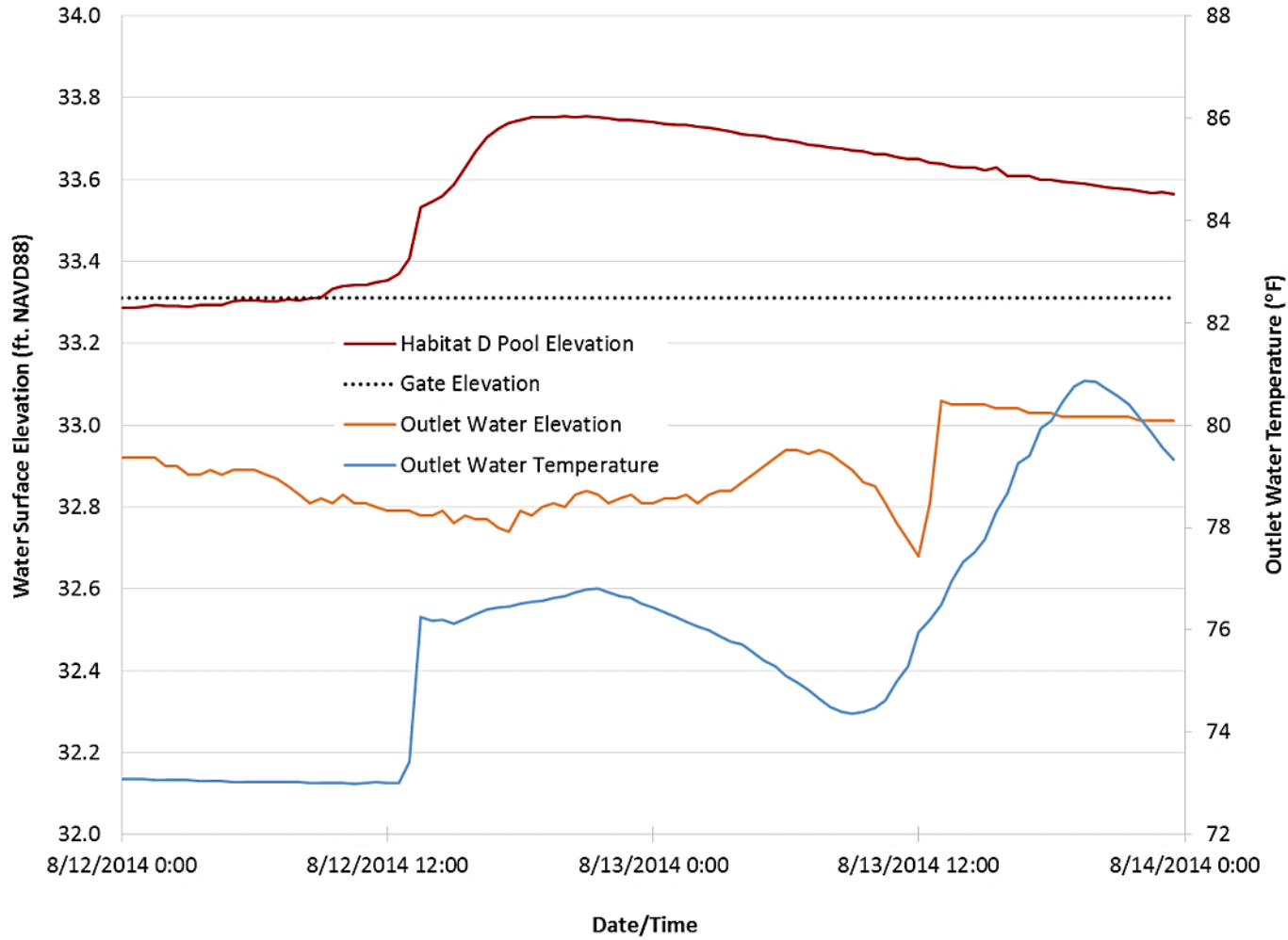


Figure 23. Changes in water surface elevation and water temperature during August 12-13, 2015 storm event. Note: gate position and water surface elevation in outlet structure are not available for this date.

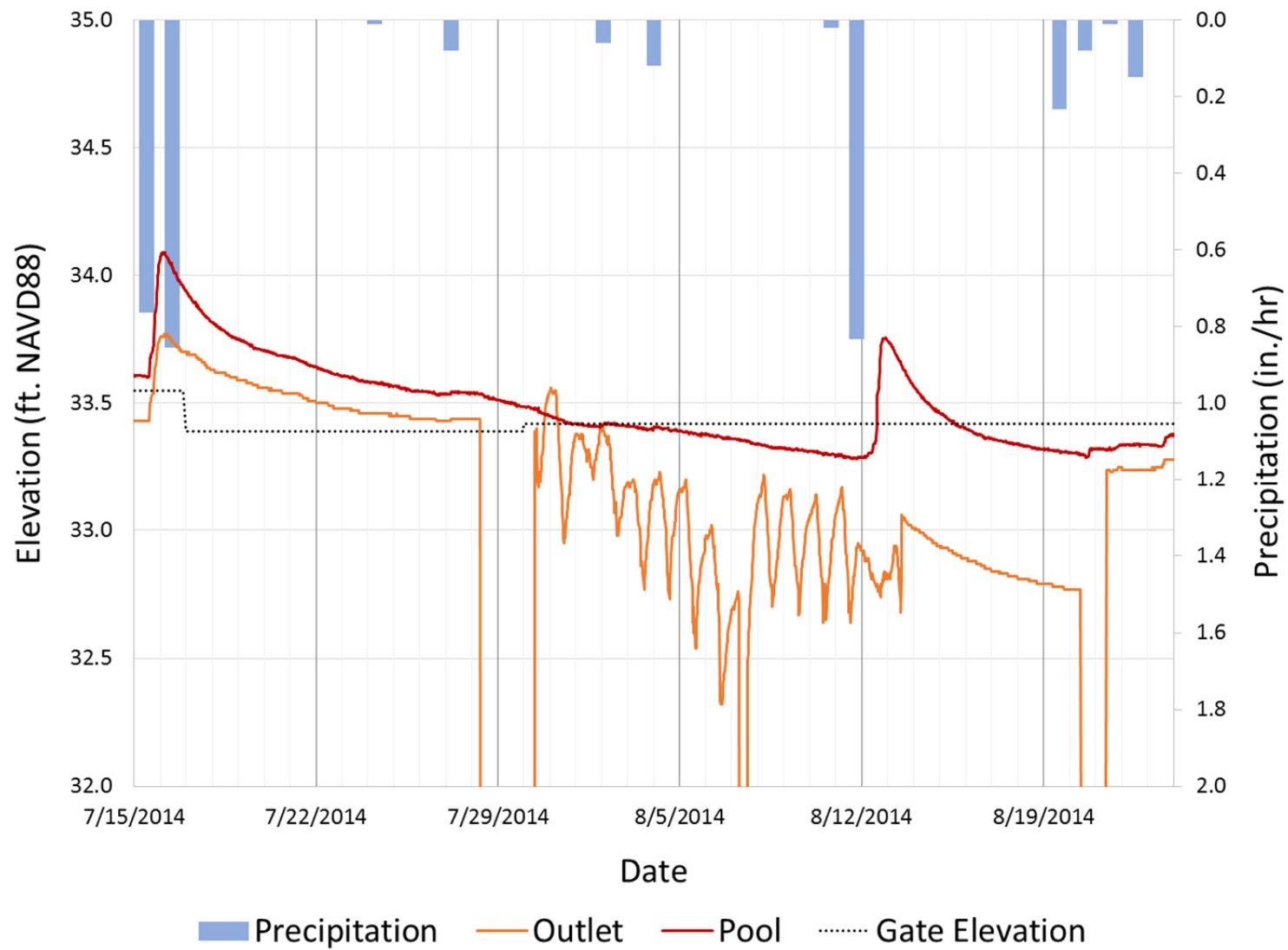


Figure 24. Precipitation rates and the corresponding water levels in Habitat D pool and the outlet structure before and after the August 12, 2014 storm event.

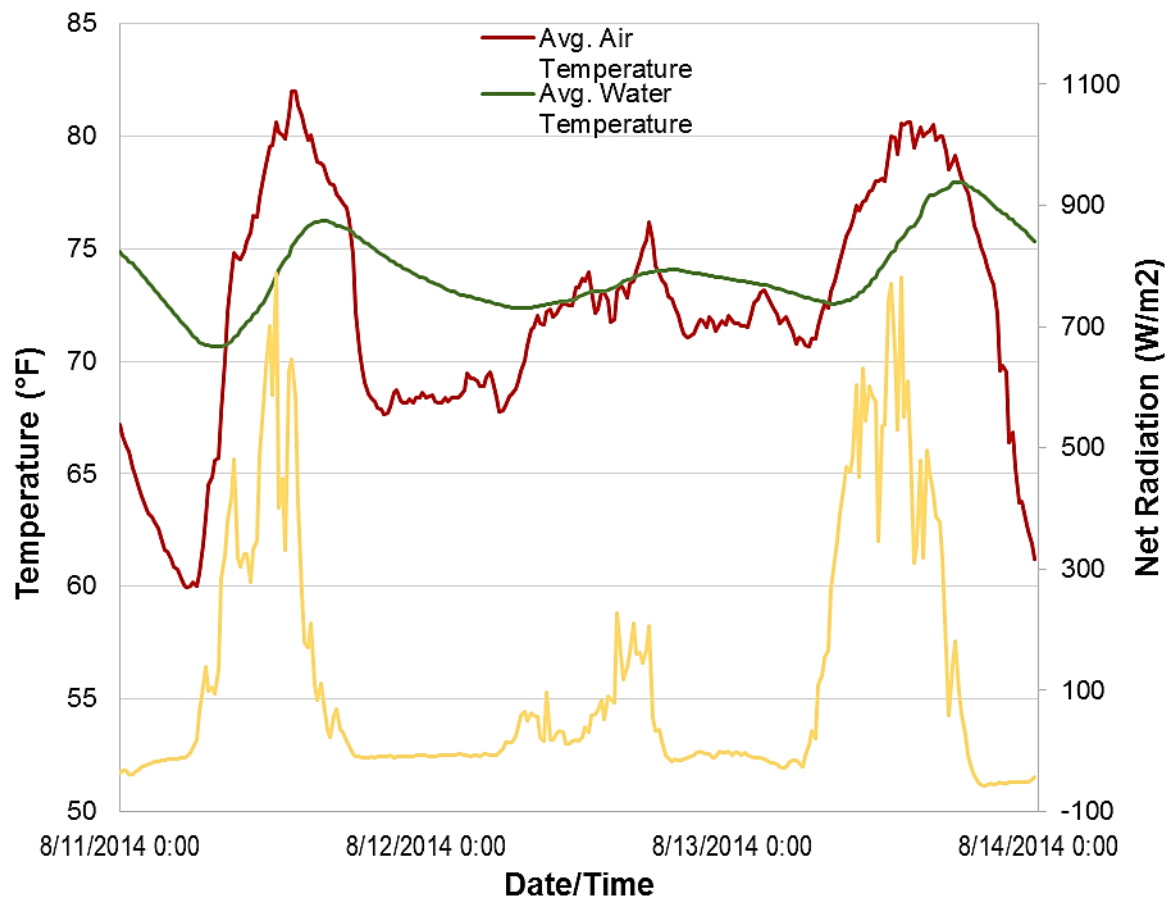


Figure 25. Net radiation and average air and water temperature at weather station during August 12-13, 2014 storm event.

Development and Deployment of Website

Immediately following the initiation of this research program, we obtained the domain name HuntleyMeadows.org for future use. In January of 2015, we launched the new website which contains (a) background information on the wetland restoration plan, (b) links to our various researchers and collaborators, (c) descriptive information on Wetbud, (d) research results and reports and (d) a link to graphical display of weather data output (Figure 26) from the weather station. We expect to add considerable content to the website over time, including certain content from this report as agreed upon by WSSI.

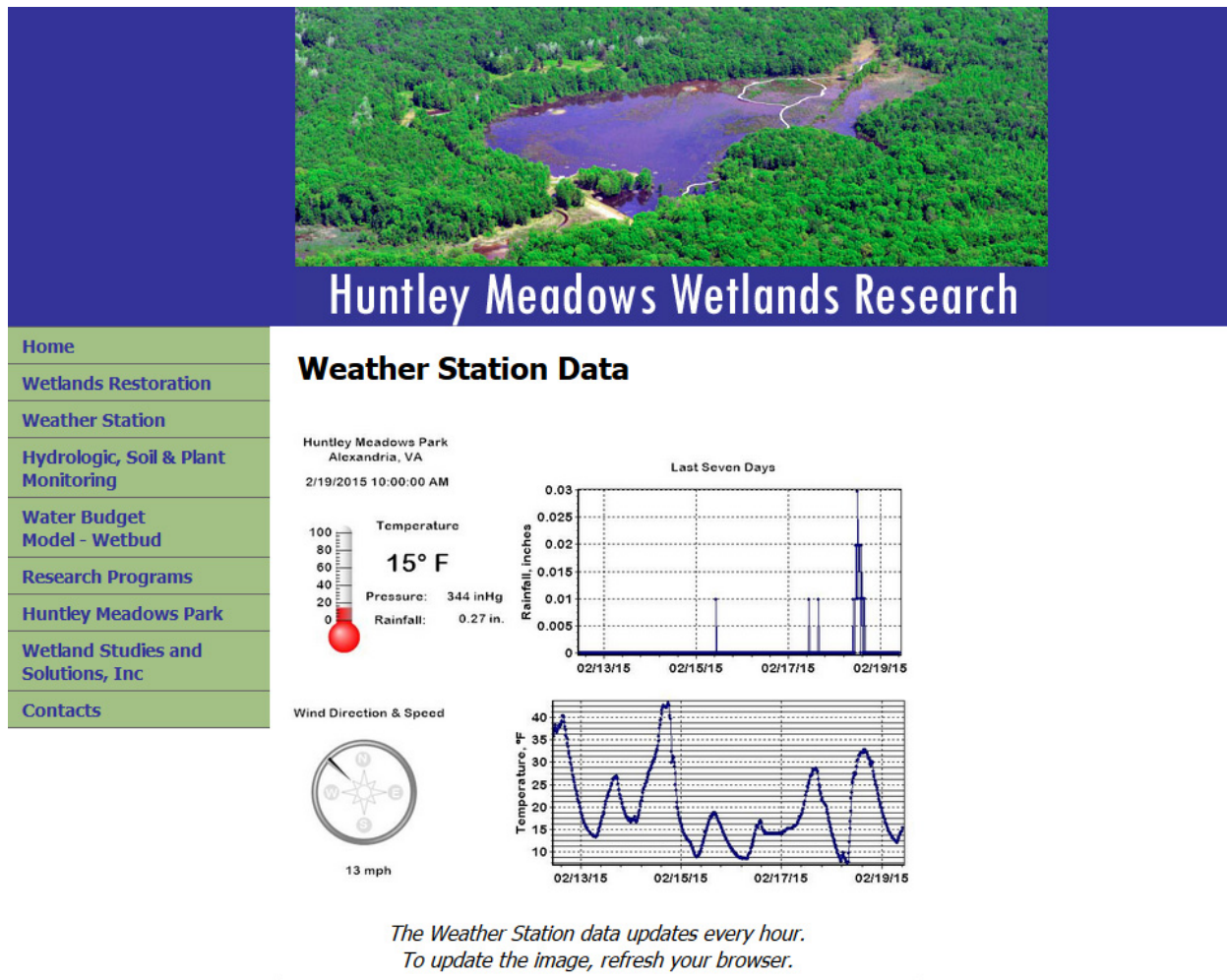


Figure 26. Weather station weather data graphic example from Huntley Meadows Restoration Research website launched in mid-January 2015. The site also includes links to background documents and cooperators and summaries of research results. The site is available at HuntleyMeadows.org.

Building a Water Budget for Huntley Meadows and Testing Wetbud

Our major overall goal with the Huntley Meadows research program is the development and validation of a site-specific water budget. As described above, we have installed an extensive array of monitoring equipment in and around the central wetlands complex at the site to develop accurate inputs for all of the components of the water budget for this site. There are very few well-documented and published water budgets for our region, the more important of which are discussed below and related to our current efforts at Huntley Meadows. Please note that we use the same ET term as the authors of the referenced studies [e.g. reference crop ET (ET_0) or potential ET (PET)] in the following summary.

Background on Regional Water Budget Studies and ET Estimates

The general water budget equation for a wetland can be expressed in several ways. Mitsch and Gosselink (2000) have summarized the general water budget for wetlands as follows:

$$\Delta V/\Delta T = P_n + S_i + G_i - ET - S_o - G_o \pm T$$

Where: $\Delta V/\Delta T$ = change in water storage volume per unit time

P_n = Precipitation (net)

S_i = Surface inflows

G_i = Groundwater inflows

ET = Evapotranspiration

S_o = Surface outflows

G_o = Groundwater outflow

T = tidal inflow/outflow (not applicable at Huntley Meadows)

Other approaches to the water budget equation balance all inputs vs. outputs with the residual accounted for as ΔS or change in storage which is also shown as $\Delta V/\Delta T$ in the equation above. It is important to point out that not all terms will apply to all wetlands. For example, Mitsch and Gosselink (2000) describe an example of a pocosin wetland (isolated from surface water exchange) on the North Carolina Coastal Plain, where a projected annual water budget (in cm/yr) might be + 117 (precipitation) – 67 (ET) – 49 (surface outflow) – 1 (groundwater outflow) = 0 ($\Delta V/\Delta T$). Thus, ET can be the major pathway for water loss from many wetlands (Drexler et al., 2004) but it is difficult and expensive to quantify it directly as discussed earlier.

In another regional study, Sanford et al. (2012) attempted to quantify hydrologic cycle components across the state of Virginia, for both watersheds and individual localities. Their yearly average values for the entire state of Virginia are shown in Figure 27. For Virginia watersheds, precipitation was estimated using PRISM (Parameter-elevation Relationships on Independent Slopes Model) climate data. Total streamflow data was obtained from the USGS

NWIS (National Water Information Service) database. Baseflow (groundwater discharge) was separated from total streamflow using differences in specific conductance, and surface runoff was calculated as total streamflow minus base flow. Infiltration was then calculated as precipitation minus surface runoff. Riparian zone ET was estimated from chemical data, recharge data, and net total outflow, and precipitation and temperature were used in a regression to estimate total evapotranspiration. Vadose zone ET was determined by subtracting riparian zone ET from total ET. For specific counties and cities in Virginia, values for each of the hydrologic cycle components were extrapolated using the watershed estimates or values obtained from regression equations based on the watershed data plus impermeable surface, climate, rock type, physiography, and/or marsh area.

A detailed and verified site-specific water budget study was developed by Virginia Tech and USGS for a created VDOT compensation wetland near Fort Lee, Virginia in the late 1990's (Daniels et al., 2000). This study also compared a range of ET predictors (Bowen-Ratio, Blaney-Cridle, Thornthwaite and White diurnal flux method) similar to those employed in this study. Over the relatively dry year studied, ET actually exceeded precipitation, but the overall water budget was clearly driven by very strong groundwater discharge into the wetland (Figure 28). The study also compared the various ET estimators and reported that (a) relative to the Bowen Ratio method, the Thornthwaite method under-predicted ET in cooler/wetter months over-predicted ET in hotter months when the soil was drier, and (b) the White (1932) method worked quite well during periods of time when its underlying assumptions were met.

Several other water budget studies from the southeastern USA are worth reviewing relative to our efforts at Huntley Meadows. Sun et al. (2002) compared the hydrology of three forested watersheds: two wetland flats (one in Florida and one in North Carolina), and one Appalachian upland in North Carolina. Within this study, they compared actual evapotranspiration (AET) to potential evapotranspiration (PET) in all sites. AET was estimated by the difference between annual precipitation and annual streamflow, while PET was calculated by Hamon's method (Lu et al., 2005), which uses temperature (measured on-site) and daylight length and saturation vapor pressure (obtained from weather records). The average AET/PET ratio for the upland North Carolina site was 0.84, while the AET/PET ratio for the wetland North Carolina site was 0.93. However, the AET/PET ratio for wetland site in Florida was 0.75, which they attributed to higher PET levels in Florida and increased exfiltration losses to groundwater caused by local sandy soils, which restricted AET. After creating models, they concluded that climate (as influenced by latitude and temperature) was the primary factor in determining long-term water balance.

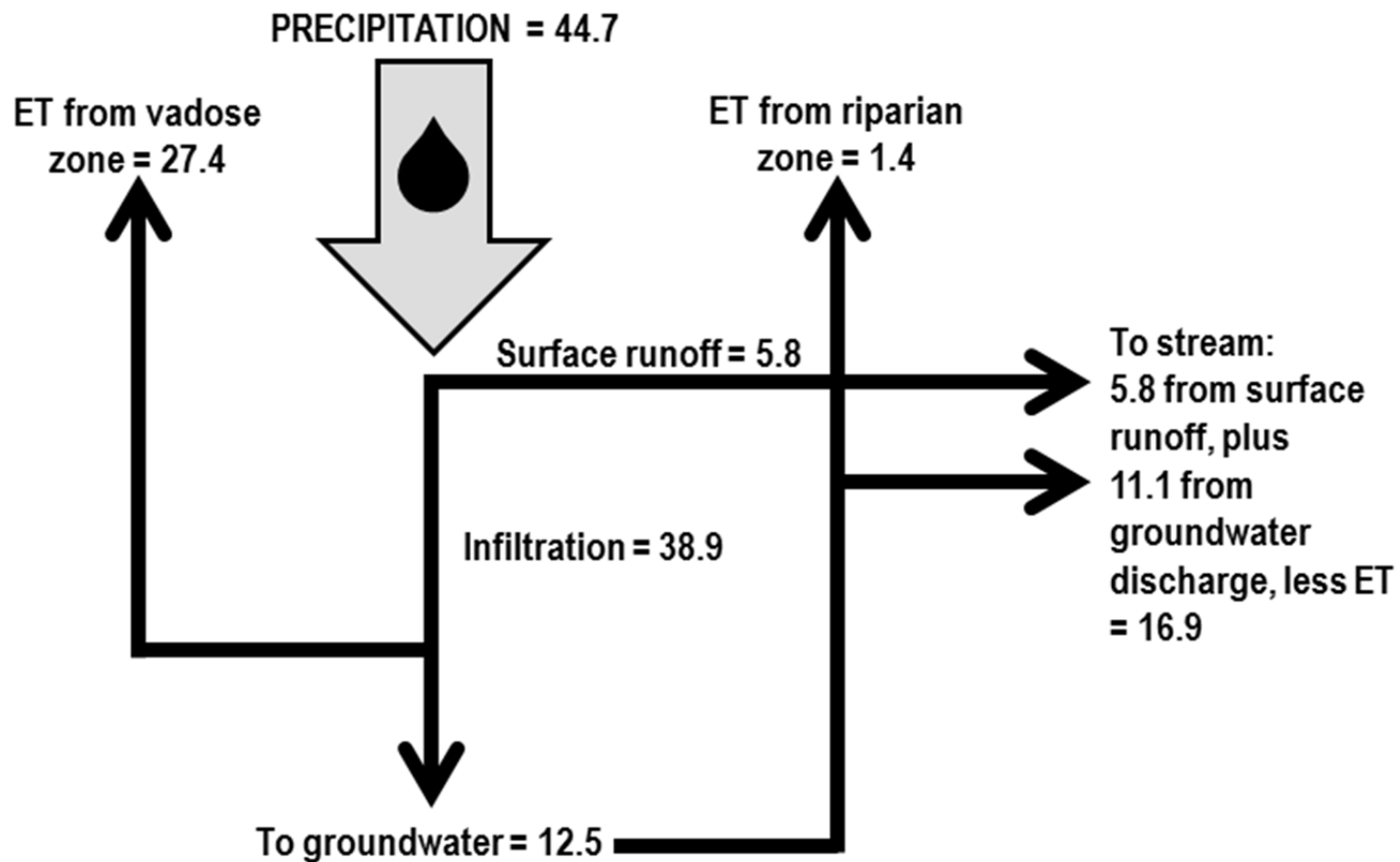


Figure 27. Yearly average values for hydrologic cycle components for the state of Virginia. Values are in inches/year. Adapted from data in Sanford et al. (2012).

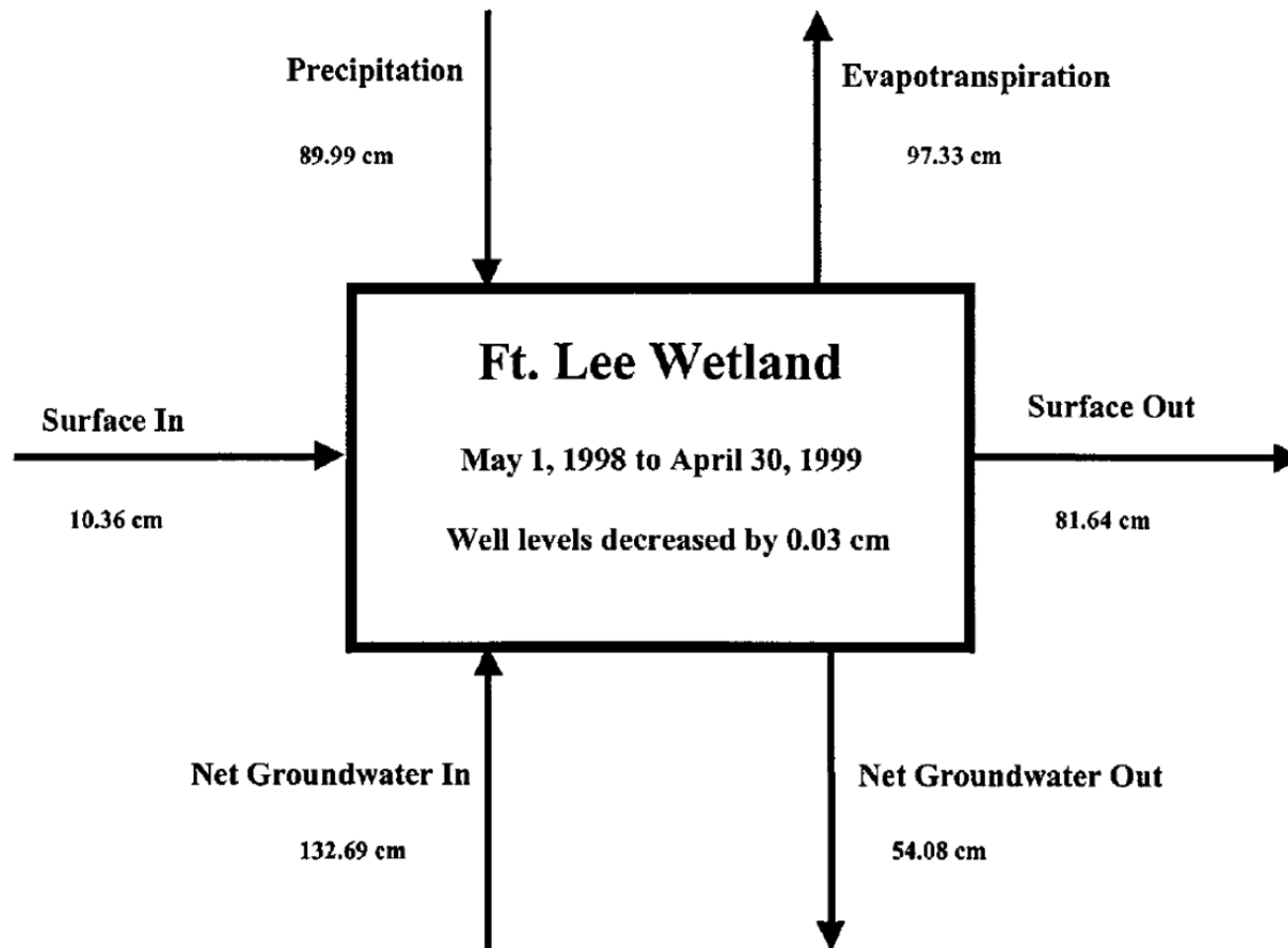


Figure 28. Fort Lee Wetland water budget parameters for May 1998 to April 1999 (Daniels et al., 2000).

Lu et al. (2003) developed a model to estimate AET using data from 39 forested watersheds in in the Southeastern U.S. AET values were approximated by using the watershed water balance method, which is essentially the difference between precipitation and streamflow. They found that AET was best predicted ($R^2 = 0.794$) by a model using the independent variables of annual precipitation, watershed latitude, watershed elevation, and percent of forest coverage, rather than a model using one or more of six popular PET calculation methods (Thornthwaite, Hamon, Hargreaves-Samani, Turc, Makkink, Priestley and Taylor).

Pyzoha et al. (2008) used Hamon's method for estimating PET (Lu et al., 2005) as part of developing a theoretical hydrologic model for a clay-based, forested Carolina bay on the South Carolina coastal plain. Precipitation and temperature were measured on site, and the rest of the weather data required were obtained from a nearby weather station. Surface water and groundwater levels were measured with transects of piezometers and wells. Although Carolina bays are often considered to be isolated wetlands, they found that this particular Carolina bay was hydrologically connected to upland during periods where precipitation exceeded evapotranspiration, with some degree of connection even during dry periods. The hydrology was similar to that of a perched wetland even though this wetland did not have a perched water table. In dry to normal years, the hydraulic gradient showed possible groundwater recharge into the bay, but in wet years and high rainfall events, the hydraulic gradient suggested either groundwater discharge from the bay, or potential groundwater flow-through.

For two years, Chaubey and Ward (2006) examined the water balance of a small (15.1 ha) shallow riparian wetland in west central Alabama's Fall Line Hills that had been created by a beaver dam on a second order stream. They found that rainfall was the dominant inflow (79-95% over the course of the study), although about 15% of rainfall was intercepted by vegetation, and ET (as estimated by the Penman-Monteith equation) was the dominant water loss (60-53%). Groundwater recharge was about 20% the total water loss. There was little annual change in water storage within the wetland.

Finally, in a more geographically distant study, Lott and Hunt (2001) both calculated and directly measured ET in a natural shrub-sedge wetland and a neighboring primarily herbaceous constructed wetland in Wisconsin. The two wetlands were approximately 300 m apart. The primary water inputs to both wetlands were precipitation and groundwater discharge, while the primary water output was ET. For this study, PET was estimated using the Penman combination equation. The data required for the equation was measured by an on-site weather station. Actual evapotranspiration (AET) was directly measured by first determining "specific yield", or the ability of soil to store water, which was approximated by 38 averaged measurements of air-filled porosity, and then using lysimeters to determine the amount of water lost to ET. In the natural wetland during the growing season, PET was lower than AET, which may have been due to the variations in microtopography and surface roughness in the natural wetland, which are not

accounted for in the Penman equation. In the constructed wetland, PET was a fairly accurate predictor of AET. The AET in the natural wetland was higher than that in the constructed wetland, even though the wetlands were so close together, apparently because of differences in plant community, soil properties, and other variables. The congruence of PET with AET varied with season in both wetlands.

Developing a Site-Specific Water Budget for Huntley Meadows

As described above, we have deployed an extensive array of monitoring equipment and sensors at Huntley Meadow that will allow us to quantify most of the critical water budget parameters (e.g. precipitation, ET, ΔS for the pond, and surface water losses) along with more general estimates for others (e.g. groundwater in-out and surface water additions). Determination of the individual water budget components over time will provide insight into which factors drive changes in water levels in the pond, as well as the hydrologic response of the wetland system to large storm events and changes in the outlet gates, allowing improved water level forecasting and management.

Our studies to date suggest that regional-scale groundwater flow passing through aquifers deep beneath Huntley Meadows do not impact the wetland significantly. However we still have not resolved if important contributions of groundwater come from small recharge sites scattered across the floor of Hybla Valley, but detailed analyses of water level records from the existing shallow water wells should resolve that issue.

Testing Wetbud

Another important aspect of our collective efforts at Huntley Meadows will be to use the various data sets obtained, particularly ET and shallow groundwater, to further test and validate Wetbud. To date, the model has been used for relatively small systems. Application of the model to a large natural system will provide a new challenge. One particular strength of our data set will be the ability to calculate actual ET via two different methods (Bowen Ratio and the White method) and then relate those measurements to PET (Thorntwaite) and ET_0 (Penman-Monteith) to determine crop coefficients for the shrub and forest vegetation in the mid-Atlantic region. Knowing the crop coefficients will permit the estimation of actual ET for similar wetlands throughout the region and will improve the design and restoration of natural wetland systems.

Another important aspect of our collective efforts at Huntley Meadows will be to use the various data sets obtained, particularly ET and shallow groundwater, to further test and validate Wetbud. At this point in time, we plan to use tools in an Advanced Model of Wetbud (e.g. irregular boundaries; multiple and sloping layers; variations in aquifer properties and elevations within the wetland; etc.) to assure their functionality. We anticipate testing Wetbud's ability to predict shallow groundwater fluctuations at several of our existing monitoring transects as verification of the model's procedures and calculations. Wetbud is designed as a planning tool for created

wetlands, however, so we are not certain that we will be able to use it to simulate the effects of changes in the central ponded/pool level at the park on the variations in water levels observed in the adjacent upgradient wells.

Overall Summary and Conclusions

Since the fall of 2012, we have installed a diverse and intensive array of groundwater, surface water, and weather monitoring instruments at Huntley Meadows Park. Results to date indicate that the implementation of the new water control strategy at the park in 2013 has not only significantly affected water levels in the central ponded portion of the wetland, but well up into the surrounding forested uplands as well. The net result of the raised open water levels appears to be an increase in overall height and duration of the winter high water table in the surrounding forested soil landscape and decrease in its short-term fluctuations during the winter. Our vegetation monitoring program has established a clear and expected relationship between local landscape position and abundance and type of hydrophytic vegetation and we expect to see significant shifts in vegetation abundance and type over time, particularly in the zone associated with the former herbaceous/forested edge.

We are confident that through this research program, we will be able to develop and validate one of the most accurate water budgets for a wetland system ever produced for the mid-Atlantic region. This knowledge will assist park administration in managing water levels to improve the quantity and quality of habitat in the park. Additionally, we will produce a much improved set of actual evapotranspiration estimators for both herbaceous and forested wetland components than currently available, which will help improve wetland design throughout the region.

Acknowledgements

We deeply appreciate the considerable and long-term support of Wetland Studies and Solutions Inc. (WSSI) and the Peterson Family Foundation for this collaborative research effort. In particular, we want to thank Mike Rolband and Jennifer Van Houten of WSSI for their continued assistance. We also want to thank Dave Lawlor and Kevin Munroe at Huntley Meadows park (Fairfax County Park Authority) for their on-site support and cooperation in all phases of this important project.

Literature Cited

- Allen, R.G., T.A. Howell, W.O. Pruitt, I.A. Walter and M.E. Jensen (ed). 1991. Lysimeters for evapotranspiration and environmental measurements. Proceedings of the International Symposium of Lysimetry. Honolulu, Hawaii. 23-25 July 1991. American Society of Civil Engineers, New York, NY.
- Allen, R.G., L.S. Pereira, T.A. Howell, and M.E. Jensen. 2011. Evapotranspiration information reporting: I. Factors governing measurement accuracy. *Agricultural Water Management*, 98(6): 899-920.
- Allen, R.G., L.S. Pereira, D. Raes, and M. Smith. 1998. Crop evapotranspiration - Guidelines for computing crop water requirements. FAO Irrigation and Drainage Paper 56. Food and Agriculture Organization of the United Nations, Rome.
- Arnold, J.G., P.M. Allen, and D.S. Morgan. 2001. Hydrologic model for design and constructed wetlands. *Wetlands* 21(2): 167-178.
- ASCE-EWRI. 2005. The ASCE standardized reference evapotranspiration equation. ASCE-EWRI Standardization of Reference Evapotranspiration Task Committee Report. Environmental and Water Resources Institute, American Society of Civil Engineers, Reston, VA.
- Baldocchi, D. D., B.B. Hincks, and T.P. Meyers. 1988. Measuring biosphere-atmosphere exchanges of biologically related gases with micrometeorological methods. *Ecology* 69: 1331-1340.
- Bos, M.G., R.A.L. Kselik, R.G. Allen, and D. Molden. 2009. Water requirements for irrigation and the environment. Springer, New York, NY.
- Bowen, I.S. 1926. The ratio of heat losses by conduction and by evaporation from any water surface. *Physical Review* 27(6): 779-787.
- Bradley, C. 2002. Simulation of the annual water table dynamics of a floodplain wetland, Narborough Bog, UK. *Journal of Hydrology* 261(1): 150-172.
- Brunt, D. 2011. Physical and dynamical meteorology: Cambridge University Press, Cambridge U.K.
- Bryla, D. R., T.J. Trout, and J.E. Ayars. 2010. Weighing lysimeters for developing crop coefficients and efficient irrigation practices for vegetable crops. *HortScience* 45(11): 1597-1604.
- Chaubey, I., and G.M. Ward. 2007. Hydrologic budget analysis of a small natural wetland in Southeast USA. *Journal of Environmental Informatics* 8(1): 10-21.

Cheng, D., Y. Li, X. Chen, W. Wang, G. Hou, and C. Wang, 2013. Estimation of groundwater evapotranspiration using diurnal water table fluctuations in the Mu Us Desert, northern China. *Journal of Hydrology* 490: 106-113.

Daniels W.L., A. Cummings, M. Schmidt, N. Fomchenko, G. Spieran, M. Focazio, and G. M. Fitch. 2000. Evaluation of methods to calculate a wetland water balance. Final contract report to the Virginia Department of Transportation. VTRC 01-CR1. Virginia Tech, Blacksburg, VA and Virginia Transportation Research Council, Charlottesville, VA.

Denbow, T. J., D. Klements, D.W. Rothman, E. Garbisch, C. Bartoldus, M.L. Kraus, D.R. MacLean, and G.A. Thunhorst. 1996. Guidelines for the development of wetland replacement areas. Report 379. Transportation Research Board, National Research Council. National Academy Press, Washington, DC.

Drexler, J.Z., R.L. Snyder, D. Spano, and K.T. Paw U. 2004. A review of models and micrometeorological methods used to estimate wetland evapotranspiration. *Hydrological Processes* 18: 2071–2101.

Droogers, P. and R.G. Allen. 2002. Estimating reference evapotranspiration under inaccurate data conditions. *Irrigation and Drainage Systems* 16(1): 33-45.

Dyer, A. 1965. Discussion on “Change of terrain roughness and the wind profile, by H.A. Panofsky and A.A. Townsend”. *Quarterly Journal of the Royal Meteorological Society* 91: 241.

Feddes, R.A., and K.J. Lenselink. 1994. Evapotranspiration. p. 145-173. *In* H.P Ritzema, Drainage principles and applications. International Institute for Land Reclamation and Improvement, Wageningen, Netherlands.

Feltrin, R.M., J.B.D. de Paiva, E.M.C.D. de Paiva, and F.A. Beling. 2011. Lysimeter soil water balance evaluation for an experiment developed in the Southern Brazilian Atlantic Forest region. *Hydrological Processes* 25(15): 2321-2328.

Freeze, R.A., and J.A. Cherry. 1977. *Groundwater*. Prentice-Hall. Englewood Cliffs, New Jersey.

Hargreaves, G.H., and R.G. Allen. History and evaluation of Hargreaves evapotranspiration equation. *Journal of Irrigation and Drainage Engineering* 129(1): 53-63.

Hargreaves, G.L., G.H. Hargreaves, and J.P. Riley. 1985. Irrigation water requirements for Senegal River basin. *Journal of Irrigation and Drainage Engineering* 111(3): 265-275.

Heilman, J., C. Brittin, C., and C. Neale. 1989. Fetch requirements for Bowen ratio measurements of latent and sensible heat fluxes. *Agricultural and Forest Meteorology* 44(3): 261-273.

Hu, S., C. Zhao, J. Li, F. Wang, and Y. Chen. 2014. Discussion and reassessment of the method used for accepting or rejecting data observed by a Bowen ratio system. *Hydrological Processes* 28(15): 4506-4510.

Irmak, S., A. Kilic, and S. Chatterjee. 2014. On the equality assumption of latent and sensible heat energy transfer coefficients of the Bowen Ratio Theory for evapotranspiration estimations: Another look at the potential causes of inequalities. *Climate* 2(3): 181-205.

Jensen, M.E., R.D. Burman, and R.G. Allen (ed). 1990. Evapotranspiration and irrigation water requirements. ASCE Manuals and Reports on Engineering Practices No. 70. American Society of Civil Engineers, New York, NY.

Litwin, R.J., J.P. Smoot, M.J. Pavich, H.W. Markewich, G. Brook, and S. Verado. 2010. Hybla Cores 7 & 8: An 80,000-year Late Pleistocene climate record from the mid-Atlantic Coastal Plain of North America. *Geological Society of America Abstracts with Programs* 42(1): 151. Vol. 42, No. 1, p. 151

Loheide, S.P., J.J. Butler, and S.M. Gorelick. 2005. Estimation of groundwater consumption by phreatophytes using diurnal water table fluctuations: A saturated-unsaturated flow assessment. *Water Resources Research* 41(7) doi: 10.1029/2005WR003942.

Loheide, I., and P. Steven. 2008. A method for estimating subdaily evapotranspiration of shallow groundwater using diurnal water table fluctuations. *Ecohydrology* 1(1): 59-66.

Lott, R.B., and R.J. Hunt. 2001. Estimating evapotranspiration in natural and constructed wetlands. *Wetlands* 21(4): 614-628.

Lu, J., G. Sun, S.G. McNulty, and D. M. Amatya. 2003. Modeling actual evapotranspiration from forested watersheds across the southeastern United States. *Journal of the American Water Resources Association* 39(4): 886-896.

Lu, J., G. Sun, S.G. McNulty, and D. M. Amatya. 2005. A comparison of six potential evapotranspiration methods for regional use in the southeastern United States. *Journal of the American Water Resources Association* 41: 621-633.

Maidment, D.R. 1992. *Handbook of hydrology*: McGraw-Hill Inc., New York, NY.

Malek, E., and G.E. Bingham. Comparison of the Bowen ratio-energy balance and the water balance methods for the measurement of evapotranspiration. *Journal of Hydrology* 146: 209-220.

Maltby, E., and T. Barker (ed). 2009. *The wetlands handbook*. John Wiley & Sons. New York, NY.

Massman, W., and X. Lee, 2002. Eddy covariance flux corrections and uncertainties in long-term studies of carbon and energy exchanges. *Agricultural and Forest Meteorology* 113(1): 121-144.

- Mitsch, W.J. and J.G. Gosselink. 2000. Wetlands. 3rd edition. John Wiley & Sons, New York, NY.
- Mixon, R.B., C.R. Berquist, Jr., W.L. Newell, G.H. Johnson, D.S. Powars, J.S. Schindler, and E.K. Rader. 1989. Geologic map and generalized cross sections of the Coastal Plain and adjacent parts of the Piedmont, Virginia: U. S. Geological Survey Miscellaneous Investigation Series Map I-2033. U.S. Geological Survey, Reston, VA.
- Monteith, J. L. 1965. Evaporation and environment. *Symposia of the Society for Experimental Biology* 19: 205–224.
- Ohmura, A. 1982. Objective criteria for rejecting data for Bowen ratio flux calculations. *Journal of Applied Meteorology* 21(4): 595-598.
- Panofsky, H.A., and A. Townsend. 1964. Change of terrain roughness and the wind profile. *Quarterly Journal of the Royal Meteorological Society* 90(384): 147-155.
- Pavich, M.J, H.W. Markewich, R.J. Litwin, J. Smoot, and G. Brook, 2010. Significance of marine oxygen isotope stage OIS5a and OIS3 OSL dates from estuarine sediments flanking Chesapeake Bay: *Geological Society of America Abstracts with Programs* 42(1): 101.
- Perez, P., F. Castellvi, M. Ibanez, and J. Rosell. 1999. Assessment of reliability of Bowen ratio method for partitioning fluxes. *Agricultural and Forest Meteorology* 97(3): 141-150.
- Pyzoha, J.E., T.J. Callahan, G. Sun, C.C. Trettin, and M. Miwa. 2008. A conceptual hydrologic model for a forested Carolina bay depressional wetland on the Coastal Plain of South Carolina, USA. *Hydrological Processes* 22: 2689-2698.
- Rosenberg, N.J. 1983. *Microclimate: The biological environment*. John Wiley & Sons. New York, NY.
- Sanford, W.E., D.L. Nelms., J.P. Pope, and D.L. Selnick. 2012. Quantifying components of the hydrologic cycle in Virginia using chemical hydrograph separation and multiple regression analysis. U.S. Geological Survey Scientific Investigations Report 2011-1598. U.S. Geological Survey, Reston, VA.
- Savage, M., C. Everson, and B. Metelerkamp. 2009. Bowen ratio evaporation measurement in a remote montane grassland: Data integrity and fluxes. *Journal of Hydrology* 376(1): 249-260.
- Schrader, F., W. Durner, J. Fank, S. Gebler, T. Pütz, M.Hannes, and U. Wollschläger. 2013. Estimating precipitation and actual evapotranspiration from precision lysimeter measurements. *Procedia Environmental Sciences* 19: 543-552.
- Senay, G., S. Leake, P. Nagler, G. Artan, J. Dickinson, J. Cordova, and E. Glenn. 2011. Estimating basin scale evapotranspiration (ET) by water balance and remote sensing methods. *Hydrological Processes* 25(26): 4037-4049.

- Smith, K.A., and M.S. Cresser. 2003. Soil and environmental analysis: Modern instrumental techniques. CRC Press, Boca Raton, FL.
- Sumner, D. M., and J.M. Jacobs. 2005. Utility of Penman–Monteith, Priestley–Taylor, reference evapotranspiration, and pan evaporation methods to estimate pasture evapotranspiration. *Journal of Hydrology* 308(1) 81-104.
- Sun, G., S.G. McNulty, D.M. Amatya, R.W. Skaggs, L.W. Swift Jr., J.P. Shepard, and H. Riekerk. 2002. A comparison of the watershed hydrology of coastal forested wetlands and the mountainous uplands in the Southern US. *Journal of Hydrology* 263: 92-104.
- Thornthwaite, C.W. 1948. An approach toward a rational classification of climate. *Geographical Review* 38(1): 55-94.
- Trajkovic, S., and S. Kolakovic. 2009. Evaluation of reference evapotranspiration equations under humid conditions. *Water Resources Management* 23(14):3057-3067.
- Verma, S.B., N.J. Rosenberg, and B.L. Blad. 1978. Turbulent exchange coefficients for sensible heat and water vapor under advective conditions. *Journal of Applied Meteorology* 17(3): 330-338.
- Viessman, Jr., W., and G.L. Lewis. 1996. Introduction to hydrology. Harper Collins College Publishers, New York, NY.
- Walter, I.A., R.G. Allen, R. Elliott, M.E. Jensen, D. Itenfisu, B. Mecham, T.A. Howell, R. Snyder, P. Brown, S. Echings, T. Spofford, M. Hattendorf, R.H. Cuenca, J.L. Wright, and D. Martin. 2000. ASCE's standardized reference evapotranspiration equation. *Watershed Management and Operations Management 2000*: 1-11. American Society of Civil Engineers, New York, NY.
- Wetland Studies and Solutions. 2013. Huntley Meadows Park Wetlands Restoration Project, Fairfax County, Virginia. Operations, Monitoring and Maintenance Plan.
http://www.huntleymeadows.org/wetland_restoration.html
- White, W.N. 1932. A method of estimating ground-water supplies based on discharge by plants and evaporation from soil: Results of investigations in Escalante Valley, Utah. U.S. Geological Survey Water-Supply Paper 659. U.S. Government Printing Office, Washington, DC.
- Wu, C. and S. Shukla. 2014. Eddy covariance-based evapotranspiration for a subtropical wetland. *Hydrological Processes* 28(24): 5879-5896.

Appendix 1. Groundwater Well Logs

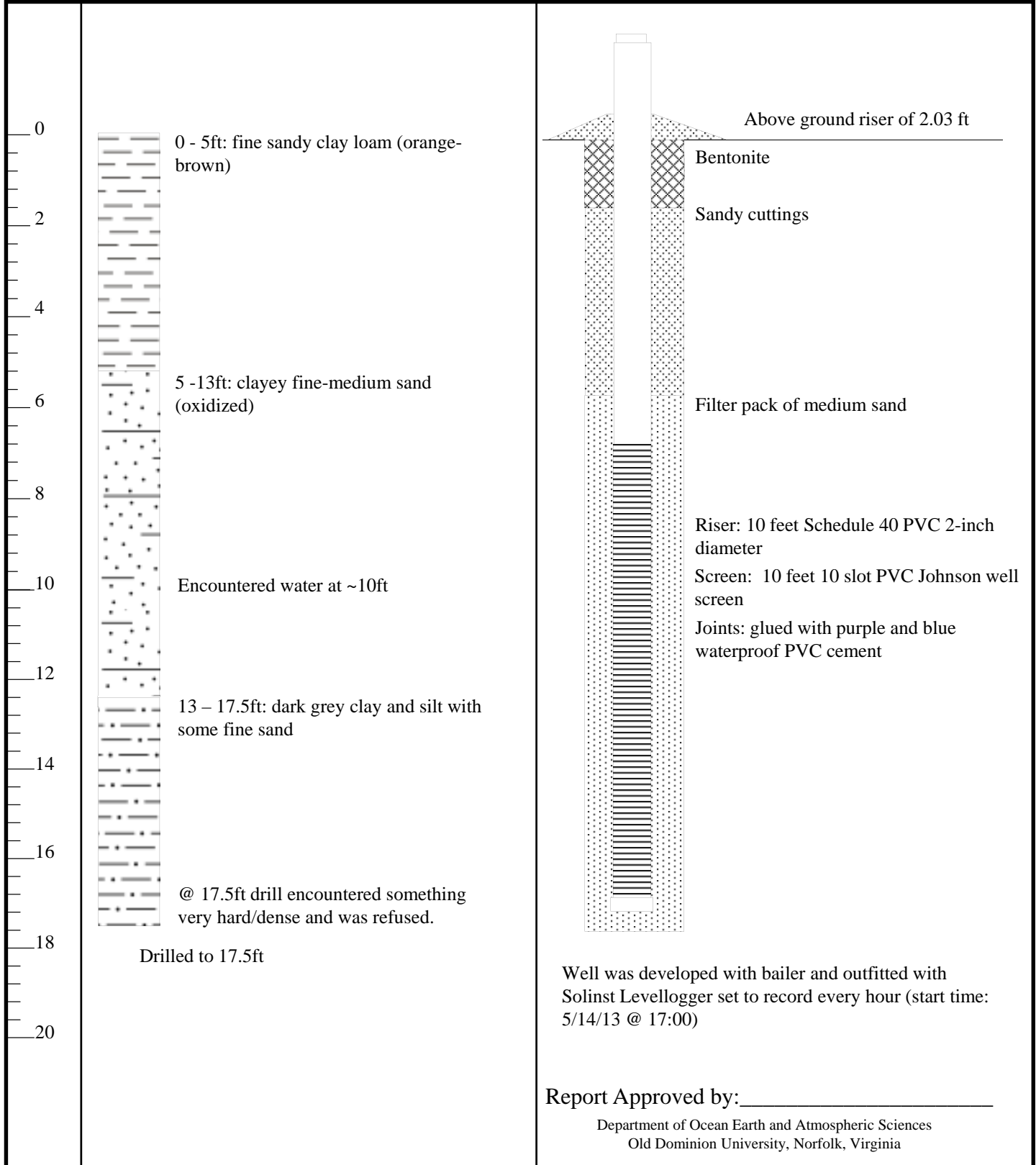
Well Completion Report

Project: Huntley Meadows Water Monitoring
Location: Corner of meadow south of HM office
 Lat: 38.76001
 Long: -77.11718
Top of casing elevation: *Not surveyed yet*

Well Name: VTHD1
Constructed by: S. Nagle, R. Konow, W. Myers
 M. Richardson, K. Dobbs, J. Parker
Construction Date: 5/14/13
Auger Type: Drilled with 6-inch hollow-stem auger

Scale (ft) Borehole Information

Well Construction Information



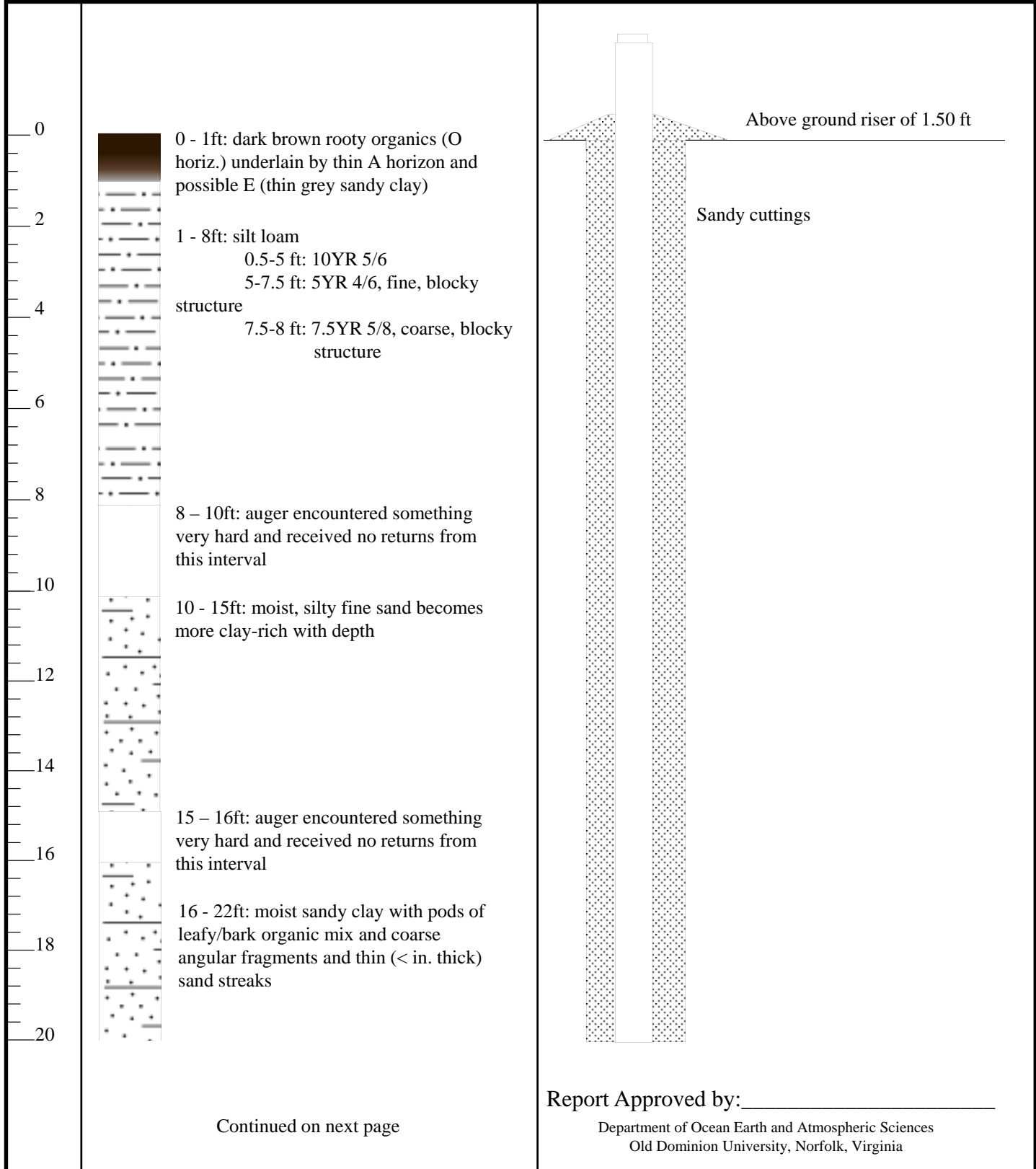
Well Completion Report

Project: Huntley Meadows Water Monitoring
Location: South end of HM near Muddy Hole Park
 Lat: 38.74389
 Long: -77.11527
Top of casing elevation: *Not surveyed yet*

Well Name: VTHD2
Constructed by: S. Nagle (Drill operator), W. Myers, K. Dobbs, M. Richardson, J. Parker
Construction Date: 5/14/13
Auger Type: Drilled with 6-inch hollow-stem auger

Scale (ft) Borehole Information

Well Construction Information



Continued on next page

Report Approved by: _____

Department of Ocean Earth and Atmospheric Sciences
 Old Dominion University, Norfolk, Virginia

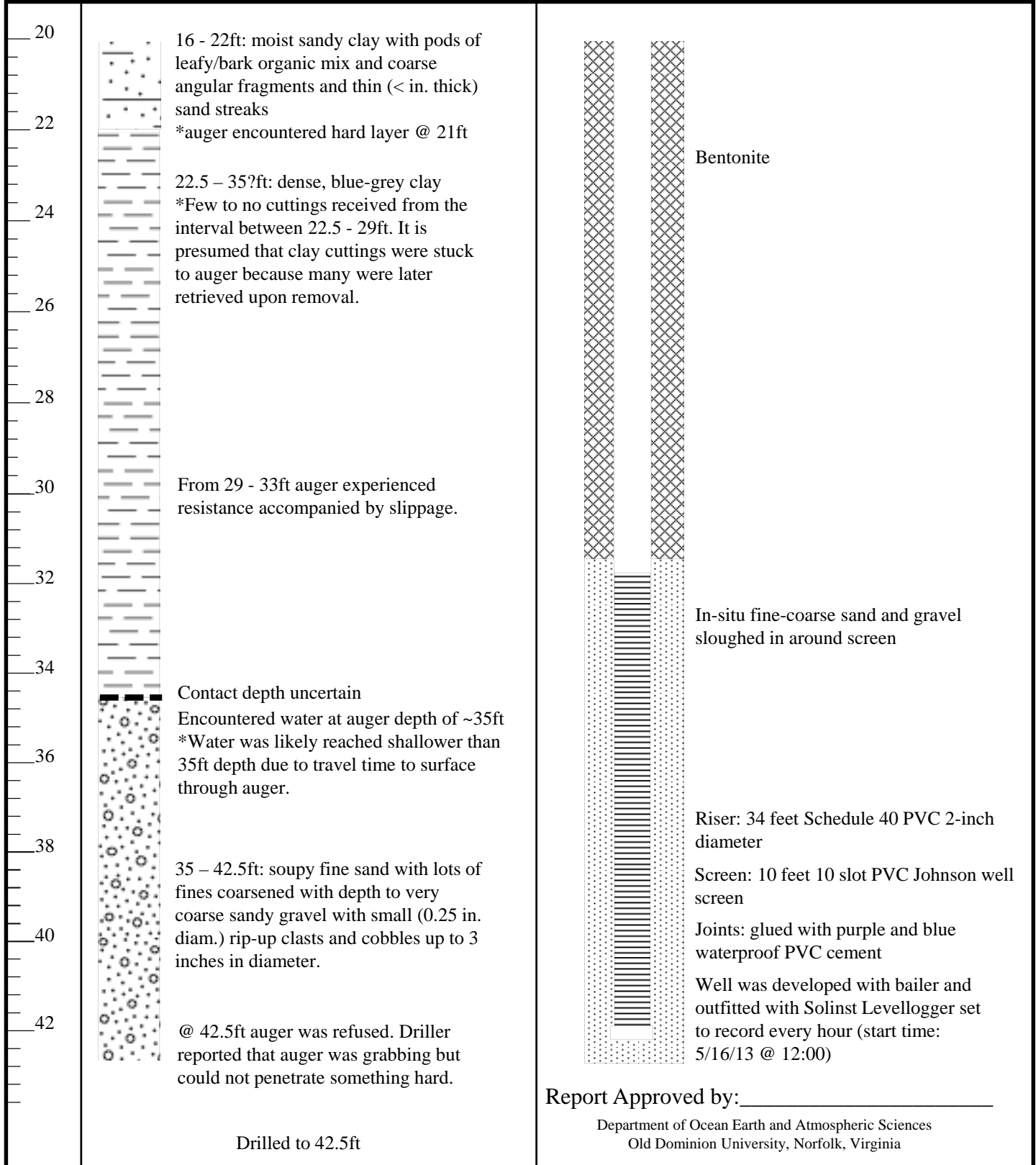
Well Completion Report (cont.)

Project: Huntley Meadows Water Monitoring
Location: South end of HM near Muddy Hole Park
 Lat: 38.74389
 Long: -77.11527
Top of casing elevation: *Not surveyed yet*

Well Name: VTHD2
Constructed by: S. Nagle (Drill operator), W. Myers, K. Dobbs, M. Richardson, J. Parker
Construction Date: 5/14/13
Auger Type: Drilled with 6-inch hollow-stem auger

Scale (ft) Borehole Information

Well Construction Information



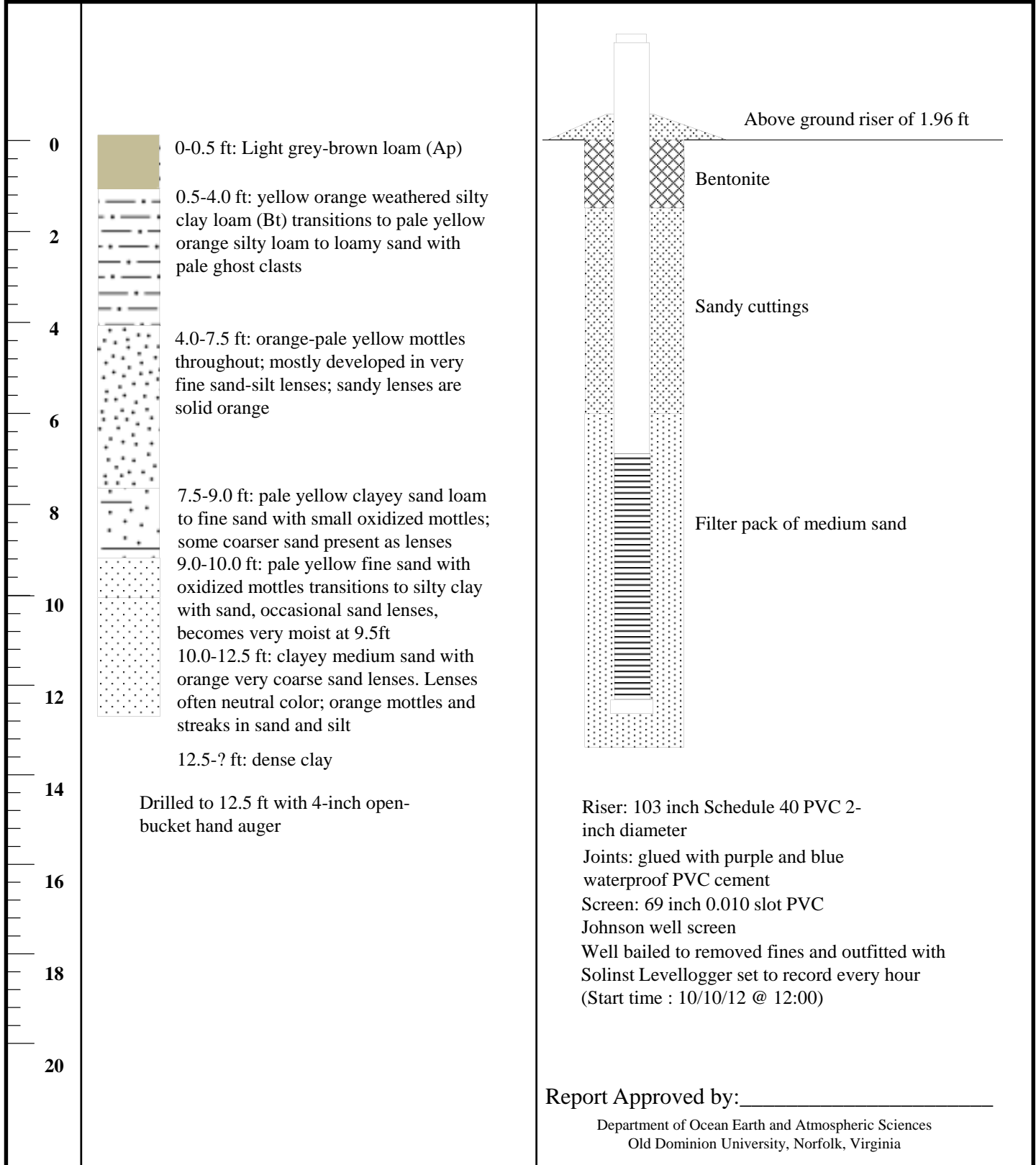
Well Completion Report

Project: Huntley Meadows Water Monitoring
Location: Huntley Meadows main entrance
 Lat: 38.76022
 Long: -77.09599
Top of casing elevation: *Not surveyed yet*

Well Name: VTHD3
Constructed by: K. Dobbs and R. Whittecar
Construction Date: 10/9/12
Auger type: 4-inch open-bucket hand auger

Scale (ft) Borehole Information

Well Construction Information



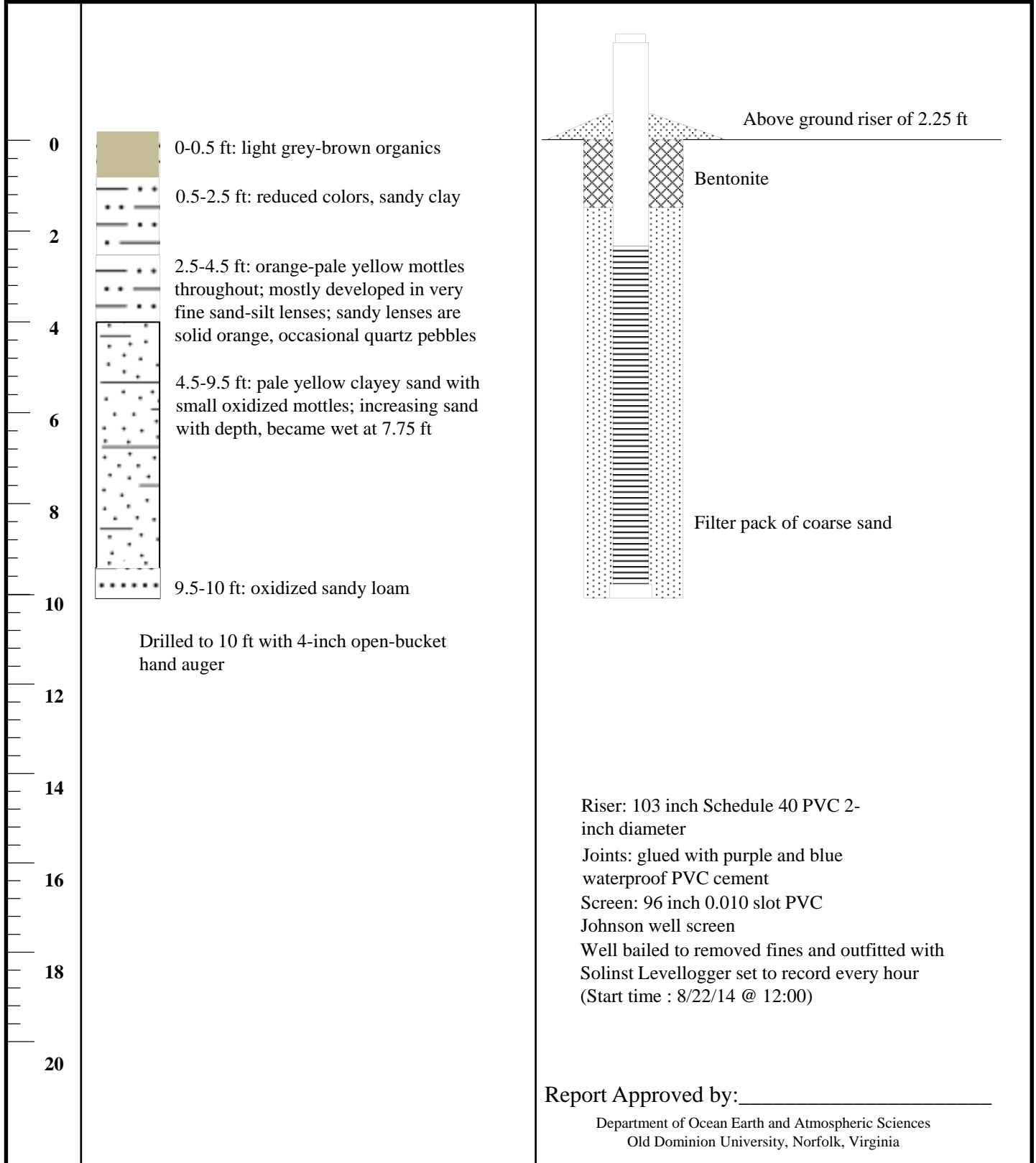
Well Completion Report

Project: Huntley Meadows Water Monitoring
Location: Near VT Stream gage east of main entrance
 Lat: 38.759517
 Long: -77.093433
Top of casing elevation: *Not surveyed yet*

Well Name: ODU_ET1
Constructed by: S. Stone and B. Hiza
Construction Date: 8/19/14
Auger type: 4-inch open-bucket hand auger

Scale (ft) Borehole Information

Well Construction Information



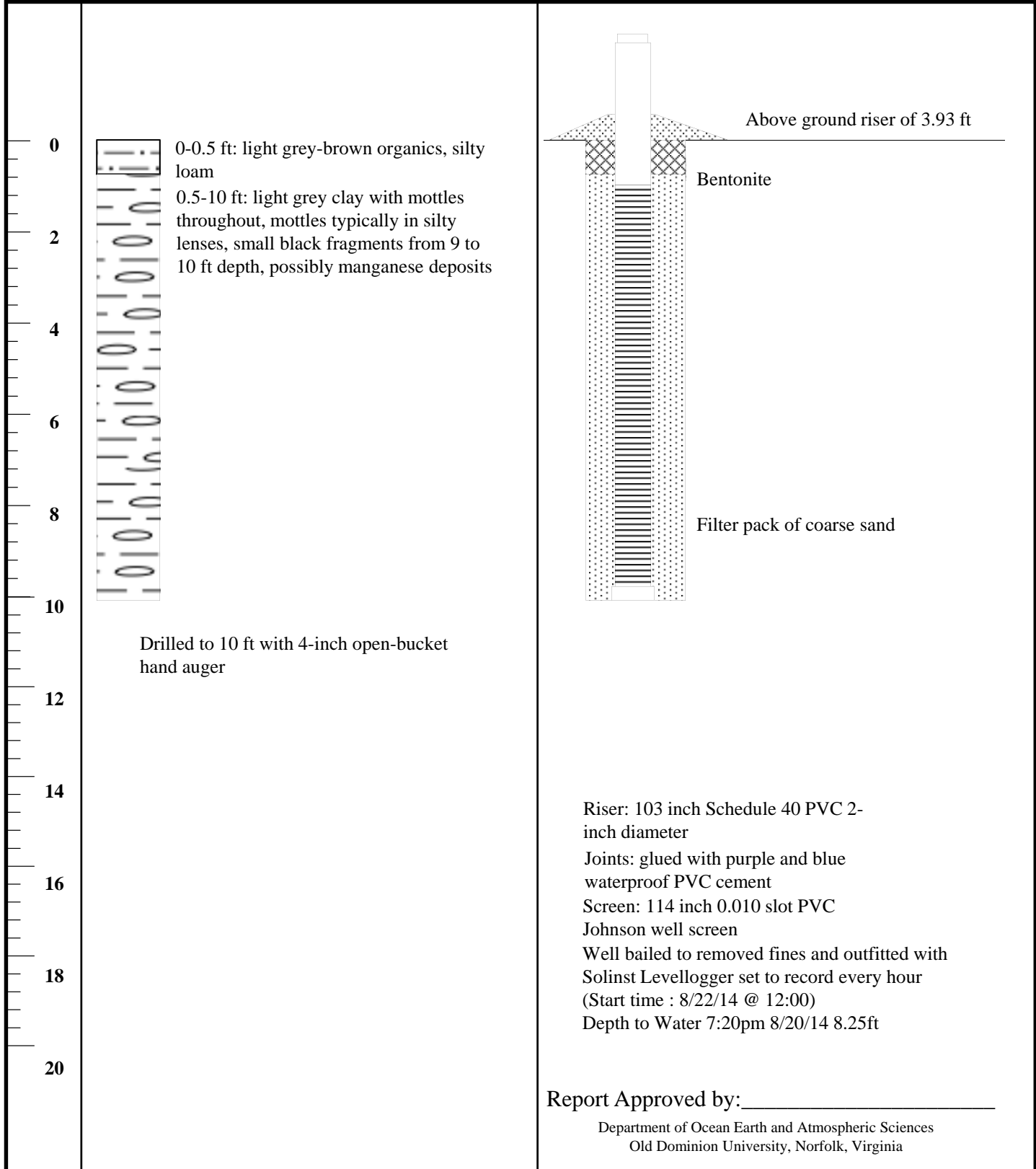
Well Completion Report

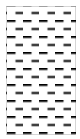
Project: Huntley Meadows Water Monitoring
Location: Near confluence of small streams north of ponded area, mapped as scrub/shrub wetland by NWI
 Lat: 38.757609 Long: -77.102559
Top of casing elevation: *Not surveyed yet*

Well Name: ODU_ET2
Constructed by: S. Stone and B. Hiza
Construction Date: 8/20/14
Auger type: 4-inch open-bucket hand auger

Scale (ft) Borehole Information

Well Construction Information





Clay



Clay with sand lenses



Sandy clay



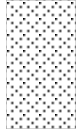
Sand and coarse angular gravel



Silt/silty loam



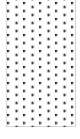
Gneissic Saprolite



Fine sand



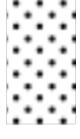
Granitic Saprolite



Medium sand



Bentonite



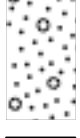
Coarse sand



Peat/Organics



Sand with some gravel



Sand and gravel



Clayey sand



Clay with sand and gravel lenses



Gravel



Sandy loam